

Critical Fields in Heavy Nuclei and Massive Nuclear Cores

Contents

1. Topics	433
2. Participants	435
2.1. ICRA Net participants	435
2.2. Past collaborators	435
2.3. On going collaborations	435
2.4. Ph.D. Students	435
3. Introduction	437
4. Brief description	441
4.1. On gravitationally and electro dy nami cally bound massive nu- clear density cores	441
4.2. On the relativistic Thomas-Fermi treatment of compressed atoms and compressed massive nuclear density cores	441
4.3. Electro dy nami c s for Nuclear Matter in Bulk	442
4.4. On the Charge to Mass ratio of Neutron Cores and Heavy Nuclei	442
4.5. Supercritical fields on the surface of massive nuclear cores: neutral core v.s. charged core	443
4.6. The extended nuclear matter model with smooth transition surface	443
4.7. Electron-positron pairs production in an electric potential of massive cores	443
4.8. On the self-consistent general relativistic equilibrium equations of neutron stars	444
4.9. The Crust of Neutron Stars and its connection with the Fireshell Model of GRBs	444
4.10. The Role of Thomas Fermi approach in Neutron Star Matter .	445
5. Publications (before 2008)	447
6. Publications (2008-2009)	449
7. Invited talks in international conferences	455
8. APPENDICES	457

A. Solution to Thomas-Fermi Equation for large nuclear cores	459
A.1. On gravitationally and electrostatically bound massive nuclear density cores	459
A.2. On the relativistic Thomas-Fermi treatment of compressed atoms and compressed massive nuclear density cores	471
A.3. Electrodynamics for Nuclear Matter in Bulk	488
A.4. On the Charge to Mass Ratio of Neutron Cores and Heavy Nuclei	496
A.5. Supercritical fields on the surface of massive nuclear cores: neutral core v.s. charged core	504
A.6. The Extended Nuclear Matter Model with Smooth Transition Surface	507
B. Electron-positron pairs production in an electric potential of massive cores	511
B.1. Introduction	511
B.2. Classical description of electrons in potential of cores	513
B.2.1. Effective potentials for particle's radial motion	513
B.2.2. Stable classical orbits (states) outside the core.	514
B.2.3. Stable classical orbits inside the core.	515
B.3. Semi-Classical description	517
B.3.1. Bohr-Sommerfeld quantization	517
B.3.2. Stability of semi-classical states	518
B.4. Production of electron-positron pair	520
B.5. Summary and remarks	522
C. On the self-consistent general relativistic equilibrium equations of neutron stars	525
D. The Outer Crust of Neutron Stars	531
E. The Role of Thomas - Fermi approach in Neutron Star Matter	537
Bibliography	551

1. Topics

- On gravitationally and electrostatically bound massive nuclear density cores
- On the relativistic Thomas-Fermi treatment of compressed atoms and compressed massive nuclear density cores
- Electrodynamics for Nuclear Matter in Bulk
- On the Charge to Mass ratio of Neutron Cores and Heavy Nuclei
- Supercritical fields on the surface of massive nuclear cores: neutral core v.s. charged core
- The extended nuclear matter model with smooth transition surface
- Electron-positron pairs production in an electric potential of massive cores
- On the self-consistent general relativistic equilibrium equations of neutron stars
- The Crust of Neutron Stars and its connection with the Fireshell Model of GRBs

2. Participants

2.1. ICRAANet participants

- D. Arnett (Steward Observatory, University of Arizona, USA)
- H. Kleinert (Free University of Berlin , Germany)
- V. Popov (ITEP, Moscow, Russia)
- M. Rotondo (ICRAANet, University of Rome, Italy)
- R. Ruffini (ICRAANet, University of Rome, Italy)
- G.'t Hooft (Institute for Theoretical Physic Universiteit Utrecht)
- S.-S. Xue (ICRAANet)

2.2. Past collaborators

- L. Stella (Rome Astronomical Observatory, Italy)
- W. Greiner (Institut für Theoretical Physics Johann Wolfgang Goethe-Universität, Frankfurt am Main)

2.3. On going collaborations

2.4. Ph.D. Students

- B. Patricelli (ICRAANet, University of Rome, Italy)
- Jorge A. Rueda (ICRAANet, University of Rome, Italy)

3. Introduction

One of the most active field of research has been to analyse a general approach to Neutron Stars based on the Thomas-Fermi ultrarelativistic equations amply adopted in the study of superheavy nuclei. The aim is to have a unified approach both to superheavy nuclei, up to atomic numbers of the order of 10^5 – 10^6 , and to what we have called “Massive Nuclear Density Cores”. These massive nuclear density cores are

- characterized by atomic number of the order of 10^{57} ;
- composed by neutrons, protons and electrons in β –equilibrium;
- expected to be kept at nuclear density by self gravity.

The analysis of superheavy nuclei has historically represented a major field of research, developed by Prof. V. Popov and Prof. W. Greiner and their schools. This same problem was studied in the context of the relativistic Thomas-Fermi equation also by R. Ruffini and L. Stella, already in the 80s. The recent approach was started with the Ph.D. Thesis of M. Rotondo and has shown the possibility to extrapolate this treatment of superheavy nuclei to the case of Massive Nuclear Cores. The very unexpected result has been that also around these massive cores there is the distinct possibility of having an electromagnetic field close to the critical value $E_c = \frac{m_e^2 c^3}{e\hbar}$, although localized in a very narrow shell of the order of the electron Compton wavelength (see Fig. 3.1, 3.2).

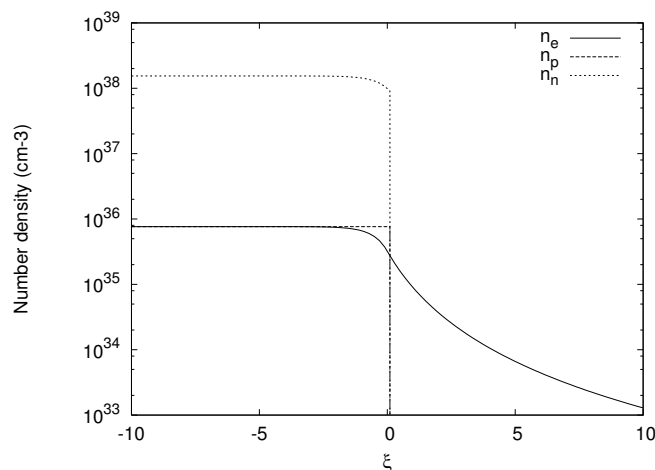


Figure 3.1.: Number density of electrons, protons and neutrons.

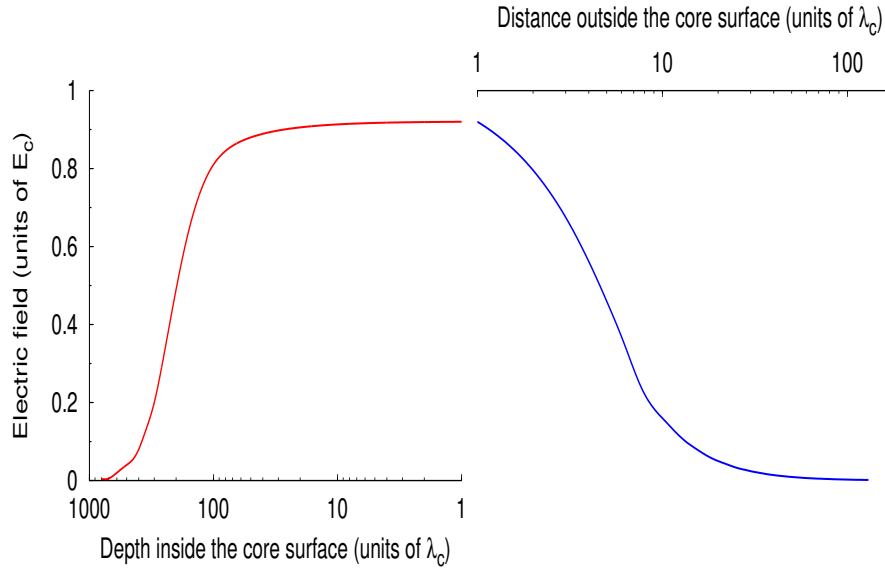


Figure 3.2.: Electric Field in units of the critical field.

The welcome result has been that all the analytic work developed by Prof. Popov and the Russian school can be applied using scaling laws to the case of massive nuclear density cores, if the β -equilibrium condition is properly taken into account. This has been the result obtained and published by Ruffini, Xue and Rotondo already in 2007. Since then, a large variety of problems has emerged, which have seen the direct participation at ICRANet of Prof. Greiner, Prof. Popov, and Prof. 't Hooft. The crucial issue to be debated is the stability of such cores under the competing effects of self gravity and Coulomb repulsion. In order to probe this stability, we have started a new approach to the problem within the framework of general relativity. However, in order to approach the more complex problem of a neutron star core and its interface with the neutron star crust, as well as a variety of new physical regimes encountered in ultra-relativistic conditions, we have proceeded by steps. We have then generalized the Feynman-Metropolis-Teller treatment of compressed atoms to relativistic regimes, and we have introduced the concept of compressed massive nuclear density cores. The object of the Ph.D thesis of Rueda has been the addressing of the existence of globally neutral neutron star configurations in contrast with the traditional ones constructed by imposing local neutrality. The equilibrium equations describing this system are the Einstein-Maxwell equations which have been solved self-consistently with the general relativistic Thomas-Fermi equations and β -equilibrium condition. The major scientific issue here is to have a unified approach solving the coupled system of the general relativistic self gravitating electro-dynamical problem with the corresponding formulation of the Thomas-Fermi equations in the framework of general relativity. Prof. 't Hooft, in a series of lectures, has forcefully expressed the opinion that necessarily, during the pro-

cess of gravitational collapse, it should occur a more extended distribution of the electromagnetic field to the entire core of the star and not only confined to a thin shell. This is a necessary condition in order to transmit the gravitational energy of the collapse to the electrodynamical component of the field giving possibly rise to large pair creation processes. Indeed, as demonstrated in our latest results, we are realizing this crucial idea of Prof. 't Hooft. As a result of the self-consistent treatment of the general relativistic equilibrium equations of neutron stars that we have mentioned above, we obtain neutron star equilibrium configurations with extended electrodynamic structure, starting from the center of the star all the way up to the core-crust interface, where the electric field can reach overcritical values. Recently, an extremely interesting observational problematic has emerged from the Chandra observations of the central compact object of the Cassiopeia A supernova remnant. It is with a similar steadily emitting and non-pulsating neutron star that our theoretical predictions can indeed be tested. In particular, the existence of a new family of neutron stars with a smaller crusts than the ones obtained when local neutrality is adopted.

4. Brief description

4.1. On gravitationally and electrostatically bound massive nuclear density cores

In a unified treatment we extrapolate results for neutral atoms with heavy nuclei to massive nuclear density cores with mass number $A \approx (m_{\text{Planck}}/m_n)^3 \sim 10^{57}$. We give explicit analytic solutions for the relativistic Thomas-Fermi equation of N_n neutrons, N_p protons and N_e electrons in beta equilibrium, full-filling global charge neutrality, with $N_p = N_e$. We give explicit expressions for the physical parameters including the Coulomb and the surface energies and we study as well the stability of such configurations. Analogous to heavy nuclei these macroscopic cores exhibit an overcritical electric field near their surface (see Appendix A.1).

4.2. On the relativistic Thomas-Fermi treatment of compressed atoms and compressed massive nuclear density cores

Using the recently established scaling laws for the solutions of the relativistic Thomas-Fermi equation we consider the two limiting cases of compressed atoms and compressed massive nuclear density cores. The Feynman, Metropolis and Teller treatment of compressed atoms is extended to the relativistic regimes. Each configuration is confined by a Wigner-Seitz cell and is characterized by a positive electron Fermi energy. There exists a limiting configuration with a maximum value of the electrons Fermi energy $(E_e^F)_{\text{max}}$ reached when the Wigner-Seitz cell radius equals the radius of the nucleus, and it can be expressed analytically in the ultra-relativistic approximation. The results are compared and contrasted to approximate treatments in the literature. This treatment is then extrapolated to compressed massive nuclear density cores with $A \simeq (m_{\text{Planck}}/m_n)^3 \sim 10^{57}$. Again an entire family of equilibrium configurations exist for selected values of the electron Fermi energy varying in the range $0 < E_e^F \leq (E_e^F)_{\text{max}}$. The configuration with $E_e^F = (E_e^F)_{\text{max}}$ has global and local charge neutrality and no electrostatic structure. The remaining configurations have electric fields on the core surface, increasing for decreasing values of the electron Fermi energy reaching values much larger

than the critical value $E_c = m_e^2 c^3 / (e\hbar)$ for $E_e^F = 0$. We compare and contrast our results with the ones of Thomas-Fermi model in strange stars. In both, the case of atoms and the massive nuclear density cores, the configuration with $E_e^F = 0$, reached when the Wigner-Seitz cell radius tends to infinity corresponds to the ground state of the system (see Appendix A.2).

4.3. Electrodynamics for Nuclear Matter in Bulk

A general approach to analyze the electrodynamics of nuclear matter in bulk is presented using the relativistic Thomas-Fermi equation generalizing to the case of $N \simeq (m_{\text{Planck}}/m_n)^3$ nucleons of mass m_n the approach well tested in very heavy nuclei ($Z \simeq 10^6$). Particular attention is given to implement the condition of charge neutrality globally on the entire configuration, versus the one usually adopted on a microscopic scale. As the limit $N \simeq (m_{\text{Planck}}/m_n)^3$ is approached the penetration of electrons inside the core increases and a relatively small tail of electrons persists leading to a significant electron density outside the core. Within a region of 10^2 electron Compton wavelength near the core surface electric fields close to the critical value for pair creation by vacuum polarization effect develop. These results can have important consequences on the understanding of physical process in neutron stars structures as well as on the initial conditions leading to the process of gravitational collapse to a black hole (see Appendix A.3).

4.4. On the Charge to Mass ratio of Neutron Cores and Heavy Nuclei

We determine theoretically the relation between the total number of protons N_p and the mass number A (the charge to mass ratio) of nuclei and neutron cores with the model recently proposed by Ruffini et al. (2007) and we compare it with other N_p versus A relations: the empirical one, related to the Periodic Table, and the semi-empirical relation, obtained by minimizing the Weizsäcker mass formula. We find that there is a very good agreement between all the relations for values of A typical of nuclei, with differences of the order of per cent. Our relation and the semi-empirical one are in agreement up to $A \approx 10^4$ for higher values, we find that the two relations differ. We interpret the different behavior of our theoretical relation as a result of the penetration of electrons (initially confined in an external shell) inside the core, that becomes more and more important by increasing A ; these effects are not taken into account in the semi-empirical mass-formula (see Appendix A.4).

4.5. Supercritical fields on the surface of massive nuclear cores: neutral core v.s. charged core

Based on the Thomas-Fermi approach, we describe and distinguish the electron distributions around extended nuclear cores: (i) in the case that cores are neutral for electrons bound by protons inside cores and proton and electron numbers are the same; (ii) in the case that super charged cores are bare, electrons (positrons) produced by vacuum polarization are bound by (fly into) cores (infinity) (see Appendix A.5).

4.6. The extended nuclear matter model with smooth transition surface

The existence of electric fields close to their critical value $E_c = \frac{m_e^2 c^3}{e\hbar}$ has been proved for massive cores of 10^7 up to 10^{57} nucleons using a distribution of constant nuclear density and a sharp step function at its boundary. We explore the modifications of this effect by considering a smoother density profile with a proton distribution fulfilling a Wood-Saxon dependence. The occurrence of a critical field has been confirmed. We discuss how the location of the maximum of the electric field as well as its magnitude is modified by the smoother distribution (see Appendix A.6).

4.7. Electron-positron pairs production in an electric potential of massive cores

Classical and semi-classical energy states of relativistic electrons bounded by a massive and charged core with the charge-mass-radius Q/M and macroscopic radius R_c are discussed. We show that the energies of semi-classical (bound) states can be much smaller than the negative electron mass-energy ($-mc^2$), and energy-level crossing to negative energy continuum occurs. Electron – positron pair production takes place by quantum tunneling, if these bound states are not occupied. Electrons fill into these bound states and positrons go to infinity. We explicitly calculate the rate of pair-production, and compare it with the rates of electron-positron production by the Sauter-Euler-Heisenberg-Schwinger in a constant electric field. In addition, the pair-production rate for the electro-gravitational balance ratio $Q/M = 10^{-19}$ is much larger than the pair-production rate due to the Hawking processes. We point out that in neutral cores with equal proton and electron numbers, the configuration of relativistic electrons in these semi-classical (bound) states should be stabilized by photon emissions (see Appendix B).

4.8. On the self-consistent general relativistic equilibrium equations of neutron stars

We address the existence of globally neutral neutron star configurations in contrast with the traditional ones constructed by imposing local neutrality. The equilibrium equations describing this system are the Einstein-Maxwell equations which must be solved self-consistently with the general relativistic Thomas-Fermi equation and β -equilibrium condition. To illustrate the application of this novel approach we adopt the Baym, Bethe, and Pethick (1971) strong interaction model of the baryonic matter in the core and of the white-dwarf-like material of the crust. We illustrate the crucial role played by the boundary conditions satisfied by the leptonic component of the matter at the interface between the core and the crust. For every central density an entire new family of equilibrium configurations exists for selected values of the Fermi energy of the electrons at the surface of the core. Each such configuration fulfills global charge neutrality and is characterized by a non-trivial electro-dynamical structure. The electric field extends over a thin shell of thickness $\sim \hbar/(m_e c)$ between the core and the crust and becomes largely overcritical in the limit of decreasing values of the crust mass (see Appendix C).

4.9. The Crust of Neutron Stars and its connection with the Fireshell Model of GRBs

We study the characteristics of the Outer Crust of Neutron Stars, that is the region of Neutron Stars characterized by a mass density less than the “neutron drip” density and composed by White Dwarf - like material (fully ionized nuclei and free electrons). In particular, we calculate its mass and its thickness (M_{crust} and ΔR_{crust} respectively) with a general relativistic model, finding that the Outer Crust is smaller in mass and in radial extension for stars with more compact Cores. We also propose a correlation with the Fireshell Model of GRBs, that assumes that GRBs originates from the gravitational collapse to a black hole. One of the parameters used in this model is the baryon loading B of the electron - positron plasma, related to the mass of the baryonic remnant of the star progenitor M_B . We propose that B originates from the Crust of Neutron Stars and we compare M_{crust} with the values of M_B used to reproduce the observed data, finding that they are compatible (see Appendix D).

4.10. The Role of Thomas Fermi approach in Neutron Star Matter

The role of the Thomas-Fermi approach in Neutron Star matter cores is presented and discussed with special attention to solutions globally neutral and not fulfilling the traditional condition of local charge neutrality. A new stable and energetically favorable configuration is found. This new solution can be of relevance in understanding unsolved issues of the gravitational collapse processes and their energetics (see Appendix E).

5. Publications (before 2008)

1. R. Ruffini, M. Rotondo and S.-S. Xue, "Electrodynamics for Nuclear Matter in Bulk ", *Int. Journ. Mod. Phys. D* Vol. 16, No. 1 (2007) 1-9.

A general approach to analyze the electrodynamics of nuclear matter in bulk is presented using the relativistic Thomas-Fermi equation generalizing to the case of $N \simeq (m_{\text{Planck}}/m_n)^3$ nucleons of mass m_n the approach well tested in very heavy nuclei ($Z \simeq 10^6$). Particular attention is given to implement the condition of charge neutrality globally on the entire configuration, versus the one usually adopted on a microscopic scale. As the limit $N \simeq (m_{\text{Planck}}/m_n)^3$ is approached the penetration of electrons inside the core increases and a relatively small tail of electrons persists leading to a significant electron density outside the core. Within a region of 10^2 electron Compton wavelength near the core surface electric fields close to the critical value for pair creation by vacuum polarization effect develop. These results can have important consequences on the understanding of physical process in neutron stars structures as well as on the initial conditions leading to the process of gravitational collapse to a black hole.

2. R. Ruffini and L. Stella, "Some comments on the relativistic Thomas-Fermi model and the Vallarta-Rosen equation", *Phys. Lett. B* 102 (1981) 442. Some basic differences between the screening of the nuclear charge due to a relativistic cloud of electrons in a neutral atom and the screening due to vacuum polarization effects induced by a superheavy ion are discussed.
3. J. Ferreira, R. Ruffini and L. Stella, "On the relativistic Thomas-Fermi model", *Phys. Lett. B* 91, (1980) 314. The relativistic generalization of the Thomas-Fermi model of the atom is derived. It approaches the usual nonrelativistic equation in the limit $Z \ll Z_{\text{crit}}$, where Z is the total number of electrons of the atom and $Z_{\text{crit}} = (3\pi/4)^{1/2}\alpha^{-3/2}$ and α is the fine structure constant. The new equation leads to the breakdown of scaling laws and to the appearance of a critical charge, purely as a consequence of relativistic effects. These results are compared and contrasted with those corresponding to N self-gravitating degenerate relativistic fermions, which for $N \approx N_{\text{crit}} = (3\pi/4)^{1/2}(m/m_p)^3$ give rise to the concept of a critical mass against gravitational collapse. Here m is the mass of the fermion and $m_p = (\hbar c/G)^{1/2}$ is the Planck mass.

6. Publications (2008-2009)

1. Jorge A. Rueda, R. Ruffini, and S.-S. Xue, "On the self-consistent general relativistic equilibrium equations of neutron stars", submitted to Phys. Rev. Lett.

We address the existence of globally neutral neutron star configurations in contrast with the traditional ones constructed by imposing local neutrality. The equilibrium equations describing this system are the Einstein-Maxwell equations which must be solved self-consistently with the general relativistic Thomas-Fermi equation and β -equilibrium condition. To illustrate the application of this novel approach we adopt the Baym, Bethe, and Pethick (1971) strong interaction model of the baryonic matter in the core and of the white-dwarf-like material of the crust. We illustrate the crucial role played by the boundary conditions satisfied by the leptonic component of the matter at the interface between the core and the crust. For every central density an entire new family of equilibrium configurations exists for selected values of the Fermi energy of the electrons at the surface of the core. Each such configuration fulfills global charge neutrality and is characterized by a non-trivial electro-dynamical structure. The electric field extends over a thin shell of thickness $\sim \hbar/(m_e c)$ between the core and the crust and becomes largely overcritical in the limit of decreasing values of the crust mass.

2. V. Popov, M. Rotondo, R. Ruffini, and S.-S. Xue, "On gravitationally and electro-dynamically bound massive nuclear density cores", submitted to Phys. Rev. C.

In a unified treatment we extrapolate results for neutral atoms with heavy nuclei to massive nuclear density cores with mass number $A \approx (m_{\text{Planck}}/m_n)^3 \sim 10^{57}$. We give explicit analytic solutions for the relativistic Thomas-Fermi equation of N_n neutrons, N_p protons and N_e electrons in beta equilibrium, full-filling global charge neutrality, with $N_p = N_e$. We give explicit expressions for the physical parameters including the Coulomb and the surface energies and we study as well the stability of such configurations. Analogous to heavy nuclei these macroscopic cores exhibit an overcritical electric field near their surface.

3. M. Rotondo, Jorge A. Rueda, R. Ruffini, and S.-S. Xue, "On the relativistic Thomas-Fermi treatment of compressed atoms and compressed massive nuclear density cores", submitted to Phys. Rev. D.

Using the recently established scaling laws for the solutions of the relativistic Thomas-Fermi equation we consider the two limiting cases of compressed atoms and compressed massive nuclear density cores. The Feynman, Metropolis and Teller treatment of compressed atoms is extended to the relativistic regimes. Each configuration is confined by a Wigner-Seitz cell and is characterized by a positive electron Fermi energy. There exists a limiting configuration with a maximum value of the electrons Fermi energy $(E_e^F)_{max}$ reached when the Wigner-Seitz cell radius equals the radius of the nucleus, and it can be expressed analytically in the ultra-relativistic approximation. The results are compared and contrasted to approximate treatments in the literature. This treatment is then extrapolated to compressed massive nuclear density cores with $A \simeq (m_{\text{Planck}}/m_n)^3 \sim 10^{57}$. Again an entire family of equilibrium configurations exist for selected values of the electron Fermi energy varying in the range $0 < E_e^F \leq (E_e^F)_{max}$. The configuration with $E_e^F = (E_e^F)_{max}$ has global and local charge neutrality and no electro-dynamical structure. The remaining configurations have electric fields on the core surface, increasing for decreasing values of the electron Fermi energy reaching values much larger than the critical value $E_c = m_e^2 c^3 / (e\hbar)$ for $E_e^F = 0$. We compare and contrast our results with the ones of Thomas-Fermi model in strange stars. In both, the case of atoms and the massive nuclear density cores, the configuration with $E_e^F = 0$, reached when the Wigner-Seitz cell radius tends to infinity corresponds to the ground state of the system.

4. R. Ruffini, M. Rotondo and S.-S. Xue, "Neutral nuclear core vs super charged one", in Proceedings of the Eleventh Marcel Grossmann Meeting, R. Jantzen, H. Kleinert, R. Ruffini (eds.), (World Scientific, Singapore, 2008).

Based on the Thomas-Fermi approach, we describe and distinguish the electron distributions around extended nuclear cores: (i) in the case that cores are neutral for electrons bound by protons inside cores and proton and electron numbers are the same; (ii) in the case that super charged cores are bare, electrons (positrons) produced by vacuum polarization are bound by (fly into) cores (infinity).

5. R. Ruffini and S.-S. Xue, "Electron-positron pairs production in an electric potential of massive cores", to be submitted to Phys. Lett. B

Classical and semi-classical energy states of relativistic electrons bounded by a massive and charged core with the charge-mass-radius Q/M and macroscopic radius R_c are discussed. We show that the energies of semi-classical (bound) states can be much smaller than the negative electron mass-energy $(-mc^2)$, and energy-level crossing to negative energy continuum occurs. Electron-positron pair production takes place by quantum tunneling, if these bound states are not occupied. Electrons fill into these bound states and positrons go to infinity. We explicitly calculate the rate of pair-production, and compare it

with the rates of electron-positron production by the Sauter-Euler-Heisenberg-Schwinger in a constant electric field. In addition, the pair-production rate for the electro-gravitational balance ratio $Q/M = 10^{-19}$ is much larger than the pair-production rate due to the Hawking processes. We point out that in neutral cores with equal proton and electron numbers, the configuration of relativistic electrons in these semi-classical (bound) states should be stabilized by photon emissions.

6. Jorge A. Rueda, R. Ruffini, and S.-S. Xue, "On the electrostatic structure of neutron stars", to be published in the proceedings of the 1st Zel'dovich meeting, Minsk-Byelorussia (2009).

We consider neutron stars composed by, (1) a core of degenerate neutrons, protons, and electrons above nuclear density; (2) an inner crust of nuclei in a gas of neutrons and electrons; and (3) an outer crust of nuclei in a gas of electrons. We use for the strong interaction model for the baryonic matter in the core an equation of state based on the phenomenological Weizsacker mass formula, and to determine the properties of the inner and the outer crust below nuclear saturation density we adopt the well-known equation of state of Baym-Bethe-Pethick. The integration of the Einstein-Maxwell equations is carried out under the constraints of β -equilibrium and global charge neutrality. We obtain baryon densities that sharply go to zero at nuclear density and electron densities matching smoothly the electron component of the crust. We show that a family of equilibrium configurations exists fulfilling overall neutrality and characterized by a non-trivial electro-dynamical structure at the interface between the core and the crust. We find that the electric field is overcritical and that the thickness of the transition surface-shell separating core and crust is of the order of the electron Compton wavelength.

7. Jorge A. Rueda H., B. Patricelli, M. Rotondo, R. Ruffini, and S. S. Xue, "The Extended Nuclear Matter Model with Smooth Transition Surface", to be published in the Proceedings of The 3rd Stueckelberg Workshop on Relativistic Field Theories, Pescara-Italy (2008).

The existence of electric fields close to their critical value $E_c = m_e^2 c^3 / (e\hbar)$ has been proved for massive cores of 10^7 up to 10^{57} nucleons using a proton distribution of constant density and a sharp step function at its boundary. We explore the modifications of this effect by considering a smoother density profile with a proton distribution fulfilling a Woods-Saxon dependence. The occurrence of a critical field has been confirmed. We discuss how the location of the maximum of the electric field as well as its magnitude is modified by the smoother distribution.

8. B. Patricelli, M. Rotondo and R. Ruffini, "On the Charge to Mass Ratio of Neutron Cores and Heavy Nuclei", AIP Conference Proceedings, Vol. 966 (2008), pp. 143-146.

We determine theoretically the relation between the total number of protons N_p and the mass number A (the charge to mass ratio) of nuclei and neutron cores with the model recently proposed by Ruffini et al. (2007) and we compare it with other N_p versus A relations: the empirical one, related to the Periodic Table, and the semi-empirical relation, obtained by minimizing the Weizsäcker mass formula. We find that there is a very good agreement between all the relations for values of A typical of nuclei, with differences of the order of per cent. Our relation and the semi-empirical one are in agreement up to $A \approx 10^4$ for higher values, we find that the two relations differ. We interpret the different behavior of our theoretical relation as a result of the penetration of electrons (initially confined in an external shell) inside the core, that becomes more and more important by increasing A ; these effects are not taken into account in the semi-empirical mass-formula.

9. M. Rotondo, R. Ruffini and S.-S Xue, "On the Electrodynamical properties of Nuclear matter in bulk", AIP Conference Proceedings, Vol. 966 (2008), pp. 147-152.

We analyze the properties of solutions of the relativistic Thomas-Fermi equation for globally neutral cores with radius of the order of $R \approx 10$ Km, at constant densities around the nuclear density. By using numerical techniques as well as well tested analytic procedures developed in the study of heavy ions, we confirm the existence of an electric field close to the critical value $E_c = m_e^2 c^3 / e \hbar$ in a shell $\Delta R \approx 10^4 \hbar / m_\pi c$ near the core surface. For a core of ≈ 10 Km the difference in binding energy reaches 10^{49} ergs. These results can be of interest for the understanding of very heavy nuclei as well as physics of neutron stars, their formation processes and further gravitational collapse to a black hole.

10. B. Patricelli, M. Rotondo, J. A. Rueda H. and R. Ruffini, "The Electrodynamics of the Core and the Crust components in Neutron Stars", AIP Conference Proceedings, Vol. 1059 (2008), pp. 68-71.

We study the possibility of having a strong electric field (E) in Neutron Stars. We consider a system composed by a core of degenerate relativistic electrons, protons and neutrons, surrounded by an oppositely charged leptonic component and show that at the core surface it is possible to have values of E of the order of the critical value for electron-positron pair creation, depending on the mass density of the system. We also describe Neutron Stars in general relativity, considering a system composed by the core and an additional component: a crust of white dwarf - like material. We study the characteristics of the crust, in particular we calculate its mass M_{crust} . We propose that, when the mass density of the star increases, the core undergoes the process of gravitational collapse to a black hole, leaving the crust as a remnant; we compare M_{crust} with the mass of the baryonic remnant considered in the fireshell model of GRBs and find that their values are compatible.

11. R. Ruffini, "The Role of Thomas-Fermi approach in Neutron Star Matter", to be published in the Proceedings of the 9th International Conference "Path Integrals - New trends and perspectives", Max Planck Institute for the Physics of Complex Systems, Dresden, Germany, September 23 - 28 2007, World Scientific 207 - 218 (2008), eds. W. Janke and A. Pelster

The role of the Thomas-Fermi approach in Neutron Star matter cores is presented and discussed with special attention to solutions globally neutral and not fulfilling the traditional condition of local charge neutrality. A new stable and energetically favorable configuration is found. This new solution can be of relevance in understanding unsolved issues of the gravitational collapse processes and their energetics.

7. Invited talks in international conferences

1. 11th Italian-Korean Symposium on Relativistic Astrophysics, November 2–4 2009, Seoul (Korea).
2. 1st Galileo-Xu Guangqi Meeting, October 26–30 2009, Shanghai (China).
3. XIIth Marcel Grossmann Meeting On General Relativity, July 12–18 2009, Paris (France).
4. 6th Italian-Sino Workshop on Relativistic Astrophysics, June 29–July 1 2009, Pescara (Italy).
5. 1st Sobral Meeting, May 26–29 2009, Fortaleza (Brazil).
6. Probing stellar populations out to the distant universe, September 7–19 2008, Cefalù (Italy).
7. XIII Brazilian School of Cosmology and Gravitation, July 20–August 2 2008, Rio de Janeiro (Brazil).
8. 3rd Stueckelberg Workshop, July 8–18 2008, Pescara (Italy).
9. 5th Italian-Sino Workshop, May 28–June 1 2008, Taipei (Taiwan).
10. APS April meeting, April 12–15 2008, Saint Louis (USA).
11. Path Integrals - New Trends and Perspectives, September 23–28 2007, Dresden (Germany).
12. APS April meeting, April 14–17 2007, Jacksonville (USA).
13. XIth Marcel Grossmann Meeting on General Relativity, July 23–29 2006, Berlin (Germany).

8. APPENDICES

A. Solution to Thomas-Fermi Equation for large nuclear cores

A.1. On gravitationally and electrostatically bound massive nuclear density cores

Introduction

Models involving e^+e^- plasmas of total energy $\leq 10^{55}$ ergs originating from a vacuum polarization process during the formation of a black hole are being studied to explain a variety of ultra-relativistic astrophysics events (1; 2; 3). The formation of such a Kerr-Newman black hole with overcritical electromagnetic fields can only occur during the process of gravitational collapse, e.g., of two coalescing neutron stars. Accordingly in this article we consider new electrostatic properties of massive nuclear density cores which have been neglected in the astrophysics literature. This issue has been overlooked in the traditional description of neutron stars by considering only neutrons (5) or by imposing *ab initio* local charge neutrality, i.e., local identity of the densities of protons and electrons $n_p = n_e$, thus bypassing the description of any possible electrostatic effect (6; 26).

The model we consider here generalizes the relativistic Thomas-Fermi treatment for neutral atoms with heavy nuclei (7; 8; 9; 10; 11; 12). The study of neutral atoms with nuclei of mass number $A \sim 10^2-10^6$ is a classic problem of theoretical physics (11; 1). Special attention has been given to a possible vacuum polarization process and the creation of e^+e^- pairs (7; 11; 1) as well as to the study of nuclear stability against Coulomb repulsion (9). The existence of electric fields larger than the critical value $E_c = m_e^2 c^3 / (e\hbar)$ near their surfaces (10) has also been shown. We have generalized these models by enforcing the beta equilibrium conditions (13).

We have then extrapolated those results by numerical integration to the case of massive nuclear density cores of mass $\approx 1M_\odot$ and radius $R_c \approx 10$ Km (13). Such a massive nuclear density core is a globally neutral system of N_n neutrons, N_p protons and N_e electrons in beta equilibrium at nuclear density having mass numbers $A \sim (m_{\text{Planck}}/m_n)^3$ where m_n (m_e) is the neutron (electron) mass and $m_{\text{Planck}} = (\hbar c/G)^{1/2}$ (13). As in the nuclear model (12), the proton distribution is here assumed to be constant up to the core radius R_c . We have obtained configurations with global charge neutrality $N_p = N_e$ but

$n_p \neq n_e$, in contrast with the local condition $n_p = n_e$ traditionally assumed in astrophysics. As a result electric fields of critical value are confirmed to exist, near the surface, also in the case of massive nuclear density cores in analogy to the case of heavy nuclei.

Recently a new dimensionless form of the relativistic Thomas-Fermi treatment for a nuclear density core has been obtained which reveals the existence of new scaling laws for this model (14).

In this article we present a unified treatment extending from heavy nuclei to massive nuclear density cores by using an explicit analytic solitonic solution of the new dimensionless form of the relativistic Thomas-Fermi equation. We confirm the existence of and give an analytic expression for the overcritical electric field near the surface of massive nuclear density cores already obtained in (13) by numerical integration. Furthermore there are a variety of new results made possible by the new analytic formulation. First we give an explicit expression for the Coulomb energy of such cores, demonstrating their stability against nuclear fission, as opposed to the case of heavy nuclei. Secondly on the basis of Newtonian gravitational energy considerations we propose the existence of a possible new island of stability for mass numbers $A > A_R = 0.039 \left(\frac{N_p}{A}\right)^{1/2} \left(\frac{m_{\text{Planck}}}{m_n}\right)^3$. The equilibrium against Coulomb repulsion originates now from the combined effect of the screening of the relativistic electrons, of the surface tension due to strong interactions and of the gravitational interaction of the massive dense cores. By enforcing the condition of beta equilibrium, we also obtain a generalized relation between the mass number A and atomic number N_p which encompasses previous phenomenological expressions.

All the above solutions have been obtained assuming the electron Fermi energy to be equal to zero. The necessity and the methodology of extending these results to the case of compressed atoms along the lines of the Feynmann-Metropolis-Teller treatment (15), corresponding to positive values of the Fermi energy of electrons, are outlined here. We also motivate the clear necessity and the general methodology of justifying the above results using a self-consistent general relativistic treatment of the system. These ideas will be pursued in detail elsewhere.

The relativistic Thomas-Fermi equation and the beta equilibrium condition

It has been known since the classic work of Fermi (16) (see also Bohr and Mottelson (21)) that the phenomenological drop model of the nucleus gives excellent results for a variety of properties including the isobaric behavior and nuclear fission. In addition to the masses of the baryonic components and the asymmetry energy and pairing term, the mass formula contains terms estimating the surface tension energy of the nucleus (17)

$$\mathcal{E}_s = 17.5 \cdot A^{2/3} \text{ MeV}, \quad (\text{A.1.1})$$

and the Coulomb energy (18)

$$\varepsilon_c = \frac{3\alpha N_p^2}{5R_c}, \quad (\text{A.1.2})$$

where $R_c = r_0 A^{1/3}$, $r_0 = 1.5 \cdot 10^{-13}$ cm and the numerical factors are derived by fitting the observational data. From the extremization of the mass formula the following relation between A and N_p is obtained (19)

$$N_p \simeq \left[\frac{2}{A} + \frac{3}{200} \frac{1}{A^{1/3}} \right]^{-1}, \quad (\text{A.1.3})$$

which in the limit of small A gives

$$N_p \simeq \frac{A}{2}. \quad (\text{A.1.4})$$

The analysis of the stability of the nucleus against finite deformation leads to a stability condition against fission given by the equality of the surface energy term to the Coulomb energy. This leads to the condition (20)

$$\frac{N_p^2}{A} < 45. \quad (\text{A.1.5})$$

A novel situation occurs when super-heavy nuclei ($A > \tilde{A} \sim 10^4$) are examined (22; 13). The distribution of electrons penetrates inside the nucleus: a much smaller effective net charge of the nucleus occurs due to the screening of relativistic electrons (12; 22). In (23) a definition of an effective nuclear charge due to the penetration of the electrons was presented. A treatment based on the relativistic Thomas-Fermi model has been developed in order to describe the penetration of the electrons and their effective screening of the positive nuclear charge. In particular, by assuming $N_p \simeq A/2$, Greiner *et al.* (7; 8; 9) and Popov *et al.* (10; 11; 12) in a series of papers were able to solve the non-linear Thomas-Fermi equation. It was demonstrated in (12) that the effective positive nuclear charge is confined to a small layer of thickness $\sim \hbar/\sqrt{\alpha}m_\pi c$ where m_π is the pion mass and as usual $\alpha = e^2/\hbar c$. Correspondingly electric fields of strength much larger than the critical value E_c for vacuum polarization at the surface of the core are created. However, the creation of electron-positron pairs due to the vacuum polarization process does not occur because of the Pauli blocking by the degenerate electrons (1; 24).

Here we generalize the work of Greiner (7; 8; 9) and Popov (10; 11; 12). We have relaxed the condition $N_p \simeq A/2$ adopted by Popov and Greiner as well as the condition $N_p \simeq [2/A + 3/200A^{1/3}]^{-1}$ adopted by Ferreira, Ruffini and Stella (22). Instead we explicitly impose the beta decay equilibrium be-

tween neutrons, protons and electrons. We then extrapolate such model to the case $A \approx (m_{\text{Planck}}/m_n)^3 \sim 10^{57}$. A supercritical field still exists in a shell of thickness $\sim \hbar/\sqrt{\alpha}m_\pi c$ at the core surface, and a charged lepton-baryonic core is surrounded by an oppositely charged leptonic component. Such massive nuclear density cores, including the leptonic component, are globally neutral.

As usual we assume that the protons are distributed at constant density n_p within a radius

$$R_c = \Delta \frac{\hbar}{m_\pi c} N_p^{1/3}, \quad (\text{A.1.6})$$

where Δ is a parameter such that $\Delta \approx 1$ ($\Delta < 1$) corresponds to nuclear (supranuclear) densities when applied to ordinary nuclei. The overall Coulomb potential satisfies the Poisson equation

$$\nabla^2 V(r) = -4\pi e [n_p(r) - n_e(r)], \quad (\text{A.1.7})$$

with the boundary conditions $V(\infty) = 0$ (due to the global charge neutrality of the system) and finiteness of $V(0)$. The density $n_e(r)$ of the electrons of charge $-e$ is determined by the Fermi energy condition on their Fermi momentum P_e^F ; we assume here

$$E_e^F = [(P_e^F c)^2 + m_e^2 c^4]^{1/2} - m_e c^2 - eV(r) = 0, \quad (\text{A.1.8})$$

which leads to

$$n_e(r) = \frac{(P_e^F)^3}{3\pi^2 \hbar^3} = \frac{1}{3\pi^2 \hbar^3 c^3} \left[e^2 V^2(r) + 2m_e c^2 eV(r) \right]^{3/2}. \quad (\text{A.1.9})$$

By introducing the dimensionless quantities $x = r/[\hbar/m_\pi c]$, $x_c = R_c/[\hbar/m_\pi c]$ and $\chi/r = eV(r)/c\hbar$, the relativistic Thomas-Fermi equation takes the form

$$\frac{1}{3x} \frac{d^2 \chi(x)}{dx^2} = -\frac{\alpha}{\Delta^3} \theta(x_c - x) + \frac{4\alpha}{9\pi} \left[\frac{\chi^2(x)}{x^2} + 2 \frac{m_e}{m_\pi} \frac{\chi}{x} \right]^{3/2}, \quad (\text{A.1.10})$$

where $\chi(0) = 0, \chi(\infty) = 0$. The neutron density $n_n(r)$ is determined by the Fermi energy condition on their Fermi momentum P_n^F imposed by beta decay equilibrium

$$\begin{aligned} E_n^F &= [(P_n^F c)^2 + m_n^2 c^4]^{1/2} - m_n c^2 \\ &= [(P_p^F c)^2 + m_p^2 c^4]^{1/2} - m_p c^2 + eV(r), \end{aligned} \quad (\text{A.1.11})$$

which in turn is related to the proton and electron densities by Eqs. (A.1.7), (A.1.9) and (A.1.10). These equations have been integrated numerically (13).

The ultra-relativistic analytic solutions

In the ultrarelativistic limit, the relativistic Thomas-Fermi equation admits an analytic solution. Introducing the new function ϕ defined by $\phi = 4^{1/3}(9\pi)^{-1/3}\Delta\chi/x$ and the new variables $\hat{x} = (12/\pi)^{1/6}\sqrt{\alpha}\Delta^{-1}x$, $\xi = \hat{x} - \hat{x}_c$, where $\hat{x}_c = (12/\pi)^{1/6}\sqrt{\alpha}\Delta^{-1}x_c$, then Eq. (A.1.10) becomes

$$\frac{d^2\hat{\phi}(\xi)}{d\xi^2} = -\theta(-\xi) + \hat{\phi}(\xi)^3, \quad (\text{A.1.12})$$

where $\hat{\phi}(\xi) = \phi(\xi + \hat{x}_c)$. The boundary conditions on $\hat{\phi}$ are: $\hat{\phi}(\xi) \rightarrow 1$ as $\xi \rightarrow -\hat{x}_c \ll 0$ (at the massive nuclear density core center) and $\hat{\phi}(\xi) \rightarrow 0$ as $\xi \rightarrow \infty$. The function $\hat{\phi}$ and its first derivative $\hat{\phi}'$ must be continuous at the surface $\xi = 0$ of the massive nuclear density core. Equation (A.1.12) admits an exact solution

$$\hat{\phi}(\xi) = \begin{cases} 1 - 3 \left[1 + 2^{-1/2} \sinh(a - \sqrt{3}\xi) \right]^{-1}, & \xi < 0, \\ \frac{\sqrt{2}}{(\xi + b)}, & \xi > 0, \end{cases} \quad (\text{A.1.13})$$

where the integration constants a and b have the values $a = \text{arcsinh}(11\sqrt{2}) \approx 3.439$, $b = (4/3)\sqrt{2} \approx 1.886$. Next we evaluate the Coulomb potential energy function

$$eV(\xi) = \left(\frac{9\pi}{4}\right)^{1/3} \frac{1}{\Delta} m_\pi c^2 \hat{\phi}(\xi), \quad (\text{A.1.14})$$

and by differentiation, the electric field

$$E(\xi) = - \left(\frac{3^5\pi}{4}\right)^{1/6} \frac{\sqrt{\alpha} m_\pi^2 c^3}{\Delta^2 e\hbar} \hat{\phi}'(\xi). \quad (\text{A.1.15})$$

Details are given in Figs. A.1 and A.2.

We now estimate three crucial quantities:

1) the Coulomb potential at the center of the configuration,

$$eV(0) \approx \left(\frac{9\pi}{4}\right)^{1/3} \frac{1}{\Delta} m_\pi c^2, \quad (\text{A.1.16})$$

2) the electric field at the surface of the core

$$E_{\text{max}} \approx 0.95\sqrt{\alpha} \frac{1}{\Delta^2} \frac{m_\pi^2 c^3}{e\hbar} = 0.95 \frac{\sqrt{\alpha}}{\Delta^2} \left(\frac{m_\pi}{m_e}\right)^2 E_c. \quad (\text{A.1.17})$$

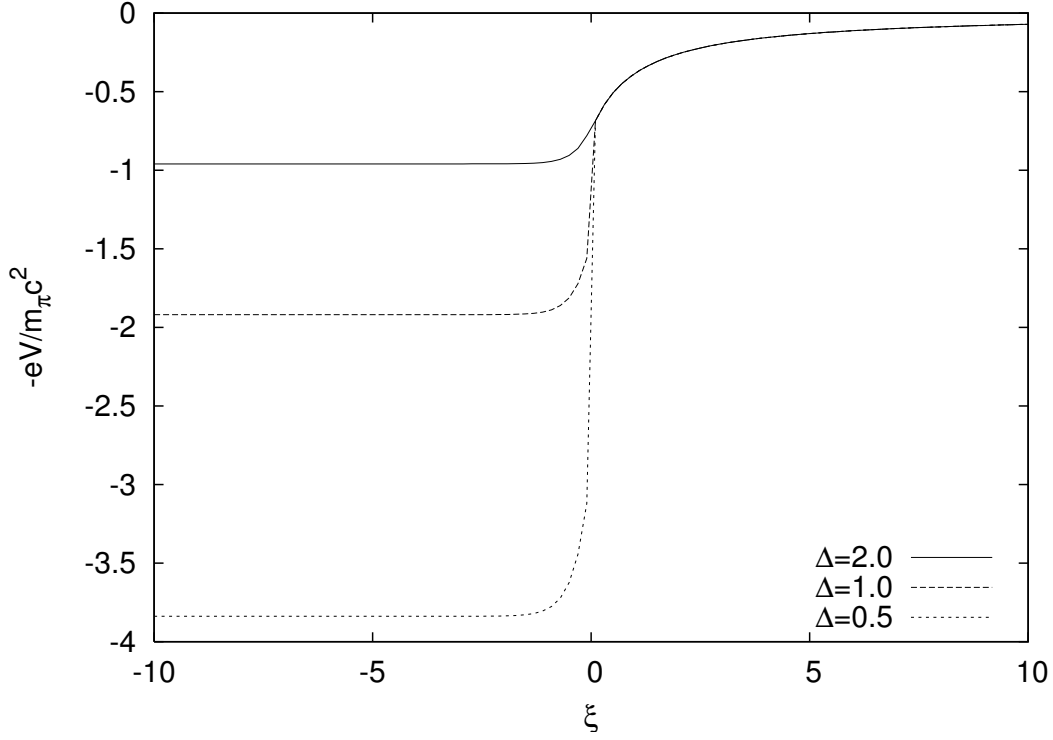


Figure A.1.: The electron Coulomb potential energy $-eV$, in units of pion mass m_π is plotted as a function of the radial coordinate $\xi = \hat{x} - \hat{x}_c$, for selected values of the density parameter Δ .

3) the Coulomb electrostatic energy of the core

$$\varepsilon_{\text{em}} = \int \frac{E^2}{8\pi} d^3r \approx 0.15 \frac{3\hbar c (3\pi)^{1/2}}{4\Delta\sqrt{\alpha}} A^{2/3} \frac{m_\pi c}{\hbar} \left(\frac{N_p}{A}\right)^{2/3}. \quad (\text{A.1.18})$$

These three quantities are functions only of the pion mass m_π , the density parameter Δ and of the fine structure constant α . Their formulas apply over the entire range from superheavy nuclei with $N_p \sim 10^3$ all the way up to massive cores with $N_p \approx (m_{\text{Planck}}/m_n)^3$.

New results derived from the analytic solutions

Starting from the analytic solutions of the previous section we obtain the following new results.

a) Using the solution (A.1.13), we have obtained a new generalized relation between A and N_p for any value of A . In the limit of small A this result agrees well with the phenomenological relations given by Eqs. (A.1.3) and (A.1.4), as is clearly shown in Fig. A.3. It appears that the explicit evaluation of the beta equilibrium, in contrast with the previously adopted Eqs.(3,4), leads to an

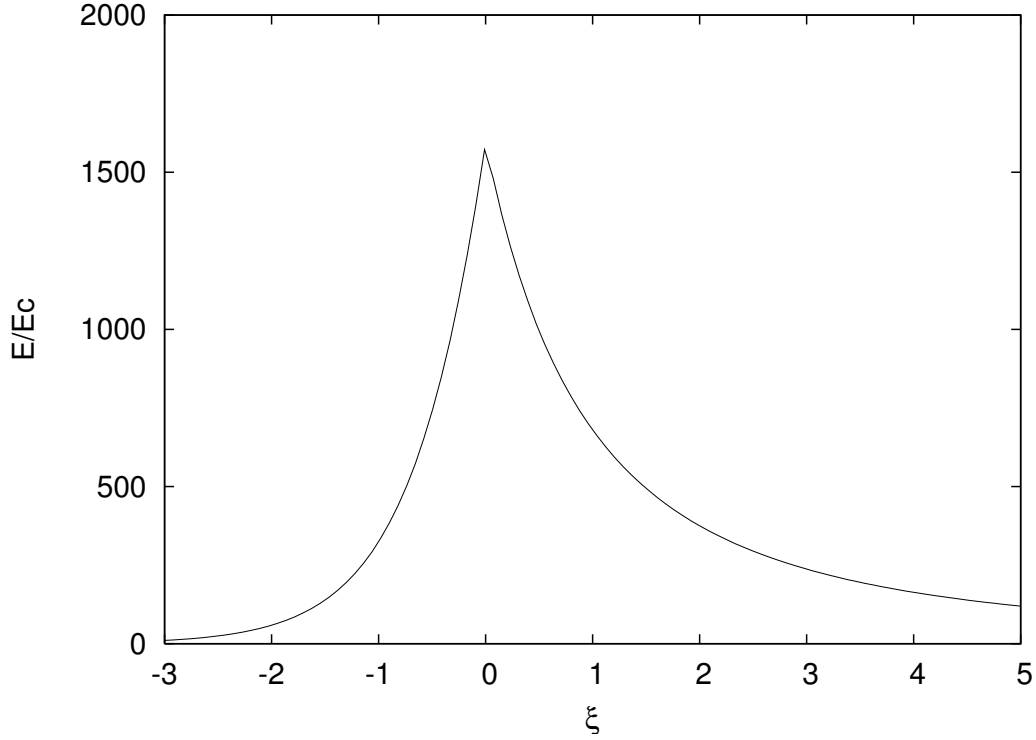


Figure A.2.: The electric field is plotted in units of the critical field E_c as a function of the radial coordinate ξ for $\Delta=2$, showing a sharp peak at the core radius.

effect comparable in magnitude and qualitatively similar to the asymmetry energy in the phenomenological liquid drop model. Details will be given in (33).

b) The charge-to-mass ratio of the effective charge Q at the core surface to the core mass M is given by

$$\frac{Q}{\sqrt{GM}} \approx \frac{E_{\max} R_c^2}{\sqrt{G} m_n A} \approx \frac{m_{\text{Planck}}}{m_n} \left(\frac{1}{N_p} \right)^{1/3} \frac{N_p}{A}. \quad (\text{A.1.19})$$

For superheavy nuclei with $N_p \approx 10^3$, the charge-to-mass ratio for the nucleus is

$$\frac{Q}{\sqrt{GM}} > \frac{1}{20} \frac{m_{\text{Planck}}}{m_n} \sim 10^{18}. \quad (\text{A.1.20})$$

Gravitation obviously plays no role in the stabilization of these nuclei.

Instead for massive nuclear density cores where $N_p \approx (m_{\text{Planck}}/m_n)^3$, the

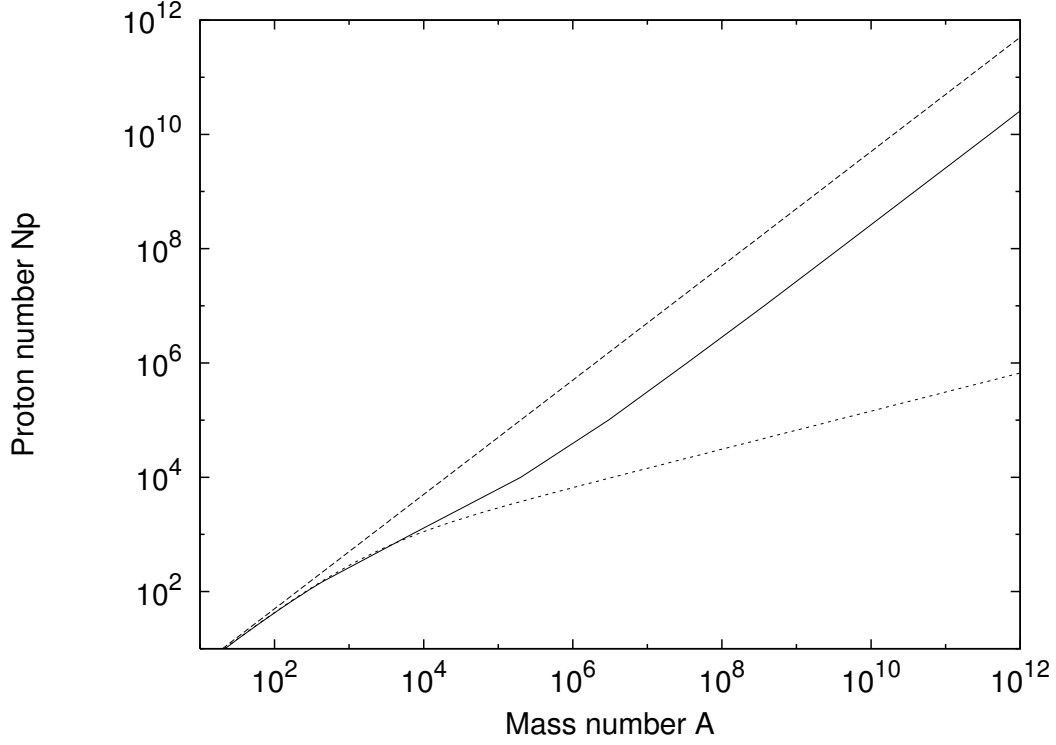


Figure A.3.: The A - N_p relation at nuclear density (solid line) obtained from first principles compared with the phenomenological expressions given by $N_p \simeq A/2$ (dashed line) and Eq. (A.1.3) (dotted line). The asymptotic value, for $A \rightarrow (m_{\text{Planck}}/m_n)^3$, is $N_p \approx 0.0046A$.

ratio Q/\sqrt{GM} given by Eq. (A.1.19) is simply

$$\frac{Q}{\sqrt{GM}} \approx \frac{N_p}{A}, \quad (\text{A.1.21})$$

which is approximately 0.0046 (see Fig. A.3). It is well-known that the charge-to-mass ratio (A.1.21) smaller than 1 evidences the equilibrium of self-gravitating mass-charge system both in Newtonian gravity and general relativity (see, e.g., (25)).

c) For a massive core at nuclear density the criterion of stability against fission ($\mathcal{E}_{em} < 2\mathcal{E}_s$) is satisfied. In order to see this we use Eqs. (A.1.1) and (A.1.18)

$$\frac{\mathcal{E}_{em}}{2\mathcal{E}_s} \approx 0.15 \frac{3}{8} \sqrt{\frac{3\pi}{\alpha}} \frac{1}{\Delta} \left(\frac{N_p}{A} \right)^{2/3} \frac{m_\pi c^2}{17.5 \text{ MeV}} \sim 0.1 < 1. \quad (\text{A.1.22})$$

Estimates of gravitational effects in a Newtonian approximation

In order to investigate the possible effects of gravitation on these massive neutron density cores we proceed to some qualitative and quantitative estimates based on the Newtonian approximation.

a) The *maximum* Coulomb energy per proton is given by Eq. (A.1.16) where the potential is evaluated at the center of the core. The Newtonian gravitational potential energy per proton (of mass m_p) in the field of a massive nuclear density core with $A \approx (m_{\text{Planck}}/m_n)^3$ is given by

$$\mathcal{E}_g = -G \frac{Mm_p}{R_c} = -\frac{1}{\Delta} \frac{m_{\text{Planck}}}{m_n} \frac{m_\pi c^2}{N_p^{1/3}} \simeq -\frac{m_\pi c^2}{\Delta} \left(\frac{A}{N_p} \right)^{1/3}. \quad (\text{A.1.23})$$

Since $A/N_p \sim 0.0046$ (see Fig. A.3) for any value of Δ , the gravitational energy is larger in magnitude than and opposite in sign to the Coulomb potential energy per proton of Eq. (A.1.16) so the system should be gravitationally stable.

b) There is yet a more accurate derivation of the gravitational stability based on the analytic solution of the Thomas-Fermi equation Eq. (A.1.12). The Coulomb energy \mathcal{E}_{em} given by (A.1.18) is mainly distributed within a thin shell of width $\delta R_c \approx \hbar \Delta / (\sqrt{\alpha} m_\pi c)$ and proton number $\delta N_p = n_p 4\pi R_c^2 \delta R_c$ at the surface. To ensure the stability of the system, the attractive gravitational energy of the thin proton shell

$$\mathcal{E}_{\text{gr}} \approx -3 \frac{G}{\Delta} \frac{A^{4/3}}{\sqrt{\alpha}} \left(\frac{N_p}{A} \right)^{1/3} m_n^2 \frac{m_\pi c}{\hbar} \quad (\text{A.1.24})$$

must be larger than the repulsive Coulomb energy (A.1.18). For small A , the gravitational energy is always negligible. However, since the gravitational energy increases proportionally to $A^{4/3}$ while the Coulomb energy only increases proportionally to $A^{2/3}$, the two must eventually cross, which occurs at

$$A_R = 0.039 \left(\frac{N_p}{A} \right)^{1/2} \left(\frac{m_{\text{Planck}}}{m_n} \right)^3. \quad (\text{A.1.25})$$

This establishes a *lower* limit for the mass number A_R necessary for the existence of an island of stability for massive nuclear density cores. The *upper* limit of the island of stability will be determined by general relativistic effects (34).

c) Having established the role of gravity in stabilizing the Coulomb interaction of the massive nuclear density core, we outline the importance of the strong interactions in determining its surface. We find for the neutron pressure at the surface:

$$P_n = \frac{9}{40} \left(\frac{3}{2\pi} \right)^{1/3} \left(\frac{m_\pi}{m_n} \right) \frac{m_\pi c^2}{(\hbar/m_\pi c)^3} \left(\frac{A}{N_p} \right)^{5/3} \frac{1}{\Delta^5}, \quad (\text{A.1.26})$$

and for the surface tension, as extrapolated from nuclear scattering experiments,

$$P_s = - \left(\frac{0.13}{4\pi} \right) \frac{m_\pi c^2}{(\hbar/m_\pi c)^3} \left(\frac{A}{N_p} \right)^{2/3} \frac{1}{\Delta^2}. \quad (\text{A.1.27})$$

We then obtain

$$\frac{|P_s|}{P_n} = 0.39 \cdot \Delta^3 \left(\frac{N_p}{A} \right) = 0.24 \cdot \frac{\rho_{\text{nucl}}}{\rho_{\text{surf}}}, \quad (\text{A.1.28})$$

where $\rho_{\text{nucl}} = 3m_n A / 4\pi R_c^3$. The relative importance of the nuclear pressure and nuclear tension is a very sensitive function of the density ρ_{surf} at the surface.

It is important to emphasize a major difference between nuclei and the massive nuclear density cores treated in this article: the gravitational binding energy in these massive nuclear density cores is instead $\varepsilon_{\text{gr}} \approx GM_\odot m_n / R_c \approx 0.1m_n c^2 \approx 93.8 \text{ MeV}$. In other words it is much bigger than the nuclear energy in ordinary nuclei $\varepsilon_{\text{nuclear}} \approx \hbar^2 / m_n r_0^2 \approx 28.8 \text{ MeV}$ (21).

Possible applications to neutron stars

All the above considerations have been made for an isolated massive core at constant density whose boundary has been sharply defined by a step function. No external forces are exerted. Consequently due to the global charge neutrality, the Fermi energy of the electrons has been assumed to be equal to zero. In the earliest description of neutron stars in the work of Oppenheimer and Volkoff (5) only a gas of neutrons was considered and the equation of equilibrium was written in the Schwarzschild metric. They considered the model of a degenerate gas of neutrons to hold from the center to the border, with the density monotonically decreasing away from the center.

In the intervening years a more realistic model has been presented challenging the original considerations of Tolman, Oppenheimer and Volkoff, (4; 5). Their TOV equations considered the existence of neutrons all the way to the surface of the star. The presence of neutrons, protons and electrons in beta equilibrium were instead introduced in (6). Still more important the neutron stars have been shown to be composed of two sharply different components: the core at nuclear and/or supra-nuclear density consisting

of neutrons, protons and electrons and a crust of white dwarf like material, namely of degenerate electrons in a nuclei lattice (6; 26). The pressure and the density of the core are mainly due to the baryons while the pressure of the crust is mainly due to the electrons with the density due to the nuclei and possibly with some free neutrons due to neutron drip (see e.g. (26)). Further works describing the nuclear interactions were later introduced (see e.g. (32)). Clearly all these considerations departed profoundly from the TOV approximation. The matching between the core component and the crust is the major unsolved problem. To this issue this article introduces some preliminary results in a simplified model which has the advantage to present explicit analytic solutions.

In all the above treatments in order to close the system of equations the condition of local charge neutrality $n_e = n_p$ was adopted without a proof. The considerations of massive neutron density cores presented in this article offer an alternative to the local charge neutrality condition $n_e = n_p$. In a specific example which can be solved also analytically such condition is substituted by the Thomas-Fermi relativistic equations implying $n_e \neq n_p$ and an overall charge neutral system ($N_e = N_p$). The condition of global charge neutrality as opposed to the local one, leads to the existence of overcritical electric fields at the core surface which may be relevant in the description of neutron stars.

Two important generalizations of the results here presented have been done :

1) we have studied the solution for massive neutron density cores with positive values of their Fermi energy of electrons, as contrasted to the one here studied with zero Fermi energy of electrons. This is a necessary step in order to take into due account the compressional effects of the neutron star crusts on the core. As we show in the accompanying paper (33), such a treatment leads, as a by-product, to the generalization of the classic work of Feynman, Metropolis and Teller considering compressed atoms in a Thomas-Fermi model (15).

2) the condition of the proton constant density adopted in this article has been relaxed by considering consistently also the gravitational self-interaction of the core. To this scope the Thomas-Fermi equations here considered has been formulated within general relativity: a covariant formulation with the metric and the electrodynamic potential fulfilling the system of the Einstein-Maxwell equations (34). The results presented in this article have been confirmed by this more general treatment.

Conclusions

We have first generalized the treatment of heavy nuclei by enforcing the condition of beta equilibrium in the relativistic Thomas-Fermi equation, avoiding the imposition of $N_p \simeq A/2$ between N_p and A traditionally assumed in the literature. In doing so we have obtained (see Fig. A.3) an $A - N_p$ relation which extends the ones adopted in the literature. Using the existence of scaling laws for the system of equations considered, we extend the results

obtained for heavy nuclei to the case of massive nuclear density cores. The novelty in this article is to show how both the considerations of heavy nuclei and of systems of macroscopic astrophysical dimensions can take advantage from a rigorous and analytic solution of the Thomas-Fermi relativistic equations and the beta equilibrium conditions. This task is achieved by obtaining explicit analytic solutions fulfilling precise boundary conditions and using the scaling laws introduced in this article.

Indeed the Thomas-Fermi treatment has been considered also in the context of quark stars with a charge and a density distribution analogous to the one of massive nuclear density cores we consider in this article (27; 28; 29; 30; 31). There are however a variety of differences both in the boundary conditions adopted and in the solution obtained (see for details (33)). In the present article we show that we can indeed obtain overcritical electric fields at nuclear density on macroscopic scales of $R_c \approx 10$ Km and $M \approx 1M_\odot$ for existing field theories involving only neutrons, protons and electrons and their fundamental interactions and no quarks present. We obtain explicit analytic solutions of the relativistic Thomas-Fermi equations, self-consistently solved with the condition of beta equilibrium. Such analytic solutions allow to give explicit expressions for the Coulomb energy, surface energy and Newtonian gravitational energy of such massive nuclear density cores.

These cores are stable against fission (see Eq. (A.1.22)), the surface tension determines the sharpness of their boundary (see Eq. (A.1.28)) and the gravitational interaction, at Newtonian level, balances the Coulomb repulsion for mass numbers larger than the critical value given by Eq. (A.1.25).

As a by-product of these results, we also conclude that the arguments often quoted concerning limits on the electric fields of an astrophysical system based on a free test particle (the dust approximation) considering only the gravitational and electric interactions

$$(E_{\max})_{\text{dust}} \approx \frac{m_e m_n c^3}{e \hbar} \frac{m_n}{m_{\text{Planck}}}, \quad (\text{A.1.29})$$

$$\left(\frac{Q}{\sqrt{GM}} \right)_{\text{dust}} \approx \sqrt{G} \frac{m_e}{e} = \frac{1}{\sqrt{\alpha}} \frac{m_e}{m_{\text{Planck}}}, \quad (\text{A.1.30})$$

appear to be inapplicable for $A \sim (m_{\text{Planck}}/m_n)^3$. Here nuclear densities are reached and the roles of *all* fundamental interactions, including weak and strong interactions in addition to the electromagnetic and gravitational ones and including as well quantum statistics, have to be taken into account through the relativistic Thomas-Fermi model. Eqs. (A.1.29) and (A.1.30) are

replaced by Eqs. (A.1.17) and (A.1.21),

$$E_{\max} \approx \frac{0.95\sqrt{\alpha} m_{\text{Planck}}}{\Delta^2 m_e} \left(\frac{m_\pi}{m_n}\right)^2 (E_{\max})_{\text{dust}}, \quad (\text{A.1.31})$$

$$\frac{Q}{\sqrt{GM}} \approx \frac{N_p}{A} \sqrt{\alpha} \frac{m_{\text{Planck}}}{m_e} \left(\frac{Q}{\sqrt{GM}}\right)_{\text{dust}}. \quad (\text{A.1.32})$$

Details are presented in (34).

A.2. On the relativistic Thomas-Fermi treatment of compressed atoms and compressed massive nuclear density cores

Introduction

In a classic article Baym, Bethe and Pethick (26) presented the problem of matching, in a neutron star, a liquid core, composed of N_n neutrons, N_p protons and N_e electrons, to the crust. After discussing the different aspects of the problem they concluded: *The details of this picture requires further elaboration; this is a situation for which the Thomas-Fermi method is useful.* This problem can indeed be approached with merit by studying the simplified but rigorous concept of a massive nuclear density core which fulfills the relativistic Thomas-Fermi equation as discussed in (13; 113).

In (13; 113) we have first generalized the treatment of heavy nuclei by enforcing the condition of beta equilibrium in the relativistic Thomas-Fermi equation. Using then the existence of scaling laws we have extended the results from heavy nuclei to the case of massive nuclear density cores. In both these treatments we had assumed the Fermi energy of the electrons $E_e^F = 0$. The aim of this article is to proceed with this dual approach and generalize both these treatments to the case of positive Fermi energy of the electrons. We consider compressed atoms and compressed massive neutron density cores both confined by a Wigner-Seitz cell of radius R_{WS} . We first recall the non-relativistic treatment of the compressed atom by Feynman, Metropolis and Teller and, following the treatment of (13; 113), we generalize that treatment to the relativistic regime by integrating the relativistic Thomas-Fermi equation, imposing also the condition of beta equilibrium. Then we compare and contrast the relativistic and the non-relativistic analysis. While in the non-relativistic treatment the Fermi energy by compression can reach infinite values as $R_{WS} \rightarrow 0$, in the relativistic treatment it reaches a perfectly finite value and grows much less than in the corresponding non-relativistic treatment.

We also compare the relativistic generalization of the Feynman, Metropolis and Teller approach with some approximate treatments in the literature.

Using the same scaling laws adopted in (13; 113) we turn to the case of

massive nuclear density cores with mass numbers $A \approx (m_{\text{Planck}}/m_n)^3 \sim 10^{57}$ where m_n is the neutron mass and $m_{\text{Planck}} = (\hbar c/G)^{1/2}$ is the Planck mass. We present the analytic solutions for the ultra-relativistic limit of the relativistic Thomas-Fermi equation. We find explicit analytic expressions for the electrostatic field and the Coulomb potential energy and we obtain:

- 1) an entire range of possible Fermi energy for the electrons between zero and a maximum value $(E_e^F)_{\text{max}}$, reached when $R_{\text{WS}} = R_c$, which can be expressed analytically.
- 2) the explicit analytic expression of the ratio between the proton number N_p and the mass number A when $R_{\text{WS}} = R_c$.

We turn then to the study of the energetic of the massive nuclear density cores for selected values of the electron Fermi energy. We show that the solution with $E_e^F = 0$ corresponds to the ground state of the system and presents the largest value of the electro-dynamical structure.

Inferences for neutron stars and confinements of ultra-relativistic plasma are outlined.

The Thomas-Fermi model for compressed atoms: the Feynman-Metropolis-Teller treatment

The Thomas-Fermi model assumes that the electrons of an atom constitute a fully degenerate gas of fermions confined in a spherical region by the Coulomb potential of a point-like nucleus of charge $+eN_p$ (114; 115). Feynman, Metropolis and Teller have shown that this model can be used to derive the equation of state of matter at high pressures by considering a Thomas-Fermi model confined in a Wigner-Seitz cell of radius R_{WS} (15).

We recall that the condition of equilibrium of the electrons in an atom, in the non-relativistic limit, is expressed by

$$\frac{(P_e^F)^2}{2m_e} - eV = E_e^F, \quad (\text{A.2.1})$$

where m_e is the electron mass, V is the electrostatic potential and E_e^F is their Fermi energy.

The electrostatic potential fulfills, for $r > 0$, the Poisson equation

$$\nabla^2 V = 4\pi e n_e, \quad (\text{A.2.2})$$

where the electron number density n_e is related to the Fermi momentum P_e^F by

$$n_e = \frac{(P_e^F)^3}{3\pi^2 \hbar^3}. \quad (\text{A.2.3})$$

For neutral atoms and ions n_e vanishes at the boundary so the electron Fermi energy is, respectively, zero or negative. In the case of compressed atoms n_e

does not vanish at the boundary while the Coulomb potential energy eV is zero. Consequently E_e^F is positive.

Assuming

$$eV(r) + E_e^F = e^2 N_p \frac{\phi(r)}{r}, \quad (\text{A.2.4})$$

we obtain the following expression for the electron number density

$$n_e(\eta) = \frac{1}{3\pi^2 \hbar^3} \frac{N_p}{4\pi b^3} \left(\frac{\phi(\eta)}{\eta} \right)^{3/2}, \quad (\text{A.2.5})$$

where the new independent variable η is related to the radial coordinate r by $r = b\eta$, where

$$b = (3\pi)^{2/3} \frac{\hbar^2}{m_e e^2} \frac{1}{2^{7/3}} \frac{1}{N_p^{1/3}}. \quad (\text{A.2.6})$$

Eq. (A.2.2) can be written in the form

$$\frac{d^2 \phi(\eta)}{d\eta^2} = \frac{\phi(\eta)^{3/2}}{\eta^{1/2}}, \quad (\text{A.2.7})$$

which is the classic Thomas-Fermi equation (17). A first boundary condition for this equation follows from the point-like structure of the nucleus

$$\phi(0) = 1. \quad (\text{A.2.8})$$

A second boundary condition comes from the conservation of the number of electrons $N_e = \int_0^{R_{WS}} 4\pi n_e(r) r^2 dr$

$$1 - \frac{N_e}{N_p} = \phi(\eta_0) - \eta_0 \phi'(\eta_0), \quad (\text{A.2.9})$$

where $\eta_0 = R_{WS}/b$ defines the radius R_{WS} of the Wigner-Seitz cell. In the case of compressed atoms $N_e = N_p$ so the Coulomb potential energy eV vanishes at the boundary R_{WS} . As a result, using Eqs. (A.2.1) and (A.2.3), the Fermi energy of electrons is given by

$$E_e^F = \frac{N_p e^2}{b} \frac{\phi(\eta_0)}{\eta_0}. \quad (\text{A.2.10})$$

Therefore in the classic treatment η_0 can approach zero and consequently the range of the possible values of the Fermi energy extends from zero to infinity.

The results are summarized in Figs. A.4 and A.5.

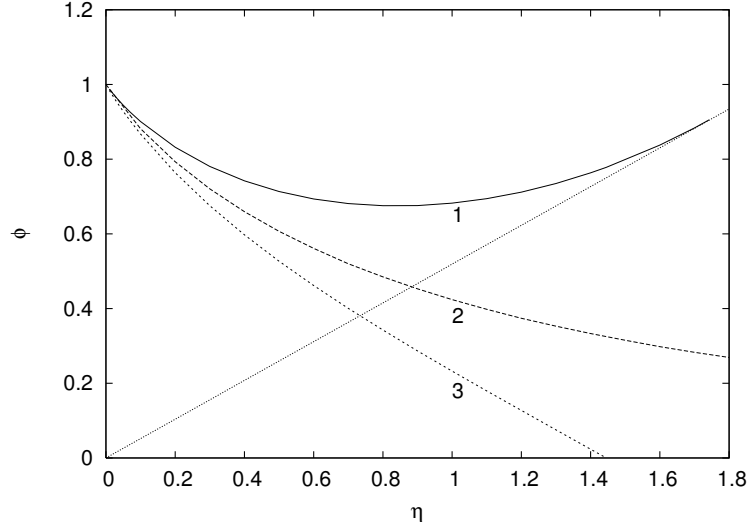


Figure A.4.: Physically relevant solutions of the Thomas-Fermi Equation (A.2.7) with the boundary conditions (A.2.8) and (A.2.9). The curve 1 refers to a neutral compressed atom. The curve 2 refers to a neutral free atom. The curve 3 refers to a positive ion. The dotted straight line is the tangent to the curve 1 at the point $(\eta_0, \phi(\eta_0))$ corresponding to overall charge neutrality (see Eq. (A.2.9)).

The relativistic generalization of the Feynman-Metropolis-Teller treatment

The main difference in the relativistic generalization of the Thomas-Fermi equation is that the point-like approximation of the nucleus must be abandoned (22; 23) since the relativistic generalization of the equilibrium condition (A.2.1)

$$E_e^F = \sqrt{(P_e^F c)^2 + m_e^2 c^4} - m_e c^2 - eV(r) > 0, \quad (\text{A.2.11})$$

would lead to a non-integrable expression for the electron density near the origin.

Following the previous treatments (see e.g. (113)), we assume a constant distribution of protons confined in a radius R_c defined by

$$R_c = \Delta \frac{\hbar}{m_\pi c} N_p^{1/3}, \quad (\text{A.2.12})$$

where m_π is the pion mass and Δ is a parameter such that $\Delta \approx 1$ ($\Delta < 1$) corresponds to nuclear (supranuclear) densities when applied to ordinary nuclei.

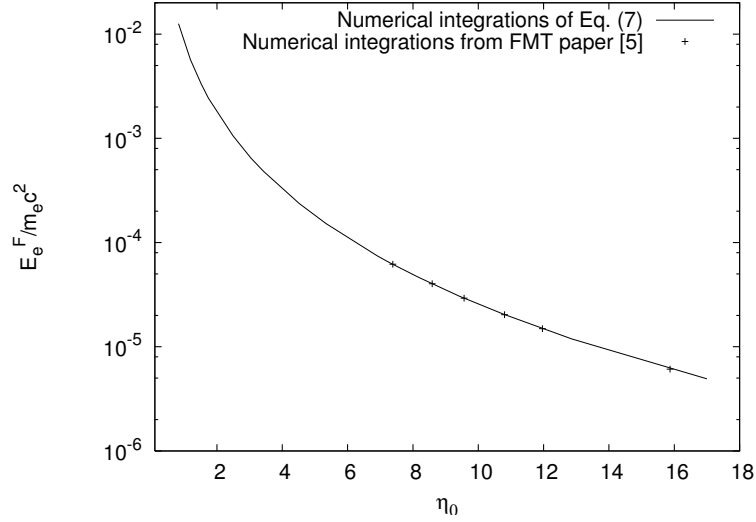


Figure A.5.: The electron Fermi energies for iron, in units of the electron mass, are plotted as a function of the dimensionless compression parameter η_0 . Points refer to the numerical integrations of the Thomas-Fermi equation (A.2.7) performed originally by Feynman, Metropolis and Teller in (15).

Consequently, the proton density can be written as

$$n_p(r) = \frac{N_p}{\frac{4}{3}\pi R_c^3} \theta(r - R_c) = \frac{3}{4\pi} \frac{m_\pi^3 c^3}{\hbar^3} \frac{1}{\Delta^3} \theta(r - R_c), \quad (\text{A.2.13})$$

and the electron density is given by

$$n_e(r) = \frac{(P_e^F)^3}{3\pi^2 \hbar^3} = \frac{1}{3\pi^2 \hbar^3 c^3} \left[e^2 \hat{V}^2(r) + 2m_e c^2 e \hat{V}(r) \right]^{3/2}, \quad (\text{A.2.14})$$

where $e\hat{V} = eV + E_e^F$.

The overall Coulomb potential satisfies the Poisson equation

$$\nabla^2 V(r) = -4\pi e [n_p(r) - n_e(r)], \quad (\text{A.2.15})$$

with the boundary conditions $V'(R_{WS}) = 0$ and $V(R_{WS}) = 0$ due to global charge neutrality.

By introducing the dimensionless quantities $x = r/\lambda_\pi$, $x_c = R_c/\lambda_\pi$ and $\chi/r = e\hat{V}(r)/(c\hbar)$ with $\lambda_\pi = \hbar/(m_\pi c)$, and replacing the particle densities (A.2.13) and (A.2.14) into the Poisson equation (A.2.15) we obtain the rela-

tivistic Thomas-Fermi equation

$$\frac{1}{3x} \frac{d^2\chi(x)}{dx^2} = -\frac{\alpha}{\Delta^3} \theta(x_c - x) + \frac{4\alpha}{9\pi} \left[\frac{\chi^2(x)}{x^2} + 2 \frac{m_e}{m_\pi} \frac{\chi}{x} \right]^{3/2}, \quad (\text{A.2.16})$$

where $\chi(0) = 0$, $\chi(x_{WS}) \geq 0$, $x_{WS} = R_{WS}/\lambda_\pi$ and, as usual $\alpha = e^2/\hbar c$. The neutron density $n_n(r)$, related to the neutron Fermi momentum $P_n^F = (3\pi^2\hbar^3 n_n)^{1/3}$, is determined, as in the previous case (113), by imposing the condition of beta equilibrium

$$\begin{aligned} E_n^F &= \sqrt{(P_n^F c)^2 + m_n^2 c^4} - m_n c^2 \\ &= \sqrt{(P_p^F c)^2 + m_p^2 c^4} - m_p c^2 + eV(r) + E_e^F, \end{aligned} \quad (\text{A.2.17})$$

which in turn is related to the proton density n_p and the electron density by Eqs. (A.2.14), (A.2.15).

Electron Fermi energy in the relativistic and the non-relativistic Feynman-Metropolis-Teller analysis

In order to compare and contrast the Fermi energy of a compressed atom in the non-relativistic and the relativistic limit we first express the non-relativistic equations in terms of the dimensionless variables used for the relativistic treatment. We then have

$$x = \frac{r}{\lambda_\pi}, \quad \frac{\chi}{r} = \frac{e\hat{V}}{c\hbar}, \quad (\text{A.2.18})$$

and the non-relativistic limit of Eq. (A.2.16) becomes

$$\frac{d^2\chi(x)}{dx^2} = \frac{2^{7/2}}{3\pi} \alpha \left(\frac{m_e}{m_\pi} \right)^{3/2} \frac{\chi^{3/2}}{x^{1/2}}, \quad (\text{A.2.19})$$

with the boundary conditions

$$\chi(0) = \alpha N_p, \quad x_{WS} \chi(x_{WS})' = \chi(x_{WS}), \quad (\text{A.2.20})$$

and dimensionless variable $x_{WS} = R_{WS}/\lambda_\pi$.

In these new variables the electron Fermi energy is given by

$$E_e^F = \frac{\chi(x_{WS})}{x_{WS}} m_\pi c^2. \quad (\text{A.2.21})$$

The two treatment, the relativistic and the non-relativistic one can be now directly compared by using the same units (see Fig. A.6).

There are two major differences:

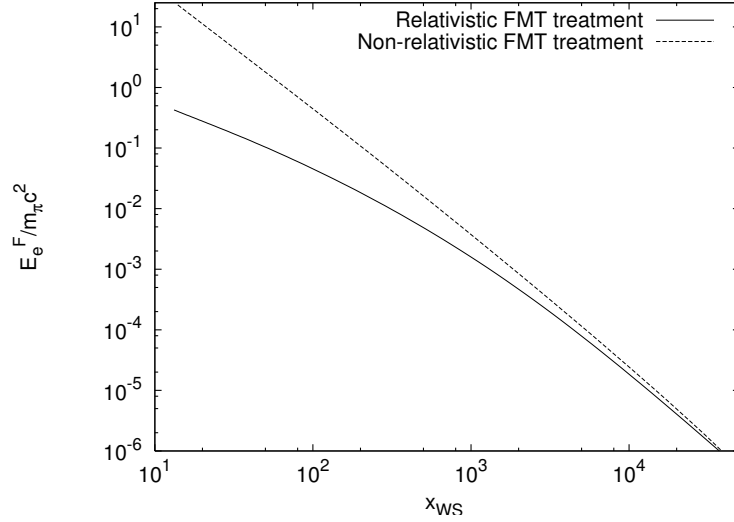


Figure A.6.: The electron Fermi energies E_e^F for iron in units of the pion rest mass, are plotted as a function of different compressions x_{WS} respectively in the non-relativistic and in the relativistic Feynman-Metropolis-Teller (FMT) treatment.

- 1) By compression the Fermi energy in the non-relativistic treatment increases much more than the one obtained in the relativistic treatment.
- 2) While in the non-relativistic treatment, by compression the Fermi energy can reach infinite values as $R_{WS} \rightarrow 0$, in the relativistic treatment it reaches a perfectly finite value given by

$$E_e^F \simeq \left[-\frac{m_e}{m_\pi} + \sqrt{\left(\frac{m_e}{m_\pi}\right)^2 + \left(\frac{3\pi^2}{2}\right)^{2/3} \left(\frac{N_p}{A}\right)^{2/3}} \right] m_\pi c^2, \quad (\text{A.2.22})$$

when R_{WS} coincides with the nuclear radius R_c .

Comparison and contrast with approximate treatments There exist in the literature a large variety of semi-qualitative approximations adopted in order to describe the electron component of a compressed atom (see e.g. (116)). We can see how the compression factor determined by the size of the Wigner-Seitz cell, affects all the current analysis of compressed atoms in the literature and deserves the necessary attention. To do this we compare the relativistic treatment described in Sec. A.2 with the one considered in (116) where, for a given nuclear charge $+eN_p$, the Wigner-Seitz cell radius R_{WS} is defined by

$$N_p = \frac{4\pi}{3} R_{WS}^3 n_e, \quad (\text{A.2.23})$$

where $n_e = (P_e^F)^3 / (3\pi^2 \hbar^3)$. The Eq. (A.2.23) is equivalent to assume a uniform distribution of electrons. The corresponding electron Fermi energy can be written as

$$E_e^F \simeq \left[-\frac{m_e}{m_\pi} + \sqrt{\left(\frac{m_e}{m_\pi}\right)^2 + \left(\frac{9\pi}{4}\right)^{2/3} \frac{N_p^{2/3}}{x_{WS}^2}} \right] m_\pi c^2. \quad (\text{A.2.24})$$

Results are given in Fig. A.7. Any analysis of nuclear composition, determined in function of the electron Fermi energy E_e^F , will be definitely very sensitive to the approximation adopted. Any approximation which does not follow the results obtained from the relativistic Thomas-Fermi equation presented above, leads necessarily to incorrect results. The difference represented in Fig. A.7 has been obtained for a specific model of the nucleus. We expect that in the case of a different nuclear model the dependence of the Fermi energy from compression may be different. For any fixed nuclear model, however, the approximation given by Eq. (A.2.24) and the correct one obtained using the relativistic Thomas-Fermi equation, will remain.

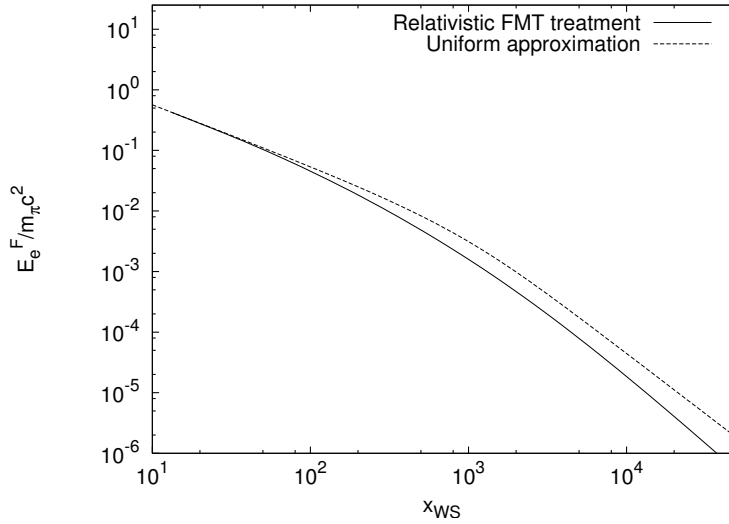


Figure A.7.: The electron Fermi energies E_e^F for iron in units of the pion rest mass, are plotted as a function of different compressions x_{WS} by using the relativistic Feynman-Metropolis-Teller (FMT) treatment and correspondingly the uniform approximation for the electron distribution inside the Wigner-Seitz cell.

Application to massive nuclear density cores

We turn now to massive nuclear density cores for $A \simeq (m_{\text{Planck}}/m_n)^3 \sim 10^{57}$. Following the treatment presented in Popov et al.,(113), we use the existence of scaling laws and proceed to the ultra-relativistic limit of Eqs. (A.2.13),

(A.2.14), (A.2.16), (A.2.17). For positive values of the Fermi energy E_e^F , we introduce the new function $\phi = 4^{1/3}(9\pi)^{-1/3}\chi\Delta/x$ and the new variable $\hat{x} = kx$ where $k = (12/\pi)^{1/6}\sqrt{\alpha}\Delta^{-1}$, as well as the variable $\xi = \hat{x} - \hat{x}_c$ in order to describe better the region around the core radius.

Eq. (A.2.16) becomes

$$\frac{d^2\hat{\phi}(\xi)}{d\xi^2} = -\theta(-\xi) + \hat{\phi}(\xi)^3, \quad (\text{A.2.25})$$

where $\hat{\phi}(\xi) = \phi(\xi + \hat{x}_c)$ and the curvature term $2\hat{\phi}'(\xi)/(\xi + \hat{x}_c)$ has been neglected.

The Coulomb potential energy is given by

$$eV(\xi) = \left(\frac{9\pi}{4}\right)^{1/3} \frac{1}{\Delta} m_\pi c^2 \hat{\phi}(\xi) - E_e^F, \quad (\text{A.2.26})$$

corresponding to the electric field

$$E(\xi) = -\left(\frac{3^5\pi}{4}\right)^{1/6} \frac{\sqrt{\alpha} m_\pi^2 c^3}{\Delta^2 e\hbar} \hat{\phi}'(\xi), \quad (\text{A.2.27})$$

and the electron number-density

$$n_e(r) = \frac{1}{3\pi^2\hbar^3 c^3} \left(\frac{9\pi}{4}\right) \frac{1}{\Delta^3} (m_\pi c^2)^3 \hat{\phi}^3(\xi). \quad (\text{A.2.28})$$

In the core center we must have $n_e = n_p$. From Eqs. (A.2.13, A.2.28) we then have that, for $\xi = -\hat{x}_c$, $\hat{\phi}(-\hat{x}_c) = 1$. In order to consider a compressed massive nuclear density core, we then introduce a Wigner-Seitz cell determining the outer boundary of the electron distribution which, in the new radial coordinate ξ is characterized by ξ^{WS} . In view of the global charge neutrality of the system the electric field goes to zero at $\xi = \xi^{WS}$. This implies, from Eq. (A.2.27), $\hat{\phi}'(\xi^{WS}) = 0$.

We now turn to the determination of the Fermi energy of the electrons in this compressed core. The function $\hat{\phi}$ and its first derivative $\hat{\phi}'$ must be continuous at the surface $\xi = 0$ of the massive nuclear density core.

This boundary-value problem can be solved analytically and indeed Eq. (A.2.25) has the first integral,

$$2[\hat{\phi}'(\xi)]^2 = \begin{cases} \hat{\phi}^4(\xi) - 4\hat{\phi}(\xi) + 3, & \xi < 0, \\ \hat{\phi}^4(\xi) - \phi^4(\xi^{WS}), & \xi > 0, \end{cases} \quad (\text{A.2.29})$$

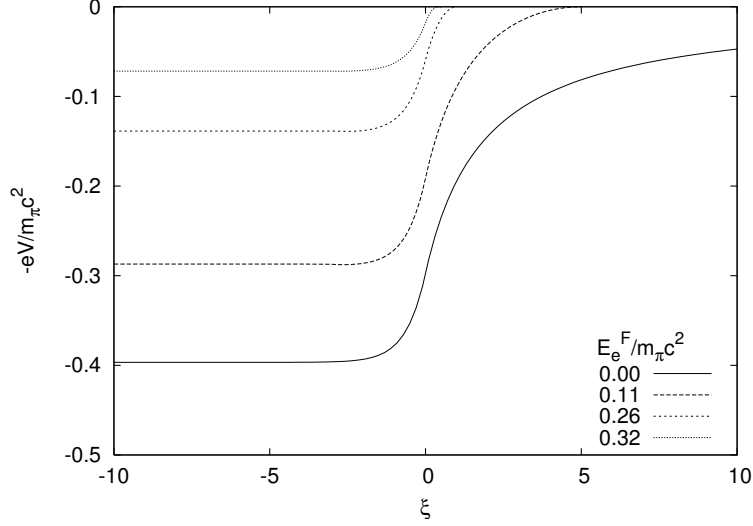


Figure A.8.: The electron Coulomb potential energies in units of the pion rest mass in a massive nuclear density core with $A \simeq^{57}$ and $R_c \approx 10^6$ cm, are plotted as a function of the dimensionless variable ξ , for different values of the electron Fermi energy also in units of the pion rest mass. The solid line corresponds to the case of null electron Fermi energy and presents the maximum binding energy. By increasing the value of the electron Fermi energy the electron Coulomb potential energy depth is reduced.

with boundary conditions at $\xi = 0$:

$$\begin{aligned}\hat{\phi}(0) &= \frac{\hat{\phi}^4(\xi^{WS}) + 3}{4}, \\ \hat{\phi}'(0) &= -\sqrt{\frac{\hat{\phi}^4(0) - \hat{\phi}^4(\xi^{WS})}{2}}.\end{aligned}\quad (\text{A.2.30})$$

Having fulfilled the continuity condition we integrate Eq. (A.2.29) obtaining for $\xi \leq 0$

$$\hat{\phi}(\xi) = 1 - 3 \left[1 + 2^{-1/2} \sinh(a - \sqrt{3}\xi) \right]^{-1}, \quad (\text{A.2.31})$$

where the integration constant a has the value

$$\sinh(a) = \sqrt{2} \left(\frac{11 + \hat{\phi}^4(\xi^{WS})}{1 - \hat{\phi}^4(\xi^{WS})} \right). \quad (\text{A.2.32})$$

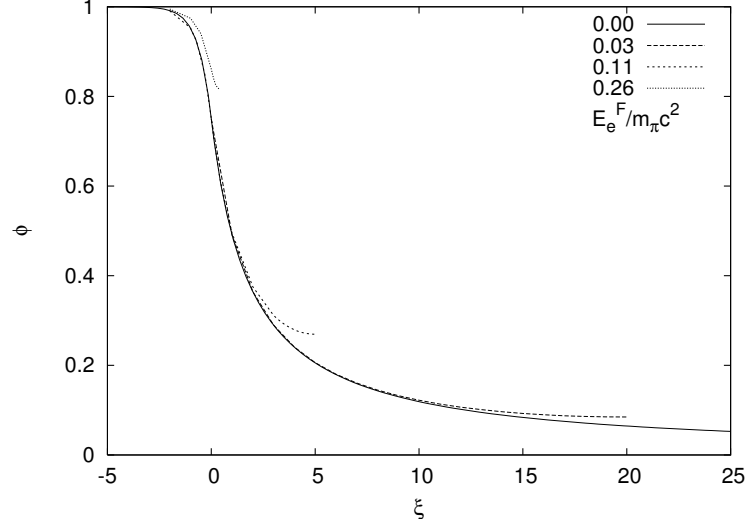


Figure A.9.: Solutions of the ultrarelativistic Thomas-Fermi equation (A.2.25) for different values of the Wigner-Seitz cell radius R_{WS} and correspondingly of the electron Fermi energy in units of the pion rest mass as in Fig. A.8, near the core surface. The solid line corresponds to the case of null electron Fermi energy.

In the interval $0 \leq \xi \leq \xi^{WS}$, the field $\hat{\phi}(\xi)$ is implicitly given by

$$F\left(\arccos\frac{\hat{\phi}(\xi^{WS})}{\hat{\phi}(\xi)}, \frac{1}{\sqrt{2}}\right) = \hat{\phi}(\xi^{WS})(\xi - \xi^{WS}), \quad (\text{A.2.33})$$

where $F(\varphi, k)$ is the elliptic function of the first kind, and $F(0, k) \equiv 0$. For $F(\varphi, k) = u$, the inverse function $\varphi = F^{-1}(u, k) = \text{am}(u, k)$ is the well known Jacobi amplitude. In terms of it, we can express the solution (A.2.33) for $\xi > 0$ as,

$$\hat{\phi}(\xi) = \hat{\phi}(\xi^{WS}) \left\{ \cos \left[\text{am} \left(\hat{\phi}(\xi^{WS})(\xi - \xi^{WS}), \frac{1}{\sqrt{2}} \right) \right] \right\}^{-1}. \quad (\text{A.2.34})$$

In the present case of $E_e^F > 0$ the ultra-relativistic approximation is indeed always valid up to $\xi = \xi^{WS}$ for high compression factors, i.e. for $R_{WS} \simeq R_c$. In the case $E_e^F = 0$, $\xi^{WS} \rightarrow \infty$, there is a breakdown of the ultra-relativistic approximation when $\xi \rightarrow \xi^{WS}$.

Details are given in Figs. A.8, A.9, A.10.

We can now estimate two crucial quantities of the solutions: the Coulomb potential at the center of the configuration and the electric field at the surface

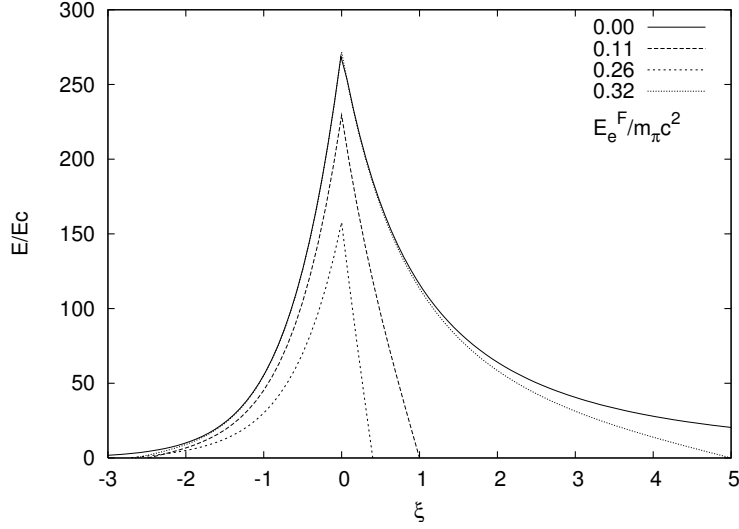


Figure A.10.: The electric field in units of the critical field E_c is plotted as a function of the coordinate ζ , for different values of the electron Fermi energy in units of the pion mass. The solid line corresponds to the case of null electron Fermi energy. To an increase of the value of the electron Fermi energy it is found a reduction of the peak of the electric field.

of the core

$$eV(0) \simeq \left(\frac{9\pi}{4}\right)^{1/3} \frac{1}{\Delta} m_\pi c^2 - E_e^F, \quad (\text{A.2.35})$$

$$E_{\max} \simeq 2.4 \frac{\sqrt{\alpha}}{\Delta^2} \left(\frac{m_\pi}{m_e}\right)^2 E_c |\hat{\phi}'(0)|, \quad (\text{A.2.36})$$

where $E_c = m_e^2 c^3 / (e\hbar)$ is the critical electric field for vacuum polarization. These functions depend on the value $\hat{\phi}(\zeta^{WS})$ via Eqs. (A.2.29)-(A.2.33). At the boundary $\zeta = \zeta^{WS}$, due to the global charge neutrality, both the electric field $E(\zeta^{WS})$ and the Coulomb potential $eV(\zeta^{WS})$ vanish. From Eq. (A.2.26), we determine the value of $\hat{\phi}(\zeta)$ at $\zeta = \zeta^{WS}$

$$\hat{\phi}(\zeta^{WS}) = \Delta \left(\frac{4}{9\pi}\right)^{1/3} \frac{E_e^F}{m_\pi c^2}, \quad (\text{A.2.37})$$

as a function of Fermi energies E_e^F . From the above Eq. (A.2.37), one can see

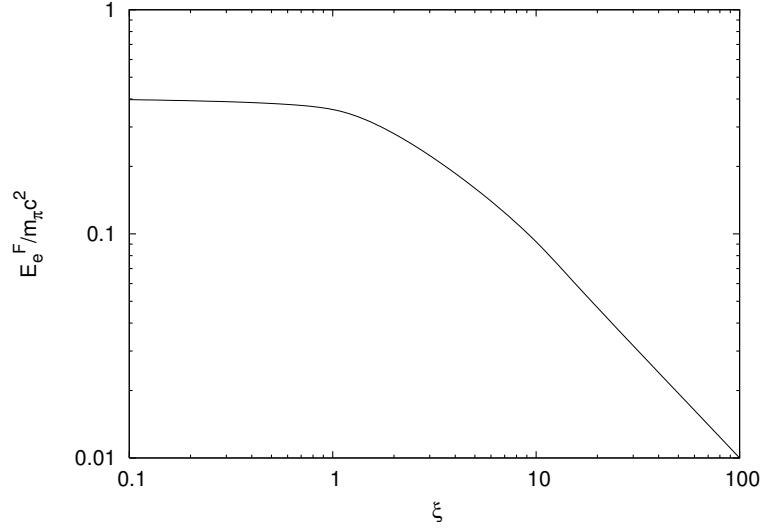


Figure A.11.: The Fermi energy of electrons in units of the pion rest mass is plotted as a function of the compression parameter ξ^{WS} in the ultra-relativistic approximation. In the limit $\xi^{WS} \rightarrow 0$ the electron Fermi energy approaches asymptotically the value $(E_e^F)_{max}$ given by Eq. (A.2.43).

that there exists a solution, characterized by the value of Fermi energy E_e^F ,

$$\frac{(E_e^F)_{max}}{m_\pi c^2} = \frac{1}{\Delta} \left(\frac{9\pi}{4} \right)^{1/3}, \quad (\text{A.2.38})$$

such that $\hat{\phi}(\xi^{WS}) = 1$. From Eq. (A.2.33) and $\xi = 0$, we also have

$$\xi^{WS}(\hat{\phi}(\xi^{WS})) = \left\{ \frac{1}{\hat{\phi}(0)} F \left[\arccos \left(4 - \frac{3}{\hat{\phi}(0)} \right), \frac{1}{\sqrt{2}} \right] \right\}. \quad (\text{A.2.39})$$

For $\hat{\phi}(\xi^{WS}) = 1$, from Eq. (A.2.30) follows $\hat{\phi}(0) = 1$ hence Eq. (A.2.39) becomes

$$\xi^{WS}(\hat{\phi}(0)) = F \left[0, \frac{1}{\sqrt{2}} \right]. \quad (\text{A.2.40})$$

It is well known that the inverse Jacobi amplitude $F[0, 1/\sqrt{2}]$ is zero, then

$$\xi^{WS}(\hat{\phi}(\xi^{WS}) = \hat{\phi}(0) = 1) = 0. \quad (\text{A.2.41})$$

Indeed from $\hat{\phi}(\xi^{WS}) = 1$ follows $\hat{\phi}(0) = 1$ and $\xi^{WS} = 0$. When $\xi^{WS} = 0$ from Eq. (A.2.30) follows $\hat{\phi}'(0) = 0$ and, using Eq. (A.2.36), $E_{max} = 0$. In other words for the value of E_e^F fulfilling Eq. (A.2.37) no electric field exists

on the boundary of the core and from Eq. (A.2.28) and Eqs. (A.2.40, A.2.13) it follows that indeed this is the solution fulfilling both global, $N_e = N_p$ as well local charge neutrality $n_e = n_p$. In this special case, starting from Eq. (A.2.17) and $A = N_p + N_n$, we obtain

$$(E_e^F)_{max}^{3/2} = \frac{\frac{9\pi}{4}(\hbar c)^3 \frac{A}{R_c^3} - (E_e^F)_{max}^3}{2^{3/2} \left[\left(\frac{9\pi}{4}(\hbar c)^3 \frac{A}{R_c^3} - (E_e^F)_{max}^3 \right)^{2/3} + m_n^2 c^4 \right]^{3/4}}. \quad (\text{A.2.42})$$

In the ultra-relativistic approximation $(E_e^F)_{max}^3 / \frac{9\pi}{4}(\hbar c)^3 \frac{A}{R_c^3} \ll 1$ so Eq. (A.2.42) can be approximated to

$$(E_e^F)_{max} = 2^{1/3} \frac{m_n}{m_\pi} \gamma \left[-1 + \sqrt{1 + \frac{\beta}{2\gamma^3}} \right]^{2/3} m_\pi c^2, \quad (\text{A.2.43})$$

where

$$\beta = \frac{9\pi}{4} \left(\frac{\hbar}{m_n c} \right)^3 \frac{A}{R_c^3}, \quad \gamma = \sqrt{1 + \beta^{2/3}}. \quad (\text{A.2.44})$$

The corresponding limiting value to the N_p/A ratio is obtained as follows

$$\frac{N_p}{A} = \frac{2\gamma^3}{\beta} \left[-1 + \sqrt{1 + \frac{\beta}{2\gamma^3}} \right]^2. \quad (\text{A.2.45})$$

Inserting Eqs. (A.2.43), (A.2.44) in Eq. (A.2.45) one obtains the ultra-relativistic limit of Eq. (A.2.22), since the electron Fermi energy, in view of the scaling laws introduced in (113), is independent of the value of A and depends only on the density of the core.

In Fig. A.11 we plot the Fermi energy of electrons, in units of the pion rest mass, as a function of the dimensionless parameter ζ^{WS} and, as $\zeta^{WS} \rightarrow 0$, the limiting value given by Eq. (A.2.43) is clearly displayed.

In ref. (29), in order to study the electro-dynamical properties of strange stars, the ultra-relativistic Thomas-Fermi equation was numerically solved in the case of bare strange stars as well as in the case of strange stars with a crust (see e.g. curves (a) and (b) in Fig. 6 of ref. (29)). In Fig. 6 of (29) was plotted what they called the Coulomb potential energy, which we will denote as V_{Alcock} . The potential V_{Alcock} was plotted for different values of the electron Fermi momentum at the edge of the crust. Actually, such potential V_{Alcock} is not the Coulomb potential eV but it coincides with our function $e\hat{V} = eV + E_e^F$. Namely, the potential V_{Alcock} corresponds to the Coulomb potential shifted by the the Fermi energy of the electrons. We then have from

Eq. (A.2.26)

$$e\hat{V}(\xi) = \left(\frac{9\pi}{4}\right)^{1/3} \frac{1}{\Delta} m_\pi c^2 \hat{\phi}(\xi) = V_{\text{Alcock}}. \quad (\text{A.2.46})$$

This explains why in (29), for different values of the Fermi momentum at the crust the depth of the potential V_{Alcock} remains unchanged. Instead, the correct behaviour of the Coulomb potential is quite different and, indeed, its depth decreases with increasing of compression as can be seen in Fig. A.8.

Energetics of compressed massive nuclear density cores

We turn now to the energetics of these family of compressed nuclear density cores each characterized by a different Fermi energy of the electrons. The kinematic energy-spectra of complete degenerate electrons, protons and neutrons are

$$\epsilon^i(p) = \sqrt{(pc)^2 + m_i^2 c^4}, \quad p \leq P_i^F, \quad i = e, p, n. \quad (\text{A.2.47})$$

So the total energy of the system is given by

$$\mathcal{E}_{\text{tot}} = \mathcal{E}_B + \mathcal{E}_e + \mathcal{E}_{\text{em}}, \quad \mathcal{E}_B = \mathcal{E}_p + \mathcal{E}_n, \quad (\text{A.2.48})$$

$$\mathcal{E}_i = 2 \int_i \frac{d^3 r d^3 p}{(2\pi\hbar)^3} \epsilon^i(p), \quad i = e, p, n, \quad \mathcal{E}_{\text{em}} = \int \frac{E^2}{8\pi} d^3 r. \quad (\text{A.2.49})$$

Using the analytic solution (A.2.34) we calculate the energy difference between two systems, *I* and *II*,

$$\Delta\mathcal{E}_{\text{tot}} = \mathcal{E}_{\text{tot}}(E_e^F(\text{II})) - \mathcal{E}_{\text{tot}}(E_e^F(\text{I})), \quad (\text{A.2.50})$$

with $E_e^F(\text{II}) > E_e^F(\text{I}) \geq 0$, at fixed A and R_c .

We first consider the infinitesimal variation of the total energy $\delta\mathcal{E}_{\text{tot}}$ with respect to the infinitesimal variation of the electron Fermi energy δE_e^F

$$\delta\mathcal{E}_{\text{tot}} = \left[\frac{\partial\mathcal{E}_{\text{tot}}}{\partial N_p} \right]_{VWS} \left[\frac{\partial N_p}{\partial E_e^F} \right] \delta E_e^F + \left[\frac{\partial\mathcal{E}_{\text{tot}}}{\partial VWS} \right]_{N_p} \left[\frac{\partial VWS}{\partial E_e^F} \right] \delta E_e^F. \quad (\text{A.2.51})$$

For the first term of this relation we have

$$\left[\frac{\partial\mathcal{E}_{\text{tot}}}{\partial N_p} \right]_{VWS} = \left[\frac{\partial\mathcal{E}_p}{\partial N_p} + \frac{\partial\mathcal{E}_n}{\partial N_p} + \frac{\partial\mathcal{E}_e}{\partial N_p} + \frac{\partial\mathcal{E}_{\text{em}}}{\partial N_p} \right]_{VWS} \simeq \left[E_p^F - E_n^F + E_e^F + \frac{\partial\mathcal{E}_{\text{em}}}{\partial N_p} \right]_{VWS}, \quad (\text{A.2.52})$$

where the general definition of chemical potential $\partial\epsilon_i/\partial n_i = \partial\mathcal{E}_i/\partial N_i$ is used ($i = e, p, n$) neglecting the mass defect $m_n - m_p - m_e$. Further using the

condition of the beta-equilibrium (A.2.17) we have

$$\left[\frac{\partial \mathcal{E}_{\text{tot}}}{\partial N_p} \right]_{V^{WS}} = \left[\frac{\partial \mathcal{E}_{\text{em}}}{\partial N_p} \right]_{V^{WS}}. \quad (\text{A.2.53})$$

For the second term of the Eq. (A.2.51) we have

$$\left[\frac{\partial \mathcal{E}_{\text{tot}}}{\partial V^{WS}} \right]_{N_p} = \left[\frac{\partial \mathcal{E}_p}{\partial V^{WS}} + \frac{\partial \mathcal{E}_n}{\partial V^{WS}} + \frac{\partial \mathcal{E}_e}{\partial V^{WS}} + \frac{\partial \mathcal{E}_{\text{em}}}{\partial V^{WS}} \right]_{N_p} = \left[\frac{\partial \mathcal{E}_e}{\partial V^{WS}} \right]_{N_p} + \left[\frac{\partial \mathcal{E}_{\text{em}}}{\partial V^{WS}} \right]_{N_p}, \quad (\text{A.2.54})$$

since in the process of increasing the electron Fermi energy namely, by decreasing the radius of the Wigner-Seitz cell, the system by definition maintains the same number of baryons A and the same core radius R_c .

Now $\delta \mathcal{E}_{\text{tot}}$ reads

$$\delta \mathcal{E}_{\text{tot}} = \left\{ \left[\frac{\partial \mathcal{E}_e}{\partial V^{WS}} \right]_{N_p} \frac{\partial V^{WS}}{\partial E_e^F} + \left[\frac{\partial \mathcal{E}_{\text{em}}}{\partial V^{WS}} \right]_{N_p} \frac{\partial V^{WS}}{\partial E_e^F} + \left[\frac{\partial \mathcal{E}_{\text{em}}}{\partial N_p} \right]_{V^{WS}} \frac{\partial N_p}{\partial E_e^F} \right\} \delta E_e^F, \quad (\text{A.2.55})$$

so only the electromagnetic energy and the electron energy give non-null contributions.

From this equation it follows that

$$\Delta \mathcal{E}_{\text{tot}} = \Delta \mathcal{E}_{\text{em}} + \Delta \mathcal{E}_e, \quad (\text{A.2.56})$$

where $\Delta \mathcal{E}_{\text{em}} = \mathcal{E}_{\text{em}}(E_e^F(II)) - \mathcal{E}_{\text{em}}(E_e^F(I))$ and $\Delta \mathcal{E}_e = \mathcal{E}_e(E_e^F(II)) - \mathcal{E}_e(E_e^F(I))$.

In the particular case in which $E_e^F(II) = (E_e^F)_{\text{max}}$ and $E_e^F(I) = 0$ we obtain

$$\Delta \mathcal{E}_{\text{tot}} \simeq 0.75 \frac{3^{5/3}}{2} \left(\frac{\pi}{4} \right)^{1/3} \frac{1}{\Delta \sqrt{\alpha}} \left(\frac{\pi}{12} \right)^{1/6} N_p^{2/3} m_\pi c^2, \quad (\text{A.2.57})$$

which is positive.

The total energy of a massive nuclear density core increases with its electron Fermi energy. The ground state is the one which corresponds to $E_e^F = 0$.

Inference for neutron stars and confinements of ultra-relativistic plasma

We consider the study of massive nuclear density cores to be necessary to clarify basic conceptual issues prior to a correct description of a neutron star. Neutron stars are composed of two sharply different components: the liquid core at nuclear and/or supra-nuclear density consisting of neutrons, protons and electrons and a crust of white dwarf-like material, namely of degenerate electrons in a lattice of nuclei (26; 6). The pressure and the density of the core are mainly due to the baryons while the pressure of the crust is mainly due to the electrons. The density of the crust is due to the nuclei and to the free neutrons due to neutron drip when this process occurs (see e.g. (26)). Consequently the boundary conditions of the electrons at the surface of the

neutron star core will have generally a positive value of the Fermi energy in order to take into account the compressional effects of the neutron star crust on the core (34). The case of zero electron Fermi energy corresponds to the limiting case of absence of the crust.

All the considerations presented in this article and in the preceding one (113) on the massive nuclear density cores, will apply to the analysis of the neutron star cores (34), as correctly predicted by Baym, Bethe and Pethick (26). Similarly the considerations presented in this article and in (113) generalizing the study of heavy nuclei and compressed atoms certainly applies to the high energy processes occurring in overcritical electric fields and giving rise electron-positron pairs in astrophysics, in plasma confinements and in laser physics (see e.g. (1)).

Conclusions

We have first considered the problem of an atom compressed described by a relativistic Thomas-Fermi equation. As in the previous works (22; 23; 13) the protons in the nuclei have been assumed to be at constant density, the electron distribution has been derived by the Thomas-Fermi relativistic equation and the neutron component has been derived by the beta equilibrium between neutrons, protons and electrons. The effect of compression has been described by constraining the system in a Wigner-Seitz cell. In doing so we have generalized the well known classic results obtained in non-relativistic treatment by Feynman, Metropolis and Teller. There in the non-relativistic treatment the Fermi energy of electrons can vary from zero to infinity, in view of the point-like structure of the nucleus. In the relativistic Thomas-Fermi equation, a perfectly finite maximum value of the Fermi energy is reached. These results, generalize the Feynman-Metropolis-Teller treatment and will be certainly verifiable in forthcoming experiments of confined high temperature plasma (117). The relativistic generalization introduce corrections with two major results:

- 1) The softening of the dependence of the electron Fermi energy on the compression factor.
- 2) The reaching of a limiting value of the electron Fermi energy.

It is also appropriate to remark that the correct treatment via a relativistic Thomas-Fermi equation, essential in determining the electron distribution in a compressed atom, is not equivalent to current treatments which have been often adopted in the literature using a variety of approximations (see e.g.(116)).

We have then extrapolate these results to the case of massive neutron density cores for $A \approx (m_{\text{Planck}}/m_n)^3 \sim 10^{57}$. In both systems of the compressed atoms and of the massive nuclear density cores a maximum value of the Fermi energy has been reached corresponding to the case of Wigner-Seitz cell radius R_{WS} coincident with the core radius R_c . The results generalize the considerations presented in the previous article corresponding to a massive nuclear density core with null Fermi energy of the electrons (113). An

entire family of configurations exist with values of the Fermi energy of the electrons ranging from zero to the maximum value $(E_e^F)_{max}$. The configuration with $E_e^F = (E_e^F)_{max}$ corresponds to the configuration with $N_p = N_e$ and $n_p = n_e$. For this limiting value of the Fermi energy the system fulfills both the global and the local charge neutrality and correspondingly no electro-dynamical structure is present in the core. The configuration with $E_e^F = 0$ has the maximum value of the electric field at the core surface, well above the critical value E_c (see Fig. A.10). All these cores with overcritical electric fields are stable against the vacuum polarization process due to the Pauli blocking by the degenerate electrons (1). We have compared and contrasted our treatment of Thomas-Fermi solutions to the corresponding one addressed in the framework of strange stars (29) pointing out in that treatment some inconsistency in the definition of the Coulomb potential. We have finally compared the energetics of configurations with selected values of the electron Fermi energy. The configuration with local charge neutrality condition corresponds to $(E_e^F)_{max}$ and has no electro-dynamical structure. On the contrary the configuration with $E_e^F = 0$ has the maximum electro-dynamical structure. The configuration with null Fermi energy of the electrons represent the ground state of the system.

Both problems considered, the one of a compressed atom and the one of compressed massive nuclear density cores, have been treated by the solution of the relativistic Thomas-Fermi equation and by enforcing the condition of beta equilibrium. They are theoretically well defined and, in our opinion, a necessary step in order to approach a more complex problem of a neutron star core and its interface with the neutron star crust. They lead anyway to a variety of new results encountered in ultra-relativistic conditions already treated in the literature.

A.3. Electrodynamics for Nuclear Matter in Bulk

It is well know that the Thomas-Fermi equation is the exact theory for atoms, molecules and solids as $Z \rightarrow \infty$ (53). We show in this letter that the relativistic Thomas-Fermi theory developed for the study of atoms for heavy nuclei with $Z \simeq 10^6$ (7), (9), (8), (10), (11),(42), (23), (54), (55), (56), (57) gives important basic new information on the study of nuclear matter in bulk in the limit of $N \simeq (m_{\text{Planck}}/m_n)^3$ nucleons of mass m_n and on its electrodynamic properties. The analysis of nuclear matter bulk in neutron stars composed of degenerate gas of neutrons, protons and electrons, has traditionally been approached by implementing microscopically the charge neutrality condition by requiring the electron density $n_e(x)$ to coincide with the proton density $n_p(x)$,

$$n_e(x) = n_p(x). \tag{A.3.1}$$

It is clear however that especially when conditions close to the gravitational collapse occur, there is an ultra-relativistic component of degenerate electrons whose confinement requires the existence of very strong electromagnetic fields, in order to guarantee the overall charge neutrality of the neutron star. Under these conditions equation (A.3.1) will be necessarily violated. We are going to show in this letter that they will develop electric fields close to the critical value E_c introduced by Sauter (58), Heisenberg and Euler (43), and by Schwinger (59)

$$E_c = \frac{m^2 c^3}{e \hbar}. \quad (\text{A.3.2})$$

Special attention for the existence of critical electric fields and the possible condition for electron-positron (e^+e^-) pair creation out of the vacuum in the case of heavy bare nuclei, with the atomic number $Z \geq 173$, has been given by Pomeranchuk and Smorodinsky (54), Gershtein and Zel'dovich (55), Popov (10), Popov and Zel'dovich (11), Greenberg and Greiner (9), Muller, Peitz, Rafelski and Greiner (8). They analyzed the specific pair creation process of an electron-positron pair around both a point-like and extended bare nucleus by direct integration of Dirac equation. These considerations have been extrapolated to much heavier nuclei $Z \gg 1600$, implying the creation of a large number of e^+e^- pairs, by using a statistical approach based on the relativistic Thomas-Fermi equation by Muller and Rafelski (56), Migdal, Voskresenskii and Popov (57). Using substantially the same statistical approach based on the relativistic Thomas-Fermi equation, Ferreira et al. (42), Ruffini and Stella (23) have analyzed the electron densities around an extended nucleus in a neutral atom all the way up to $Z \simeq 6000$. They have shown the effect of penetration of the electron orbitals well inside the nucleus, leading to a screening of the nuclei positive charge and to the concept of an "effective" nuclear charge distribution. All the above works assumed for the radius of the extended nucleus the semi-empirical formulae (44),

$$R_c \approx r_0 A^{1/3}, \quad r_0 = 1.2 \cdot 10^{-13} \text{cm}, \quad (\text{A.3.3})$$

where the mass number $A = N_n + N_p$, N_n and N_p are the neutron and proton numbers. The approximate relation between A and the atomic number $Z = N_p$,

$$Z \simeq \frac{A}{2}, \quad (\text{A.3.4})$$

was adopted in Refs. (56; 57), or the empirical formulae

$$Z \simeq \left[\frac{2}{A} + \frac{3}{200} \frac{1}{A^{1/3}} \right]^{-1}, \quad (\text{A.3.5})$$

was adopted in Refs. (42; 23).

The aim of this letter is to outline an alternative approach of the description of nuclear matter in bulk: it generalizes, to the case of $N \simeq (m_{\text{Planck}}/m_n)^3$ nucleons, the above treatments, already developed and tested for the study of heavy nuclei. This more general approach differs in many aspects from the ones in the current literature and recovers, in the limiting case of A smaller than 10^6 , the above treatments. We shall look for a solution implementing the condition of overall charge neutrality of the star as given by

$$N_e = N_p, \quad (\text{A.3.6})$$

which significantly modifies Eq. (A.3.1), since now $N_e(N_p)$ is the total number of electrons (protons) of the equilibrium configuration. Here we present only a simplified prototype of this approach. We outline the essential relative role of the four fundamental interactions present in the neutron star physics: the gravitational, weak, strong and electromagnetic interactions. In addition, we also implement the fundamental role of Fermi-Dirac statistics and the phase space blocking due to the Pauli principle in the degenerate configuration. The new results essentially depend from the coordinated action of the five above theoretical components and cannot be obtained if any one of them is neglected. Let us first recall the role of gravity. In the case of neutron stars, unlike in the case of nuclei where its effects can be neglected, gravitation has the fundamental role of defining the basic parameters of the equilibrium configuration. As pointed out by Gamow (60), at a Newtonian level and by Oppenheimer and Volkoff (5) in general relativity, configurations of equilibrium exist at approximately one solar mass and at an average density around the nuclear density. This result is obtainable considering only the gravitational interaction of a system of Fermi degenerate self-gravitating neutrons, neglecting all other particles and interactions. It can be formulated within a Thomas-Fermi self-gravitating model (see e.g. (61)). In the present case of our simplified prototype model directed at evidencing new electrodynamic properties, the role of gravity is simply taken into account by considering, in line with the generalization of the above results, a mass-radius relation for the baryonic core

$$R^{NS} = R_c \approx \frac{\hbar}{m_\pi c} \frac{m_{\text{Planck}}}{m_n}. \quad (\text{A.3.7})$$

This formula generalizes the one given by Eq. (A.3.3) extending its validity to $N \approx (m_{\text{Planck}}/m_n)^3$, leading to a baryonic core radius $R_c \approx 10\text{km}$. We also recall that a more detailed analysis of nuclear matter in bulk in neutron stars (see e.g. Bethe et al. (62) and Cameron (63)) shows that at mass densities

larger than the "melting" density of

$$\rho_c = 4.34 \cdot 10^{13} \text{ g/cm}^3, \quad (\text{A.3.8})$$

all nuclei disappear. In the description of nuclear matter in bulk we have to consider then the three Fermi degenerate gas of neutrons, protons and electrons. In turn this naturally leads to consider the role of strong and weak interactions among the nucleons. In the nucleus, the role of the strong and weak interaction, with a short range of one Fermi, is to bind the nucleons, with a binding energy of 8 MeV, in order to balance the Coulomb repulsion of the protons. In the neutron star case we have seen that the neutrons confinement is due to gravity. We still assume that an essential role of the strong interactions is to balance the effective Coulomb repulsion due to the protons, partly screened by the electrons distribution inside the neutron star core. We shall verify, for self-consistency, the validity of this assumption on the final equilibrium solution we are going to obtain. We now turn to the essential weak interaction role in establishing the relative balance between neutrons, protons and electrons via the direct and inverse β -decay

$$p + e \longrightarrow n + \nu_e, \quad (\text{A.3.9})$$

$$n \longrightarrow p + e + \bar{\nu}_e. \quad (\text{A.3.10})$$

Since neutrinos escape from the star and the Fermi energy of the electrons is null, as we will show below, the only non-vanishing terms in the equilibrium condition given by the weak interactions are:

$$[(P_n^F c)^2 + M_n^2 c^4]^{1/2} - M_n c^2 = [(P_p^F c)^2 + M_p^2 c^4]^{1/2} - M_p c^2 + |e| V_{\text{coul}}^p \quad (\text{A.3.11})$$

where P_n^F and P_p^F are respectively, the neutron and proton Fermi momenta, and V_{coul}^p is the Coulomb potential of protons. At this point, having fixed all these physical constraints, the main task is to find the electrons distributions fulfilling in addition to the Dirac-Fermi statistics also the Maxwell equations for the electrostatic. The condition of equilibrium of the Fermi degenerate electrons implies the null value of the Fermi energy:

$$[(P_e^F c)^2 + m^2 c^4]^{1/2} - m c^2 + e V_{\text{coul}}(r) = 0, \quad (\text{A.3.12})$$

where P_e^F is the electron Fermi momentum and $V_{\text{coul}}(r)$ the Coulomb potential. In line with the procedure already followed for the heavy atoms (42),(23) we here adopt the relativistic Thomas-Fermi Equation:

$$\frac{1}{x} \frac{d^2 \chi(x)}{dx^2} = -4\pi\alpha \left\{ \theta(x - x_c) - \frac{1}{3\pi^2} \left[\left(\frac{\chi(x)}{x} + \beta \right)^2 - \beta^2 \right]^{3/2} \right\}, \quad (\text{A.3.13})$$

where $\alpha = e^2/(\hbar c)$, $\theta(x - x_c)$ represents the normalized proton density distribution, the variables x and χ are related to the radial coordinate and the electron Coulomb potential V_{coul} by

$$x = \frac{r}{R_c} \left(\frac{3N_p}{4\pi} \right)^{1/3}; \quad eV_{\text{coul}}(r) \equiv \frac{\chi(r)}{r}, \quad (\text{A.3.14})$$

and the constants $x_c(r = R_c)$ and β are respectively

$$x_c \equiv \left(\frac{3N_p}{4\pi} \right)^{1/3}; \quad \beta \equiv \frac{mcR_c}{\hbar} \left(\frac{4\pi}{3N_p} \right)^{1/3}. \quad (\text{A.3.15})$$

The solution has the boundary conditions

$$\chi(0) = 0; \quad \chi(\infty) = 0, \quad (\text{A.3.16})$$

with the continuity of the function χ and its first derivative χ' at the boundary of the core R_c . The crucial point is the determination of the eigenvalue of the first derivative at the center

$$\chi'(0) = \text{const.}, \quad (\text{A.3.17})$$

which has to be determined by fulfilling the above boundary conditions (A.3.16) and constraints given by Eq. (A.3.11) and Eq. (A.3.6). The difficulty of the integration of the Thomas-Fermi Equations is certainly one of the most celebrated chapters in theoretical physics and mathematical physics, still challenging a proof of the existence and uniqueness of the solution and strenuously avoiding the occurrence of exact analytic solutions. We recall after the original papers of Thomas (64) and Fermi (65), the works of Scorza Dragoni (66), Sommerfeld (67), Miranda (68) all the way to the many hundredth papers reviewed in the classical articles of Lieb and Simon (53), Lieb (69) and Spruch (70). The situation here is more difficult since we are working on the special relativistic generalization of the Thomas-Fermi Equation. Also in this case, therefore, we have to proceed by numerical integration. The difficulty of this numerical task is further enhanced by a consistency check in order to fulfill all different constraints. It is so that we start the computations by assuming a total number of protons and a value of the core radius R_c . We integrate the Thomas-Fermi Equation and we determine the number of neutrons from the Eq. (A.3.11). We iterate the procedure until a value of A is reached consistent with our choice of the core radius. The paramount difficulty of the problem is the numerical determination of the eigenvalue in Eq. (A.3.17) which already for $A \approx 10^4$ had presented remarkable numerical difficulties (42). In the present context we have been faced for a few months by an apparently unsurmountable numerical task: the determination of the

eigenvalue seemed to necessitate a significant number of decimals in the first derivative (A.3.17) comparable to the number of the electrons in the problem! We shall discuss elsewhere the way we overcame the difficulty by splitting the problem on the ground of the physical interpretation of the solution (71). The solution is given in Fig. (A.12) and Fig. (A.13).

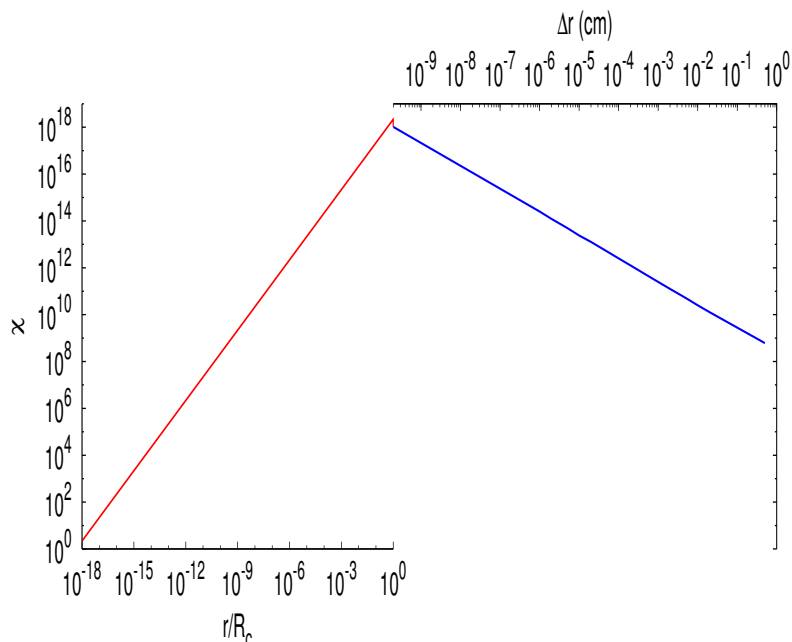


Figure A.12.: The solution χ of the relativistic Thomas-Fermi Equation for $A = 10^{57}$ and core radius $R_c = 10\text{km}$, is plotted as a function of radial coordinate. The left red line corresponds to the internal solution and it is plotted as a function of radial coordinate in unit of R_c in logarithmic scale. The right blue line corresponds to the solution external to the core and it is plotted as function of the distance Δr from the surface in the logarithmic scale in centimeter.

A relevant quantity for exploring the physical significance of the solution is given by the number of electrons within a given radius r :

$$N_e(r) = \int_0^r 4\pi(r')^2 n_e(r') dr'. \quad (\text{A.3.18})$$

This allows to determine, for selected values of the A parameter, the distribution of the electrons within and outside the core and follow the progressive penetration of the electrons in the core at increasing values of A [see Fig. (A.14)]. We can then evaluate, generalizing the results in (42), (23), the net charge inside the core

$$N_{\text{net}} = N_p - N_e(R_c) < N_p, \quad (\text{A.3.19})$$

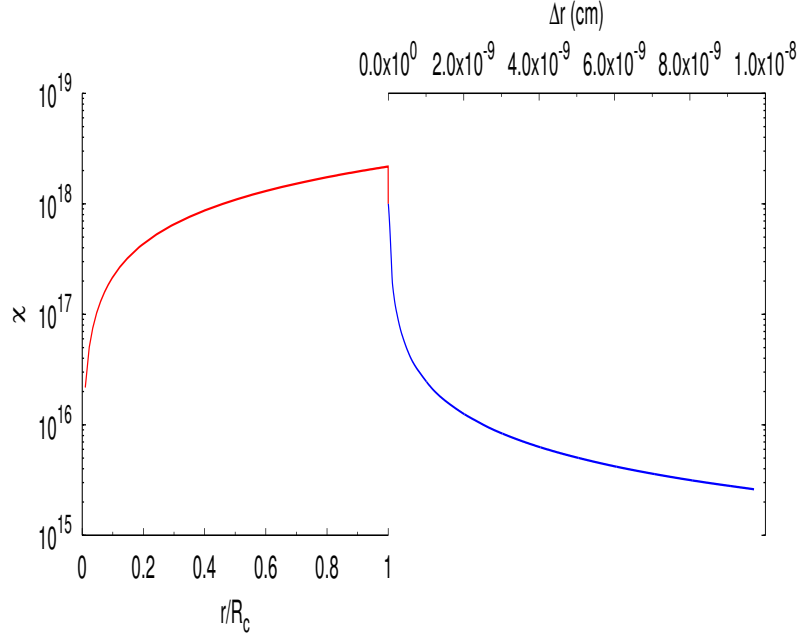


Figure A.13.: The same as Fig. (A.12): enlargement around the core radius R_c showing explicitly the continuity of function χ and its derivative χ' from the internal to the external solution.

and consequently determine of the electric field at the core surface, as well as within and outside the core [see Fig. (A.8)] and evaluate as well the Fermi degenerate electron distribution outside the core [see Fig. (A.16)]. It is interesting to explore the solution of the problem under the same conditions and constraints imposed by the fundamental interactions and the quantum statistics and imposing instead of Eq. (A.3.1) the corresponding Eq. (A.3.6). Indeed a solution exist and is much simpler

$$n_n(x) = n_p(x) = n_e(x) = 0, \quad \chi = 0. \quad (\text{A.3.20})$$

Before concluding as we announce we like to check on the theoretical consistency of the solution. We obtain an overall neutral configuration for the nuclear matter in bulk, with a positively charged baryonic core with

$$N_{\text{net}} = 0.92 \left(\frac{m}{m_\pi} \right)^2 \left(\frac{e}{m_n \sqrt{G}} \right)^2 \left(\frac{1}{\alpha} \right)^2, \quad (\text{A.3.21})$$

and an electric field on the baryonic core surface (see Fig. (A.15))

$$\frac{E}{E_c} = 0.92. \quad (\text{A.3.22})$$

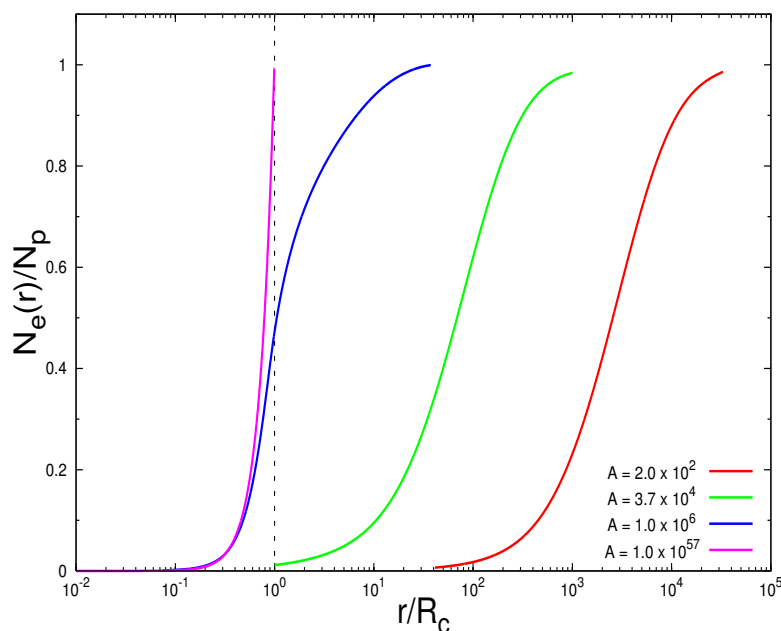


Figure A.14.: The electron number (A.3.18) in the unit of the total proton number N_p , for selected values of A , is given as function of radial distance in the unit of the core radius R_c , again in logarithmic scale. It is clear how by increasing the value of A the penetration of electrons inside the core increases. The detail shown in Fig. (A.8) and Fig. (A.16) demonstrates how for $N \simeq (m_{\text{Planck}}/m_n)^3$ a relatively small tail of electron outside the core exists and generates on the baryonic core surface an electric field close to the critical value given in . A significant electron density outside the core is found.

The corresponding Coulomb repulsive energy per nucleon is given by

$$U_{\text{coul}}^{\text{max}} = \frac{1}{2\alpha} \left(\frac{m}{m_\pi} \right)^3 mc^2 \approx 1.78 \cdot 10^{-6} (\text{MeV}), \quad (\text{A.3.23})$$

well below the nucleon binding energy per nucleon. It is also important to verify that this charge core is gravitationally stable. We have in fact

$$\frac{Q}{\sqrt{GM}} = \alpha^{-1/2} \left(\frac{m}{m_\pi} \right)^2 \approx 1.56 \cdot 10^{-4}. \quad (\text{A.3.24})$$

The electric field of the baryonic core is screened to infinity by an electron distribution given in Fig. (A.16). As usual any new solution of Thomas-Fermi systems has relevance and finds its justification in the theoretical physics and mathematical physics domain. We expect that as in the other solutions previously obtained in the literature of the relativistic Thomas-Fermi equa-

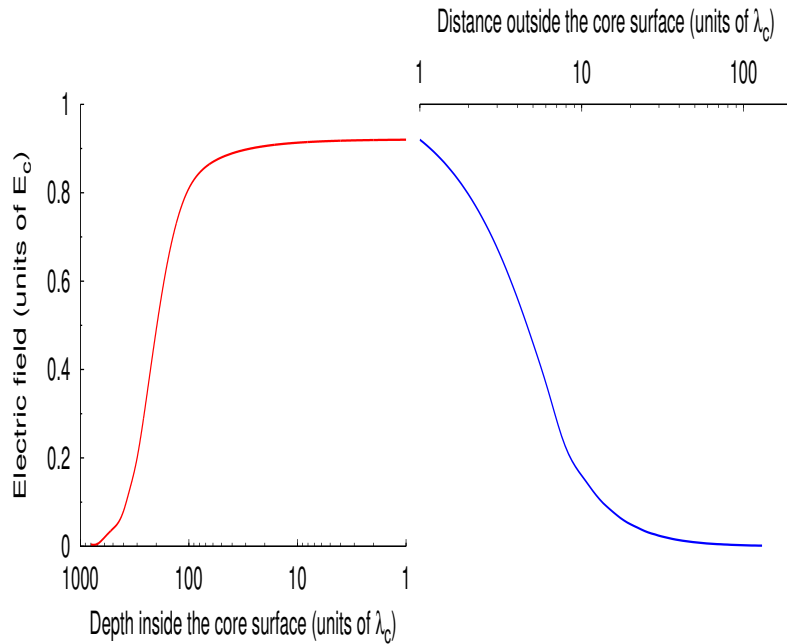


Figure A.15.: The electric field in the unit of the critical field E_c is plotted around the core radius R_c . The left (right) diagram in the red (blue) refers the region just inside (outside) the core radius plotted logarithmically. By increasing the density of the star the field approaches the critical field.

tions also this one we present in this letter will find important applications in physics and astrophysics. There are a variety of new effects that such a generalized approach naturally leads to: (1) the mass-radius relation of neutron star may be affected; (2) the electrodynamic aspects of neutron stars and pulsars will be different; (3) we expect also important consequence in the initial conditions in the physics of gravitational collapse of the baryonic core as soon as the critical mass for gravitational collapse to a black hole is reached. The consequent collapse to a black hole will have very different energetics properties.

A.4. On the Charge to Mass Ratio of Neutron Cores and Heavy Nuclei

Introduction. It is well known that stable nuclei are located, in the N_n - N_p plane (where N_n and N_p are the total number of neutrons and protons respectively), in a region that, for small values of N_p , is almost a line well described by the relation $N_n = N_p$.

In the past, several efforts have been made to explain theoretically this property, for example with the liquid drop model of atoms, that is based on two

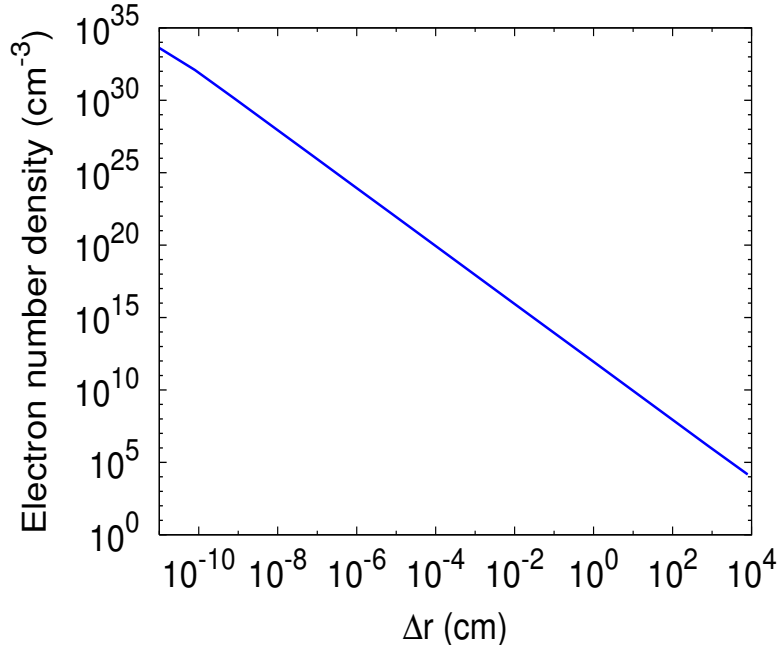


Figure A.16.: The density of electrons for $A = 10^{57}$ in the region outside the core; both scale are logarithmically.

properties common to all nuclei: their mass densities and their binding energies for nucleons are almost independent from the mass number $A = N_n + N_p$ (44). This model takes into account the strong nuclear force and the Coulombian repulsion between protons and explains different properties of nuclei, for example the relation between N_p and A (the charge to mass ratio). In this work (89) we derive theoretically the charge to mass ratio of nuclei and extend it to neutron cores (characterized by higher values of A) with the model of Ruffini et al. (13). We consider systems composed of degenerate neutrons, protons and electrons and we use the relativistic Thomas-Fermi equation and the equation of β -equilibrium to determine the number density and the total number of these particles, from which we obtain the relation between N_p and A .

The theoretical model. Following the work of Ruffini et al. (13), we describe nuclei and neutron cores as spherically symmetric systems composed of degenerate protons, electrons and neutrons and impose the condition of global charge neutrality.

We assume that the proton's number density $n_p(r)$ is constant inside the core ($r \leq R_C$) and vanishes outside the core ($r > R_C$):

$$n_p(r) = \left(\frac{3N_p}{4\pi R_C^3} \right) \theta(R_C - r), \quad (\text{A.4.1})$$

where N_p is the total number of protons and R_C is the core-radius, parametrized as:

$$R_C = \Delta \frac{\hbar}{m_\pi c} N_p^{1/3}. \quad (\text{A.4.2})$$

We choose Δ in order to have $\rho \sim \rho_N$, where ρ and ρ_N are the mass density of the system and the nuclear density respectively ($\rho_N = 2.314 \cdot 10^{14} \text{ g cm}^{-3}$).

The electron number density $n_e(r)$ is given by:

$$n_e(r) = \frac{1}{3\pi^2 \hbar^3} \left[p_e^F(r) \right]^3, \quad (\text{A.4.3})$$

where $p_e^F(r)$ is the electron Fermi momentum. It can be calculated from the condition of equilibrium of Fermi degenerate electrons, that implies the null value of their Fermi energy $\epsilon_e^F(r)$:

$$\epsilon_e^F(r) = \sqrt{[p_e^F(r)c]^2 + m_e^2 c^4} - m_e c^2 + V_c(r) = 0, \quad (\text{A.4.4})$$

where $V_c(r)$ is the Coulomb potential energy of electrons.

From this condition we obtain:

$$p_e^F(r) = \frac{1}{c} \sqrt{V_c^2(r) - 2m_e c^2 V_c(r)}, \quad (\text{A.4.5})$$

hence the electron number density is:

$$n_e(r) = \frac{1}{3\pi^2 \hbar^3 c^3} \left[V_c^2(r) - 2m_e c^2 V_c(r) \right]^{3/2}. \quad (\text{A.4.6})$$

The Coulomb potential energy of electrons, necessary to derive $n_e(r)$, can be determined as follows. Based on the Gauss law, $V_c(r)$ obeys the following Poisson equation:

$$\nabla^2 V_c(r) = -4\pi e^2 [n_e(r) - n_p(r)], \quad (\text{A.4.7})$$

with the boundary conditions $V_c(\infty) = 0$, $V_c(0) = \text{finite}$. Introducing the dimensionless function $\chi(r)$, defined by the relation:

$$V_c(r) = -\hbar c \frac{\chi(r)}{r}, \quad (\text{A.4.8})$$

and the new variable $x = rb^{-1} = r \left(\frac{\hbar}{m_\pi c} \right)^{-1}$, from eq. (A.4.7) we obtain the relativistic Thomas-Fermi equation:

$$\frac{1}{3x} \frac{d^2 \chi(x)}{dx^2} = -\alpha \left\{ \frac{1}{\Delta^3} \theta(x_c - x) - \frac{4}{9\pi} \left[\frac{\chi^2(x)}{x^2} + 2 \frac{m_e}{m_\pi} \frac{\chi(x)}{x} \right]^{3/2} \right\}. \quad (\text{A.4.9})$$

The boundary conditions for the function $\chi(x)$ are:

$$\chi(0) = 0, \quad \chi(\infty) = 0, \quad (\text{A.4.10})$$

as well as the continuity of $\chi(x)$ and its first derivative $\chi'(x)$ at the boundary of the core.

The number density of neutrons $n_n(r)$ is:

$$n_n(r) = \frac{1}{3\pi^2\hbar^3} \left[p_n^F(r) \right]^3, \quad (\text{A.4.11})$$

where $p_n^F(r)$ is the neutron Fermi momentum. It can be calculated with the condition of equilibrium between the processes

$$e^- + p \rightarrow n + \nu_e; \quad (\text{A.4.12})$$

$$n \rightarrow p + e^- + \bar{\nu}_e, \quad (\text{A.4.13})$$

Assuming that neutrinos escape from the core as soon as they are produced, this condition (condition of β -equilibrium) is

$$\epsilon_e^F(r) + \epsilon_p^F(r) = \epsilon_n^F(r). \quad (\text{A.4.14})$$

Eq. (A.4.14) can be explicitly written as:

$$\sqrt{[p_p^F(r)c]^2 + m_p^2c^4} - m_p c^2 - V_c(r) = \sqrt{[p_n^F(r)c]^2 + m_n^2c^4} - m_n c^2. \quad (\text{A.4.15})$$

N_p versus A relation. Using the previous equations, we derive $n_e(r)$, $n_n(r)$ and $n_p(r)$ and, by integrating these, we obtain the N_e , N_n and N_p . We also derive a theoretical relation between N_p and A and we compare it with the data of the Periodic Table and with the semi-empirical relation:

$$N_p = \left(\frac{A}{2} \right) \cdot \frac{1}{1 + \left(\frac{3}{400} \right) \cdot A^{2/3}} \quad (\text{A.4.16})$$

that, in the limit of low A , gives the well known relation $N_p = A/2$ (44).

Eq. (A.4.16) can be obtained by minimizing the semi-empirical mass formula, that was first formulated by Weizsäcker in 1935 and is based on empirical measurements and on theory (the liquid drop model of atoms).

The liquid drop model approximates the nucleus as a sphere composed of protons and neutrons (and not electrons) and takes into account the Coulombian repulsion between protons and the strong nuclear force. Another important characteristic of this model is that it is based on the property that the mass densities of nuclei are approximately the same, independently from A (90). In fact, from scattering experiments it was found the following expres-

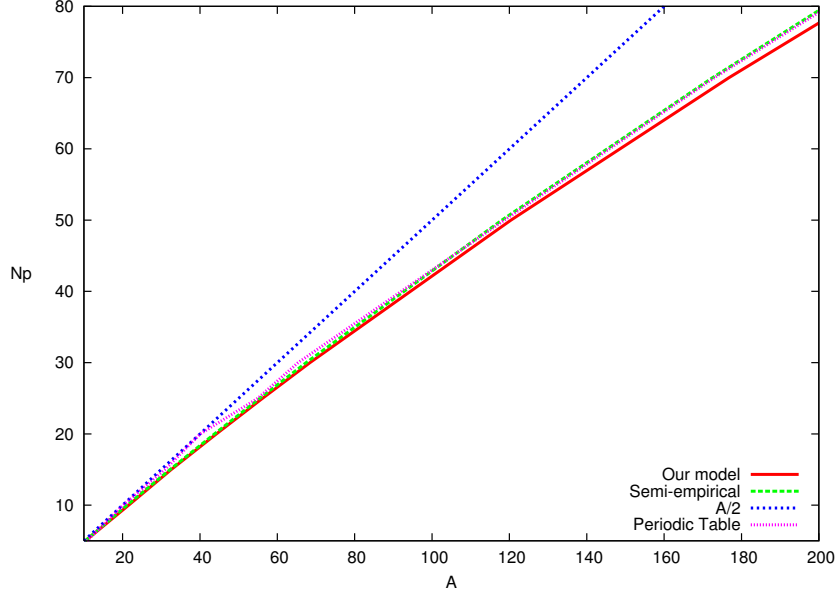


Figure A.17.: The $N_p - A$ relation obtained with our model and with the semi-empirical mass formula, the $N_p = A/2$ relation and the data of the Periodic Table; relations are plotted for values of A from 0 to 200.

sion for the nuclear radius R_N :

$$R_N = r_0 A^{1/3}, \quad (\text{A.4.17})$$

with $r_0 = 1.2$ fm. Using eq. (A.4.17) the nuclear density can be write as follows:

$$\rho_N = \frac{Am_N}{V} = \frac{3Am_N}{4\pi r_0^3 A} = \frac{3m_N}{4\pi r_0^3}, \quad (\text{A.4.18})$$

where m_N is the nucleon mass. From eq. (A.4.18) it is clear that nuclear density is independent from A , so it is constant for all nuclei.

The property of constant density for all nuclei is a common point with our model: in fact, we choose Δ in order to have the same mass density for every value of A ; in particular we consider the case $\rho \sim \rho_N$, as previously said.

In table (A.1) are listed some values of A obtained with our model and the semi-empirical mass formula, as well as the data of the Periodic Table; in fig. (A.17) and (A.18) it is shown the comparison between the various $N_p - A$ relations. It is clear that there is a good agreement between all the relations for values of A typical of nuclei, with differences of the order of per cent. Our relation and the semi-empirical one are in agreement up to $A \sim 10^4$; for higher values, we find that the two relations differ. We interpret these differences as due to the effects of penetration of electrons inside the core [see fig. (A.19)]: in our model we consider a system composed of degenerate protons, neutrons and electrons. For the smallest values of A , all the electrons are in a

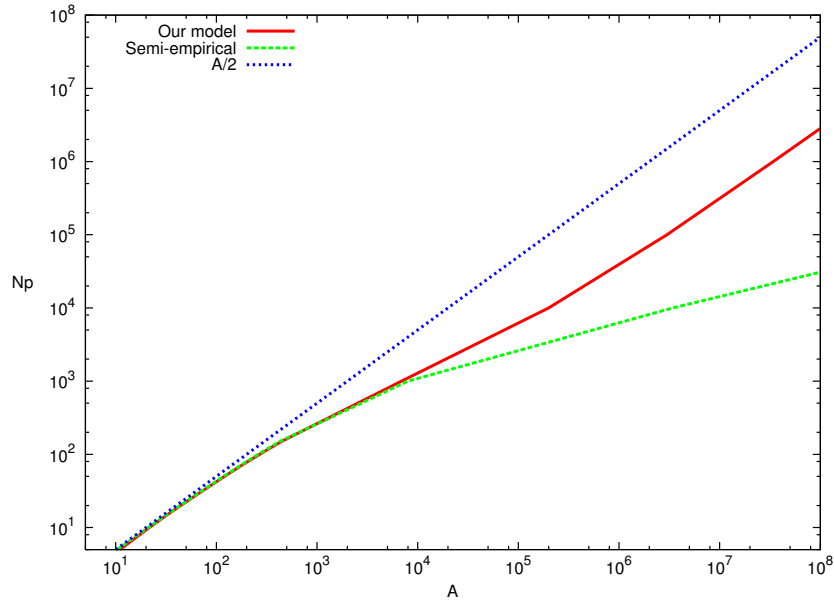


Figure A.18.: The $N_p - A$ relation obtained with our model and with the semi-empirical mass formula and the $N_p = A/2$ relation; relations are plotted for values of A from 0 to 10^8 . It is clear how the semi-empirical relation and the one obtained with our model are in good agreement up to values of A of the order of 10^4 ; for greater values of A the two relation differ because our model takes into account the penetration of electrons inside the core, which is not considered in the semi-empirical mass formula.

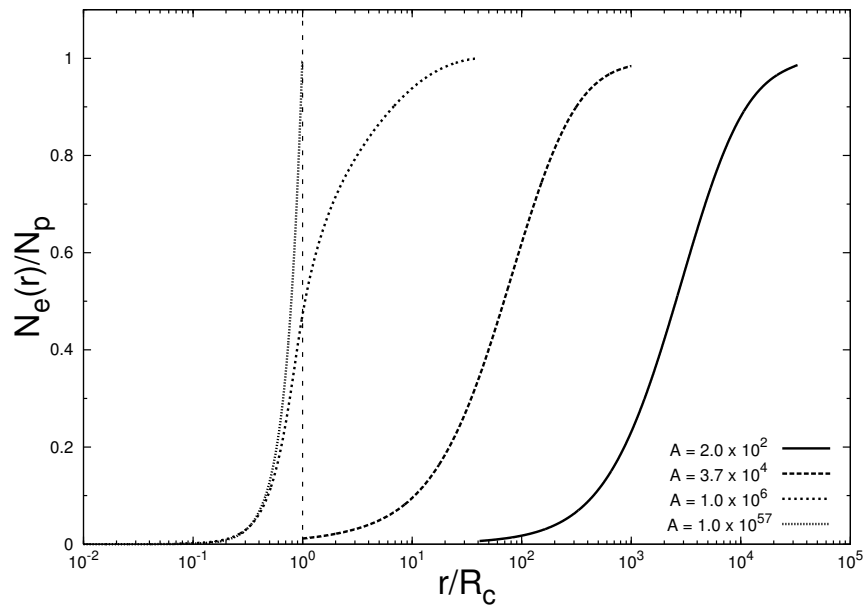


Figure A.19.: The electron number in units of the total proton number N_p as function of the radial distance in units of the core radius R_C , for different values of A . It is clear that, by increasing the value of A , the penetration of electrons inside the core increases. Figure from R. Ruffini, M. Rotondo and S. S. Xue (13).

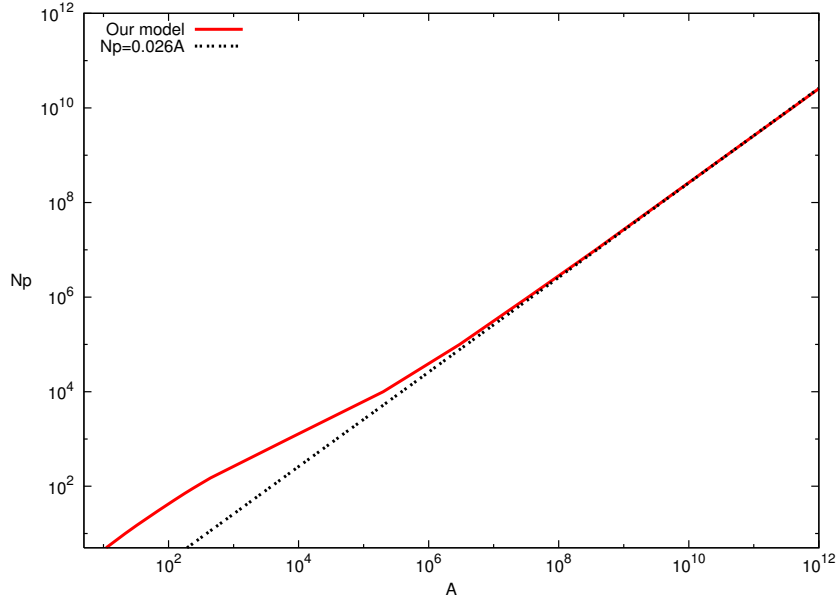


Figure A.20.: The $N_p - A$ relation obtained with our model and the asymptotic limit $N_p = 0.026A$

shell outside the core; by increasing A , they progressively penetrate into the core (13). These effects, which need the relativistic approach introduced in (13), are not taken into account in the semi-empirical mass formula.

We also note that the charge to mass ratio become constant for A greater than 10^7 ; in particular, it is well approximated by the relation $N_p = 0.026A$ [see fig. (A.20)].

Conclusions. In this work we have derived theoretically a relation between the total number of protons N_p and the mass number A for nuclei and neutron cores with the model recently proposed by Ruffini et al. (13)).

We have considered spherically symmetric systems composed of degenerate electrons, protons and neutrons having global charge neutrality and the same mass densities ($\rho \sim \rho_N$). By integrating the relativistic Thomas-Fermi equation and using the equation of β -equilibrium, we have determined the total number of protons, electrons and neutrons in the system and hence a theoretical relation between N_p and A .

We have compared this relation with the empirical data of the Periodic Table and with the semi-empirical relation, obtained by minimizing the Weizsäcker mass formula by considering systems with the same mass densities. We have shown that there's a good agreement between all the relations for values of A typical of nuclei, with differences of the order of per cent. Our relation and the semi-empirical one are in agreement up to $A \sim 10^4$; for higher values, we find that the two relations differ. We interpret the different behaviour of our theoretical relation as a result of the penetration of electrons (initially confined in an external shell) inside the core [see fig.(A.19)], that becomes more

N_p	A_M	A_{PT}	A_{SE}
5	10.40	10.811	10.36
10	21.59	20.183	21.15
15	32.58	30.9738	32.28
20	44.24	40.08	43.72
25	56.17	54.938	55.45
30	68.43	65.37	67.46
50	120.40	118.69	118.05
70	176.78	173.04	172.54
90	237.41	232.038	230.79
110	302.18	271	292.75
150	443.98		427.73
200	644.03		617.56
250	869.32		831.63
300	1119.71		1071.08
350	1395.12		1337.23
450	2019.48		1955.57
500	2367.77		2310.96
550	2739.60		2699.45
600	3134.28		3122.83
10^3	$6.9 \cdot 10^3$		$8 \cdot 10^3$
10^4	$2.0 \cdot 10^5$		$3.45 \cdot 10^6$
10^5	$3.0 \cdot 10^6$		$3.38 \cdot 10^9$
10^6	$3.4 \cdot 10^7$		$3.37 \cdot 10^{12}$
10^7	$3.7 \cdot 10^8$		$3.37 \cdot 10^{15}$
10^{10}	$3.9 \cdot 10^{11}$		$3.37 \cdot 10^{24}$

Table A.1.: Different values of N_p (column 1) and corresponding values of A from our model (A_M , column 2), the Periodic Table (A_{PT} , column 3) and the semi-empirical mass formula (A_{SE} , column 4).

and more important by increasing A ; these effects, which need the relativistic approach introduced in (13), are not taken into account in the semi-empirical mass-formula.

A.5. Supercritical fields on the surface of massive nuclear cores: neutral core v.s. charged core

Equilibrium of electron distribution in neutral cores. In Refs. (13; 42; 23), the Thomas-Fermi approach was used to study the electrostatic equilibrium of electron distributions $n_e(r)$ around extended nuclear cores, where total proton and electron numbers are the same $N_p = N_e$. Proton's density $n_p(r)$ is constant inside core $r \leq R_c$ and vanishes outside the core $r > R_c$,

$$n_p(r) = n_p \theta(R_c - r), \quad (\text{A.5.1})$$

where R_c is the core radius and n_p proton density. Degenerate electron density,

$$n_e(r) = \frac{1}{3\pi^2 \hbar^3} (P_e^F)^3, \quad (\text{A.5.2})$$

where electron Fermi momentum P_e^F , Fermi-energy $\mathcal{E}_e(P_e^F)$ and Coulomb potential energy $V_{\text{coul}}(r)$ are related by,

$$\mathcal{E}_e(P_e^F) = [(P_e^F c)^2 + m_e^2 c^4]^{1/2} - m_e c^2 - V_{\text{coul}}(r). \quad (\text{A.5.3})$$

The electrostatic equilibrium of electron distributions is determined by

$$\mathcal{E}_e(P_e^F) = 0, \quad (\text{A.5.4})$$

which means the balance of electron's kinetic and potential energies in Eq. (A.5.3) and degenerate electrons occupy energy-levels up to $+m_e c^2$. Eqs. (A.5.2, A.5.3, A.5.4) give the relationships:

$$P_e^F = \frac{1}{c} \left[V_{\text{coul}}^2(r) + 2m_e c^2 V_{\text{coul}}(r) \right]^{1/2}; \quad (\text{A.5.5})$$

$$n_e(r) = \frac{1}{3\pi^2 (c\hbar)^3} \left[V_{\text{coul}}^2(r) + 2m_e c^2 V_{\text{coul}}(r) \right]^{3/2}. \quad (\text{A.5.6})$$

The Gauss law leads the following Poisson equation and boundary conditions,

$$\Delta V_{\text{coul}}(r) = 4\pi\alpha [n_p(r) - n_e(r)]; \quad V_{\text{coul}}(\infty) = 0, \quad V_{\text{coul}}(0) = \text{finite} \quad (\text{A.5.7})$$

These equations describe a Thomas-Fermi model for neutral nuclear cores, and have numerically solved together with the empirical formula (42; 23) and β -equilibrium equation (13) for the proton number N_p and mass number $A = N_p + N_n$, where N_n is the neutron number.

Equilibrium of electron distribution in super charged cores In Ref. (56; 57), assuming that super charged cores of proton density (A.5.1) are bare, electrons (positrons) produced by vacuum polarization fall (fly) into cores (infinity), one studied the equilibrium of electron distribution when vacuum polarization process stop. When the proton density is about nuclear density, super charged core creates a negative Coulomb potential well $-V_{\text{coul}}(r)$, whose depth is much more profound than $-m_e c^2$ (see Fig. [A.21]), production of electron-positron pairs take places, and electrons bound by the core and screen down its charge. Since the phase space of negative energy-levels $\epsilon(p)$

$$\epsilon(p) = [(pc)^2 + m_e^2 c^4]^{1/2} - V_{\text{coul}}(r), \quad (\text{A.5.8})$$

below $-m_e c^2$ for accommodating electrons is limited, vacuum polarization process completely stops when electrons fully occupy all negative energy-levels up to $-m_e c^2$, even electric field is still critical. Therefore an equilibrium of degenerate electron distribution is expected when the following condition is satisfied,

$$\epsilon(p) = [(pc)^2 + m_e^2 c^4]^{1/2} - V_{\text{coul}}(r) = -m_e c^2, \quad p = P_e^F, \quad (\text{A.5.9})$$

and Fermi-energy

$$\mathcal{E}_e(P_e^F) = \epsilon(P_e^F) - m_e c^2 = -2m_e c^2, \quad (\text{A.5.10})$$

which is rather different from Eq. (A.5.4). This equilibrium condition (A.5.10) leads to electron's Fermi-momentum and number-density (A.5.2),

$$P_e^F = \frac{1}{c} \left[V_{\text{coul}}^2(r) - 2m_e c^2 V_{\text{coul}}(r) \right]^{1/2}; \quad (\text{A.5.11})$$

$$n_e(r) = \frac{1}{3\pi^2 (c\hbar)^3} \left[V_{\text{coul}}^2(r) - 2m_e c^2 V_{\text{coul}}(r) \right]^{3/2}. \quad (\text{A.5.12})$$

which have a different sign contracting to Eqs. (A.5.5,A.5.6). Eq. (A.5.7) remains the same. However, contracting to the neutrality condition $N_e = N_p$ and $n_e(r)|_{r \rightarrow \infty} \rightarrow 0$ in the case of neutral cores, the total number of electrons is given by

$$N_e^{\text{ion}} = \int_0^{r_0} 4\pi r^2 dr n_e(r) < N_p, \quad (\text{A.5.13})$$

where r_0 is the finite radius at which electron distribution $n_e(r)$ (A.5.12) vanishes: $n_e(r_0) = 0$, i.e., $V_{\text{coul}}(r_0) = 2m_e c^2$, and $n_e(r) \equiv 0$ for the range $r > r_0$. $N^{\text{ion}} < N_p$ indicates that such configuration is not neutral. These equations describe a Thomas-Fermi model for super charged cores, and have numerically (56) and analytically (57) solved with assumption $N_p = A/2$.

Ultra-relativistic solution In analytical approach (57; 71), the ultra-relativistic approximation is adopted for $V_{\text{coul}}(r) \gg 2m_e c^2$, the term $2m_e c^2 V_{\text{coul}}(r)$ in Eqs. (A.5.5, A.5.6, A.5.11, A.5.12) is neglected. It turns out that approximated Thomas-Fermi equations are the same for both cases of neutral and charged cores, and solution $V_{\text{coul}}(r) = \hbar c (3\pi^2 n_p)^{1/3} \phi(x)$,

$$\phi(x) = \left\{ \begin{array}{ll} 1 - 3 \left[1 + 2^{-1/2} \sinh(3.44 - \sqrt{3}x) \right]^{-1}, & \text{for } x < 0, \\ \frac{\sqrt{2}}{(x+1.89)}, & \text{for } x > 0, \end{array} \right\}, \quad (\text{A.5.14})$$

where $x = 2(\pi/3)^{1/6} \alpha^{1/2} n_p^{1/3} (r - R_c) \sim 0.1(r - R_c) / \lambda_\pi$ and the pion Compton length $\lambda_\pi = \hbar / (m_\pi c)$. At the core center $r = 0 (x \rightarrow -\infty)$, $V_{\text{coul}}(0) = \hbar c (3\pi^2 n_p)^{1/3} \sim m_\pi c^2$. On core surface $r = R_c (x = 0)$, $V_{\text{coul}}(R_c) = 3/4 V_{\text{coul}}(0) \gg m_e c^2$, indicating that the ultra-relativistic approximation is applicable for $r \lesssim R_c$. This approximation breaks down at $r \gtrsim r_0$. Clearly, it is impossible to determine the value r_0 out of ultra-relativistically approximated equation, and full Thomas-Fermi equation (A.5.7) with source terms Eq. (A.5.6) for the neutral case, and Eq. (A.5.12) for the charged case have to be solved.

For $r < r_0$ where $V_{\text{coul}}(r) > 2m_e c^2$, we treat the term $2m_e c^2 V_{\text{coul}}(r)$ in Eqs. (A.5.6, A.5.12) as a small correction term, and find the following inequality is always true

$$n_e^{\text{neutral}}(r) > n_e^{\text{charged}}(r), \quad r < r_0, \quad (\text{A.5.15})$$

where $n_e^{\text{neutral}}(r)$ and $n_e^{\text{charged}}(r)$ stand for electron densities of neutral and super charged cores. For the range $r > r_0$, $n_e^{\text{charged}}(r) \equiv 0$ in the case of super charged core, while $n_e^{\text{neutral}}(r) \rightarrow 0$ in the case of neutral core, which should be calculated in non-relativistic approximation: the term $V_{\text{coul}}^2(r)$ in Eq. (A.5.6) is neglected.

In conclusion, the physical scenarios and Thomas-Fermi equations of neutral and super charged cores are slightly different. When the proton density n_p of cores is about nuclear density, ultra-relativistic approximation applies for the Coulomb potential energy $V_{\text{coul}}(r) \gg m_e c^2$ in $0 < r < r_0$ and $r_0 > R_c$, and approximate equations and solutions for electron distributions inside and around cores are the same. As relativistic regime $r \sim r_0$ and non-relativistic regime $r > r_0$ (only applied to neutral case) are approached, solutions in two cases are somewhat different, and need direct integrations.

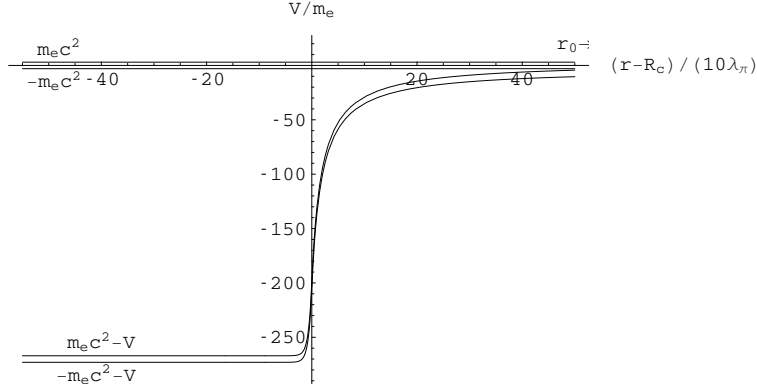


Figure A.21.: Potential energy-gap $\pm m_e c^2 - V_{\text{coul}}(r)$ and electron mass-gap $\pm m_e c^2$ in the unit of $m_e c^2$ are plotted as a function of $(r - R_c)/(10\lambda_\pi)$. The potential depth inside core ($r < R_c$) is about pion mass $m_\pi c^2 \gg m_e c^2$ and potential energy-gap and electron mass-gap are indicated. The radius r_0 where electron distribution $n_e(r_0)$ vanishes in super charged core case is indicated as r_{0-} , since it is out of plotting range.

A.6. The Extended Nuclear Matter Model with Smooth Transition Surface

The Relativistic Thomas–Fermi Equation.

Let us to introduce the proton distribution function $f_p(x)$ by mean of $n_p(x) = n_p^c f_p(x)$, where n_p^c is the central number density of protons. We use the dimensionless unit $x = (r - b)/a$, with $a^{-1} = \sqrt{4\pi\alpha\lambda_e n_p^c}$, λ_e is the electron Compton wavelength, b the length where initial conditions are given ($x = 0$) and α is the fine structure constant.

Using the Poisson’s equation and the equilibrium condition for the gas of electrons

$$E_F^e = m_e c^2 \sqrt{1 + x_e^2} - m_e c^2 - eV = 0, \quad (\text{A.6.1})$$

where e is the fundamental charge, x_e the normalized electron Fermi momentum and V the electrostatic potential, we obtain the relativistic Thomas–Fermi equation

$$\bar{\zeta}_e''(x) + \left(\frac{2}{x + b/a} \right) \bar{\zeta}_e'(x) - \frac{[\bar{\zeta}_e^2(x) - 1]^{3/2}}{\mu} + f_p(x) = 0, \quad (\text{A.6.2})$$

where $\mu = 3\pi^2 \lambda_e^3 n_p^c$ and we have introduced the normalized electron chemical potential in absence of any field $\bar{\zeta}_e = \sqrt{1 + x_e^2}$. For a given distribution

function $f_p(x)$ and a central number density of protons n_p^c , the above equation can be integrated numerically with the boundary conditions

$$\xi_e(0) = \sqrt{1 + [\mu \delta f_p(0)]^{2/3}}, \quad \xi_e'(0) < 0, \quad (\text{A.6.3})$$

where $\delta \equiv n_e(0)/n_p(0)$.

The Woods-Saxon-like Proton Distribution Function.

We simulate a monotonically decreasing proton distribution function fulfilling a Woods-Saxon dependence

$$f_p(x) = \frac{\gamma}{\gamma + e^{\beta x}}, \quad (\text{A.6.4})$$

where $\gamma > 0$ and $\beta > 0$. In fig. A.22 we show the proton distribution function for a particular set of parameters.

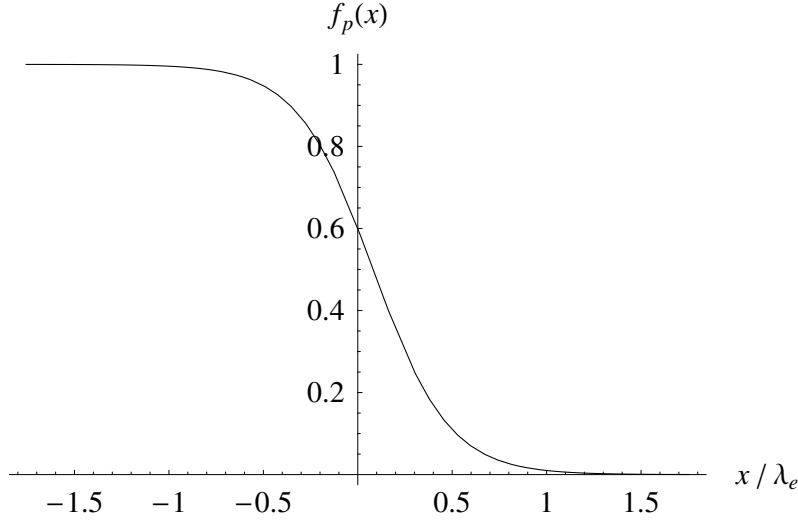


Figure A.22.: Proton distribution function for $\gamma = 1.5$, $\beta \approx 0.0585749$.

Results of the Numerical Integration.

We have integrated numerically the eq.(A.6.2) for several sets of parameters and initial conditions. As an example, we show the results for the proton distribution function shown in fig. A.22, with $n_p^c = 1.38 \times 10^{36} (cm^{-3})$. This system was integrated with $N_e = N_p = 10^{54}$, mass number $A = 1.61 \times 10^{56}$ and $\delta \approx 0.967$.

We summarize the principal features of our model in figures A.23 and A.24, where we have plotted the electric field in units of the critical field $E_c = \frac{m_e^2 c^3}{e \hbar}$, (m_e and e are the electron mass and charge), and the normalized charge separation function

$$\Delta(x) = \frac{n_p(x) - n_e(x)}{n_p(0)}. \quad (\text{A.6.5})$$

We see that the electric field is overcritical but smaller respect to the case of a sharp step proton distribution used in (13; 12). We have performed several numerical integrations expanding the transition surface and confirm the existence of overcritical fields but it is worth to mention that it could be subcritical expanding the width of the transition surface several orders of magnitude in electron Compton wavelength units.

We also see a displacement of the location of the maximum of intensity. This effect is due to the displacement of the point where $n_e = n_p$. After this point, the charge density becomes negative producing an effect of screening of the charged core up to global charged neutrality is achieved.

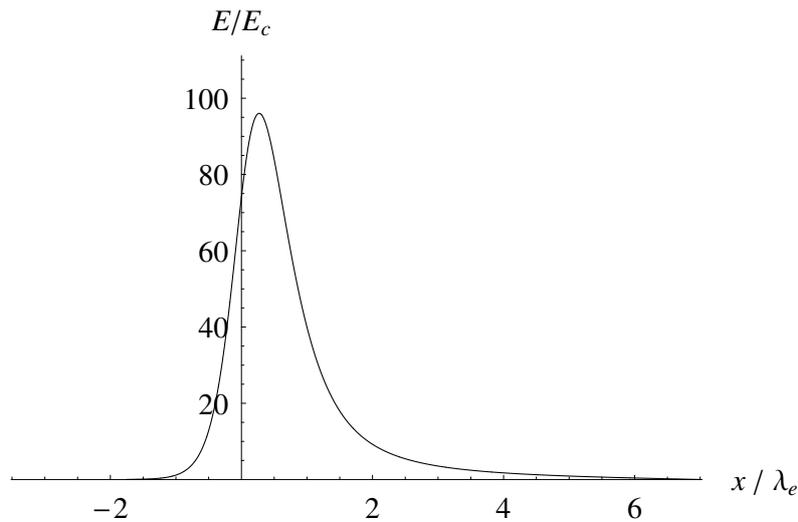


Figure A.23.: Electric field in units of the critical field E_c .

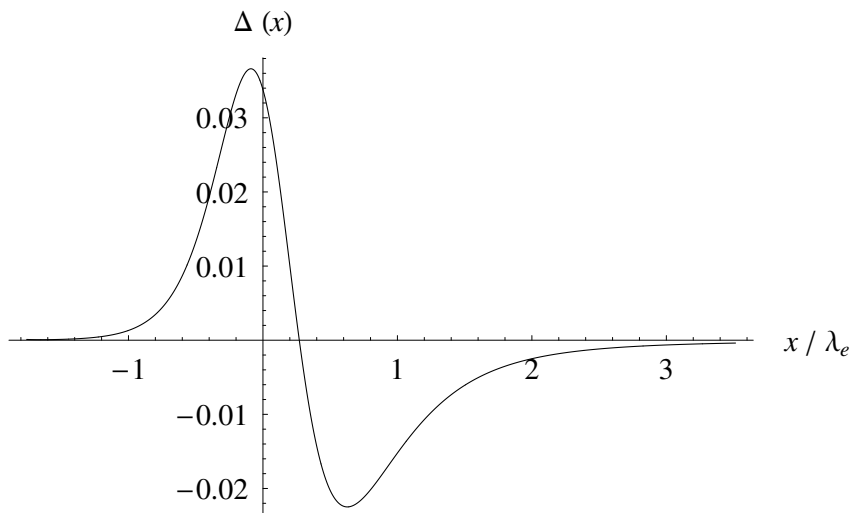


Figure A.24.: Charge separation function.

B. Electron-positron pairs production in an electric potential of massive cores

B.1. Introduction

Very soon after the Dirac equation for a relativistic electron was discovered (72; 73), Gordon (74) (for all $Z < 137$) and Darwin (75) (for $Z = 1$) found its solution in the point-like Coulomb potential $V(r) = -Z\alpha/r$, they obtained the well-known Sommerfeld's formula (76) for energy-spectrum,

$$\mathcal{E}(n, j) = mc^2 \left[1 + \left(\frac{Z\alpha}{n - |K| + (K^2 - Z^2\alpha^2)^{1/2}} \right)^2 \right]^{-1/2}, \quad (\text{B.1.1})$$

where the fine-structure constant $\alpha = e^2/\hbar c$, the principle quantum number $n = 1, 2, 3, \dots$ and

$$K = \begin{cases} -(j + 1/2) = -(l + 1), & \text{if } j = l + \frac{1}{2}, \quad l \geq 0 \\ (j + 1/2) = l, & \text{if } j = l - \frac{1}{2}, \quad l \geq 1 \end{cases} \quad (\text{B.1.2})$$

$l = 0, 1, 2, \dots$ is the orbital angular momentum corresponding to the upper component of Dirac bi-spinor, j is the total angular momentum. The integer values n and j label bound states whose energies are $\mathcal{E}(n, j) \in (0, mc^2)$. For the example, in the case of the lowest energy states, one has

$$\mathcal{E}(1S_{\frac{1}{2}}) = mc^2 \sqrt{1 - (Z\alpha)^2}, \quad (\text{B.1.3})$$

$$\mathcal{E}(2S_{\frac{1}{2}}) = \mathcal{E}(2P_{\frac{1}{2}}) = mc^2 \sqrt{\frac{1 + \sqrt{1 - (Z\alpha)^2}}{2}}, \quad (\text{B.1.4})$$

$$\mathcal{E}(2P_{\frac{3}{2}}) = mc^2 \sqrt{1 - \frac{1}{4}(Z\alpha)^2}. \quad (\text{B.1.5})$$

For all states of the discrete spectrum, the binding energy $mc^2 - \mathcal{E}(n, j)$ increases as the nuclear charge Z increases. No regular solution with $n = 1, l = 0, j = 1/2$ and $K = -1$ (the $1S_{1/2}$ ground state) is found for $Z > 137$, this was first noticed by Gordon in his pioneer paper (74). This is the problem

so-called “ $Z = 137$ catastrophe”.

The problem was solved (11; 54; 77; 78; 79; 80; 81; 82) by considering the fact that the nucleus is not point-like and has an extended charge distribution, and the potential $V(r)$ is not divergent when $r \rightarrow 0$. The $Z = 137$ catastrophe disappears and the energy-levels $\mathcal{E}(n, j)$ of the bound states $1S$, $2P$ and $2S, \dots$ smoothly continue to drop toward the negative energy continuum ($E_- < -mc^2$), as Z increases to values larger than 137. The critical values Z_{cr} for $\mathcal{E}(n, j) = -mc^2$ were found (11; 78; 80; 81; 82; 85; 86; 87): $Z_{cr} \simeq 173$ is a critical value at which the lowest energy-level of the bound state $1S_{1/2}$ encounters the negative energy continuum, while other bound states $2P_{1/2}, 2S_{3/2}, \dots$ encounter the negative energy continuum at $Z_{cr} > 173$, thus energy-level-crossings and productions of electron and positron pair takes place, provided these bound states are unoccupied. We refer the readers to (11; 80; 81; 82; 83; 84; 85; 86; 87) for mathematical and numerical details.

The energetics of this phenomenon can be understood as follow. The energy-level of the bound state $1S_{1/2}$ can be estimated as follow,

$$\mathcal{E}(1S_{1/2}) = mc^2 - \frac{Ze^2}{\bar{r}} < -mc^2, \quad (\text{B.1.6})$$

where \bar{r} is the average radius of the $1S_{1/2}$ state's orbit, and the binding energy of this state $Ze^2/\bar{r} > 2mc^2$. If this bound state is unoccupied, the bare nucleus gains a binding energy Ze^2/\bar{r} larger than $2mc^2$, and becomes unstable against the production of an electron-positron pair. Assuming this pair-production occur around the radius \bar{r} , we have energies of electron (ϵ_-) and positron (ϵ_+):

$$\epsilon_- = \sqrt{(c|\mathbf{p}_-|)^2 + m^2c^4} - \frac{Ze^2}{\bar{r}}; \quad \epsilon_+ = \sqrt{(c|\mathbf{p}_+|)^2 + m^2c^4} + \frac{Ze^2}{\bar{r}}, \quad (\text{B.1.7})$$

where \mathbf{p}_\pm are electron and positron momenta, and $\mathbf{p}_- = -\mathbf{p}_+$. The total energy required for a pair production is,

$$\epsilon_{-+} = \epsilon_- + \epsilon_+ = 2\sqrt{(c|\mathbf{p}_-|)^2 + m^2c^4}, \quad (\text{B.1.8})$$

which is independent of the potential $V(\bar{r})$. The potential energies $\pm eV(\bar{r})$ of electron and positron cancel each other and do not contribute to the total energy (B.1.8) required for pair production. This energy (B.1.8) is acquired from the binding energy ($Ze^2/\bar{r} > 2mc^2$) by the electron filling into the bound state $1S_{1/2}$. A part of the binding energy becomes the kinetic energy of positron that goes out. This is analogous to the familiar case that a proton ($Z = 1$) catches an electron into the ground state $1S_{1/2}$, and a photon is emitted with the energy not less than 13.6 eV.

In this article, we study classical and semi-classical states of electrons, electron-

positron pair production in an electric potential of macroscopic cores with charge $Q = Z|e|$, mass M and macroscopic radius R_c .

B.2. Classical description of electrons in potential of cores

B.2.1. Effective potentials for particle's radial motion

Setting the origin of spherical coordinates (r, θ, ϕ) at the center of such cores, we write the vectorial potential $A_\mu = (\mathbf{A}, A_0)$, where $\mathbf{A} = 0$ and A_0 is the Coulomb potential. The motion of a relativistic electron with mass m and charge e is described by its radial momentum p_r , total angular momenta p_ϕ and the Hamiltonian,

$$H_\pm = \pm mc^2 \sqrt{1 + \left(\frac{p_r}{mc}\right)^2 + \left(\frac{p_\phi}{mcr}\right)^2} - V(r), \quad (\text{B.2.1})$$

where the potential energy $V(r) = eA_0$, and \pm corresponds for positive and negative energies. The states corresponding to negative energy solutions are fully occupied. The total angular momentum p_ϕ is conserved, for the potential $V(r)$ is spherically symmetric. For a given angular momentum $p_\phi = mv_\perp r$, where v_\perp is the transverse velocity, the effective potential energy for electron's radial motion is

$$E_\pm(r) = \pm mc^2 \sqrt{1 + \left(\frac{p_\phi}{mcr}\right)^2} - V(r). \quad (\text{B.2.2})$$

Outside the core ($r \geq R_c$), the Coulomb potential energy $V(r)$ is given by

$$V_{\text{out}}(r) = \frac{Ze^2}{r}, \quad (\text{B.2.3})$$

where \pm indicates positive and negative effective energies. Inside the core ($r \leq R_c$), the Coulomb potential energy is given by

$$V_{\text{in}}(r) = \frac{Ze^2}{2R_c} \left[3 - \left(\frac{r}{R_c}\right)^2 \right], \quad (\text{B.2.4})$$

where we postulate the charged core has a uniform charge distribution with constant charge density $\rho = Ze/V_c$, and the core volume $V_c = 4\pi R_c^3/3$. Coulomb potential energies outside the core (B.2.3) and inside the core (B.2.4)

is continuous at $r = R_c$. The electric field on the surface of the core,

$$E_s = \frac{Q}{R_c^2} = \frac{\lambda_e}{R_c} E_c, \quad \beta \equiv \frac{Ze^2}{mc^2 R_c} \quad (\text{B.2.5})$$

where the electron Compton wavelength $\lambda_e = \hbar/(mc)$, the critical electric field $E_c = m^2 c^3 / (e\hbar)$ and the parameter β is the electric potential-energy on the surface of the core in unit of the electron mass-energy.

B.2.2. Stable classical orbits (states) outside the core.

Given different values of total angular momenta p_ϕ , the stable circulating orbits R_L (states) are determined by the minimum of the effective potential $E_+(r)$ (B.2.2) (see Fig. B.1), at which $dE_+(r)/dr = 0$. We obtain stable orbits locate at the radii R_L ,

$$R_L = \left(\frac{p_\phi^2}{Ze^2 m} \right) \sqrt{1 - \left(\frac{Ze^2}{cp_\phi} \right)^2}, \quad R_L \geq R_c, \quad (\text{B.2.6})$$

for different p_ϕ -values. Substituting Eq. (B.2.6) into Eq. (B.2.2), we find the energy of electron at each stable orbit,

$$\varepsilon \equiv \min(E_+) = mc^2 \sqrt{1 - \left(\frac{Ze^2}{cp_\phi} \right)^2}. \quad (\text{B.2.7})$$

For the condition $R_L \gtrsim R_c$, we have

$$\left(\frac{Ze^2}{cp_\phi} \right)^2 \lesssim \frac{1}{2} [\beta(4 + \beta^2)^{1/2} - \beta^2], \quad (\text{B.2.8})$$

where the semi-equality holds for the last stable orbits outside the core $R_L \rightarrow R_c + 0^+$. In the point-like case $R_c \rightarrow 0$, the last stable orbits are

$$cp_\phi \rightarrow Ze^2 + 0^+, \quad R_L \rightarrow 0^+, \quad \varepsilon \rightarrow 0^+. \quad (\text{B.2.9})$$

Eq. (B.2.7) shows that only positive or null energy solutions (states) to exists in the case of a point-like charge, which is the same as the energy-spectrum Eqs. (B.1.3,B.1.4,B.1.5) in quantum mechanic scenario. While for $p_\phi \gg 1$, radii of stable orbits $R_L \gg 1$ and energies $\varepsilon \rightarrow mc^2 + 0^-$, classical electrons in these orbits are critically bound for their banding energy goes to zero. We conclude that the energies (B.2.7) of stable orbits outside the core must be smaller than mc^2 , but larger than zero, $\varepsilon > 0$. Therefore, no energy-level crossing with the negative energy spectrum occurs.

B.2.3. Stable classical orbits inside the core.

We turn to the stable orbits of electrons inside the core. Analogously, using Eqs. (B.2.2,B.2.4) and $dE_+(r)/dr = 0$, we obtain the stable orbit radius $R_L \leq 1$ in the unit of R_c , obeying the following equation,

$$\beta^2(R_L^8 + \kappa^2 R_L^6) = \kappa^4; \quad \kappa = \frac{p_\phi}{mcR_c}. \quad (\text{B.2.10})$$

and corresponding to the minimal energy (binding energy) of these states

$$\varepsilon = \frac{Ze^2}{R_c} \left[\left(\frac{cp_\phi}{Ze^2} \right)^2 \frac{1}{R_L^4} - \frac{1}{2}(3 - R_L^2) \right]. \quad (\text{B.2.11})$$

There are 8 solutions to this polynomial equation (B.2.10), only one is physical solution R_L that has to be real, positive and smaller than one. As example, the numerical solution to Eq. (B.2.10) is $R_L = 0.793701$ for $\beta = 4.4 \cdot 10^{16}$ and $\kappa = 2.2 \cdot 10^{16}$. In following, we respectively adopt non-relativistic and ultra-relativistic approximations to obtain analytical solutions.

First considering the non-relativistic case for those stable orbit states whose the kinetic energy term characterized by angular momentum term p_ϕ , see Eq. (B.2.2), is much smaller than the rest mass term mc^2 , we obtain the following approximate equation,

$$\beta^2 R_L^8 \simeq \kappa^4, \quad (\text{B.2.12})$$

and the solutions for stable orbit radii are,

$$R_L \simeq \frac{\kappa^{1/2}}{\beta^{1/4}} = \left(\frac{cp_\phi}{Ze^2} \right)^{1/2} \beta^{1/4} < 1, \quad (\text{B.2.13})$$

and energies,

$$\varepsilon \simeq \left(1 - \frac{3}{2}\beta + \frac{1}{2}\kappa\beta^{1/2} \right) mc^2. \quad (\text{B.2.14})$$

The consistent conditions for this solution are $\beta^{1/2} > \kappa$ for $R_L < 1$, and $\beta \ll 1$ for non-relativistic limit $v_\perp \ll c$. As a result, the binding energies (B.2.14) of these states are $mc^2 > \varepsilon > 0$, are never less than zero. These in fact correspond to the stable states which have large radii closing to the radius R_c of cores and $v_\perp \ll c$.

Second considering the ultra-relativistic case for those stable orbit states whose the kinetic energy term characterized by angular momentum term p_ϕ , see Eq. (B.2.2), is much larger than the rest mass term mc^2 , we obtain the

following approximate equation,

$$\beta^2 R_L^6 \simeq \kappa^2, \quad (\text{B.2.15})$$

and the solutions for stable orbit radii are,

$$R_L \simeq \left(\frac{\kappa}{\beta}\right)^{1/3} = \left(\frac{p_{\phi}c}{Ze^2}\right)^{1/3} < 1, \quad (\text{B.2.16})$$

which gives $R_L \simeq 0.7937007$ for the same values of parameters β and κ in above. The consistent condition for this solution is $\beta > \kappa \gg 1$ for $R_L < 1$. The energy levels of these ultra-relativistic states are,

$$\varepsilon \simeq \frac{3}{2}\beta \left[\left(\frac{p_{\phi}c}{Ze^2}\right)^{2/3} - 1 \right] mc^2, \quad (\text{B.2.17})$$

and $mc^2 > \varepsilon > -1.5\beta mc^2$. The particular solutions $\varepsilon = 0$ and $\varepsilon \simeq -mc^2$ are respectively given by

$$\left(\frac{p_{\phi}c}{Ze^2}\right) \simeq 1; \quad \left(\frac{p_{\phi}c}{Ze^2}\right) \simeq \left(1 - \frac{2}{3\beta}\right)^{3/2}. \quad (\text{B.2.18})$$

These in fact correspond to the stable states which have small radii closing to the center of cores and $v_{\perp} \lesssim c$.

To have the energy-level crossing to the negative energy continuum, we are interested in the values $\beta > \kappa \gg 1$ for which the energy-levels (B.2.17) of stable orbit states are equal to or less than $-mc^2$,

$$\varepsilon \simeq \frac{3}{2}\beta \left[\left(\frac{p_{\phi}c}{Ze^2}\right)^{2/3} - 1 \right] mc^2 \leq -mc^2. \quad (\text{B.2.19})$$

As example, with $\beta = 10$ and $\kappa = 2$, $R_L \simeq 0.585$, $\varepsilon_{\min} \simeq -9.87mc^2$. The lowest energy-level of electron state is $p_{\phi}/(Ze^2) = \kappa/\beta \rightarrow 0$ with the binding energy,

$$\varepsilon_{\min} = -\frac{3}{2}\beta mc^2, \quad (\text{B.2.20})$$

locating at $R_L \simeq (p_{\phi}c/Ze^2)^{1/3} \rightarrow 0$, the bottom of the potential energy $V_{\text{in}}(0)$ (B.2.4).

B.3. Semi-Classical description

B.3.1. Bohr-Sommerfeld quantization

In order to have further understanding, we consider the semi-classical scenario. Introducing the Planck constant $\hbar = h/(2\pi)$, we adopt the semi-classical Bohr-Sommerfeld quantization rule

$$\int p_\phi d\phi \simeq h(l + \frac{1}{2}), \quad \Rightarrow \quad p_\phi(l) \simeq \hbar(l + \frac{1}{2}), \quad l = 0, 1, 2, 3, \dots, \quad (\text{B.3.1})$$

which are discrete values selected from continuous total angular momentum p_ϕ in the classical scenario. The variation of total angular momentum $\Delta p_\phi = \pm\hbar$ in the unit of the Planck constant \hbar . Substitution

$$\left(\frac{p_\phi c}{Ze^2}\right) \Rightarrow \left(\frac{2l+1}{2Z\alpha}\right), \quad (\text{B.3.2})$$

where the fine-structure constant $\alpha = e^2/(\hbar c)$, must be performed in classical solutions that we obtained in section (B.2).

1. The radii and energies of stable states outside the core (B.2.6) and (B.2.7) become:

$$R_L = \lambda \left(\frac{2l+1}{Z\alpha}\right) \sqrt{1 - \left(\frac{2Z\alpha}{2l+1}\right)^2}, \quad (\text{B.3.3})$$

$$\varepsilon = mc^2 \sqrt{1 - \left(\frac{2Z\alpha}{2l+1}\right)^2}, \quad (\text{B.3.4})$$

where λ is the electron Compton length.

2. The radii and energies of non-relativistic stable states inside the core (B.2.13) and (B.2.14) become:

$$R_L \simeq \left(\frac{2l+1}{2Z\alpha}\right)^{1/2} \beta^{1/4}, \quad (\text{B.3.5})$$

$$\varepsilon \simeq \left(1 - \frac{3}{2}\beta + \frac{\lambda(2l+1)}{4R_c}\beta^{1/2}\right) mc^2. \quad (\text{B.3.6})$$

3. The radii and energies of ultra-relativistic stable states inside the core

(B.2.16) and (B.2.17) become:

$$R_L \simeq \left(\frac{2l+1}{2Z\alpha} \right)^{1/3}, \quad (\text{B.3.7})$$

$$\varepsilon \simeq \frac{3}{2}\beta \left[\left(\frac{2l+1}{2Z\alpha} \right)^{2/3} - 1 \right] mc^2. \quad (\text{B.3.8})$$

Note that radii R_L in the second and third cases are in unit of R_c .

B.3.2. Stability of semi-classical states

When these semi-classical states are not occupied as required by the Pauli Principle, the transition from one state to another with different discrete values of total angular momentum l (l_1, l_2 and $\Delta l = l_2 - l_1 = \pm 1$) undergoes by emission or absorption of a spin-1 (\hbar) photon. Following the energy and angular-momentum conservations, photon emitted or absorbed in the transition have angular momenta $p_\phi(l_2) - p_\phi(l_1) = \hbar(l_2 - l_1) = \pm\hbar$ and energy $\varepsilon(l_2) - \varepsilon(l_1)$. In this transition of stable states, the variation of radius is $\Delta R_L = R_L(l_2) - R_L(l_1)$.

We first consider the stability of semi-classical states against such transition in the case of point-like charge, i.e., Eqs. (B.3.3, B.3.4) with $l = 0, 1, 2, \dots$. As required by the Heisenberg indeterminacy principle $\Delta\phi\Delta p_\phi \simeq 4\pi p_\phi(l) \gtrsim h$, the absolute ground state for minimal energy and angular momentum is given by the $l = 0$ state, $p_\phi \sim \hbar/2$, $R_L \sim \lambda(Z\alpha)^{-1} \sqrt{1 - (2Z\alpha)^2} > 0$ and $\varepsilon \sim mc^2 \sqrt{1 - (2Z\alpha)^2} > 0$, which corresponds to the last stable orbit (B.2.9) in the classical scenario. Thus the stability of all semi-classical states $l > 0$ is guaranteed by the Pauli principle. This is only case for $Z\alpha \leq 1/2$. While for $Z\alpha > 1/2$, there is not an absolute ground state in the semi-classical scenario. This can be understood by examining how the lowest energy states are selected by the quantization rule in the semi-classical scenario out of the last stable orbits (B.2.9) in the classical scenario. For the case of $Z\alpha \leq 1/2$, equating p_ϕ in Eq. (B.2.9) to $p_\phi = \hbar(l + 1/2)$ (B.3.1), we find the selected state $l = 0$ is only possible solution so that the ground state $l = 0$ in the semi-classical scenario corresponds to the last stable orbits (B.2.9) in the classical scenario. While for the case of $Z\alpha > 1/2$, equating p_ϕ in Eq. (B.2.9) to $p_\phi = \hbar(l + 1/2)$ (B.3.1), we find the selected semi-classical state

$$\tilde{l} = \frac{Z\alpha - 1}{2} > 0, \quad (\text{B.3.9})$$

in the semi-classical scenario corresponds to the last stable orbits (B.2.9) in the classical scenario. This state $l = \tilde{l} > 0$ is not protected by the Heisenberg indeterminacy principle from quantum-mechanically decaying in \hbar -steps to the

states with lower angular momenta and energies (correspondingly smaller radius R_L (B.3.3)) via photon emissions. This clearly shows that the “ $Z = 137$ -catastrophe” corresponds to $R_L \rightarrow 0$, falling to the center of the Coulomb potential and all semi-classical states (l) are unstable.

Then we consider the stability of semi-classical states against such transition in the case of charged cores $R_c \neq 0$. Substituting p_ϕ in Eq. (B.3.1) into Eq. (B.2.8), we obtain the selected semi-classical state \tilde{l} corresponding to the last stable orbit outside the core,

$$\tilde{l} = \sqrt{2} \left(\frac{R_c}{\lambda} \right) \left[\left(\frac{4R_c}{Z\alpha\lambda} + 1 \right)^{1/2} - 1 \right]^{-1/2} \approx (Z\alpha)^{1/4} \left(\frac{R_c}{\lambda} \right)^{3/4} > 0. \quad (\text{B.3.10})$$

Analogously to Eq. (B.3.9), the same argument concludes the instability of this semi-classical state, which must quantum-mechanically decay to states with angular momentum $l < \tilde{l}$ inside the core, provided these semi-classical states are not occupied. This conclusion is independent of $Z\alpha$ -value.

We go on to examine the stability of semi-classical states inside the core. In the non-relativistic case ($1 \gg \beta > \kappa^2$), the last classical stable orbits locate at $R_L \rightarrow 0$ and $p_\phi \rightarrow 0$ given by Eqs. (B.2.13,B.2.14), corresponding to the lowest semi-classical state (B.3.5,B.3.6) with $l = 0$ and energy $mc^2 > \mathcal{E} > 0$. In the ultra-relativistic case ($\beta > \kappa \gg 1$), the last classical stable orbits locate at $R_L \rightarrow 0$ and $p_\phi \rightarrow 0$ given by Eqs. (B.2.16,B.2.17), corresponding to the lowest semi-classical state (B.3.7,B.3.8) with $l = 0$ and minimal energy,

$$\mathcal{E} \simeq \frac{3}{2}\beta \left[\left(\frac{1}{2Z\alpha} \right)^{2/3} - 1 \right] mc^2 \approx -\frac{3}{2}\beta mc^2. \quad (\text{B.3.11})$$

This concludes that the $l = 0$ semi-classical state inside the core is an absolute ground state in both non- and ultra-relativistic cases. The Pauli principle assure that all semi-classical states $l > 0$ are stable, provided all these states accommodate electrons. The electrons can be either present inside the neutral core or produced from the vacuum polarization, later will be discussed in details.

We are particular interested in the ultra-relativistic case $\beta > \kappa \gg 1$, i.e., $Z\alpha \gg 1$, the energy-levels of semi-classical states can be profound than $-mc^2$ ($\mathcal{E} < -mc^2$), energy-level crossings and pair-productions occur if these states are unoccupied, as discussed in introductory section. It is even more important to mention that neutral cores like neutron stars of proton number $Z \sim 10^{52}$, the Thomas-Fermi approach has to be adopted to find the configuration of electrons in these semi-classical states, which has the depth of energy-levels $\mathcal{E} \sim -m_\pi c^2$ to accommodate electrons and a supercritical electric field ($E > E_c$) on the surface of the core (13; 71).

B.4. Production of electron-positron pair

When the energy-levels of semi-classical (bound) states $\mathcal{E} \leq -mc^2$ (B.2.19), energy-level crossings between these energy-levels (B.2.17) and negative energy continuum (B.2.2) for $p_r = 0$, as shown in Fig. B.2. The energy-level-crossing indicates that \mathcal{E} (B.2.17) and E_- (B.2.2) are equal,

$$\mathcal{E} = E_-, \quad (\text{B.4.1})$$

where angular momenta p_ϕ in \mathcal{E} (B.3.8) and E_- (B.2.2) are the same for angular-momentum conservation. The production of electron-positron pairs must takes place, provided these semi-classical (bound) states are unoccupied. The phenomenon of pair production can be understood as a quantum-mechanical tunneling process of relativistic electrons. The energy-levels \mathcal{E} of semi-classical (bound) states are given by Eq. (B.3.8) or (B.2.19). The probability amplitude for this process can be evaluated by a semi-classical calculation using WKB method (87):

$$W_{\text{WKB}}(|\mathbf{p}_\perp|) \equiv \exp \left\{ -\frac{2}{\hbar} \int_{R_b}^{R_n} p_r dr \right\}, \quad (\text{B.4.2})$$

where $|\mathbf{p}_\perp| = p_\phi/r$ is transverse momenta and the radial momentum,

$$p_r(r) = \sqrt{(c|\mathbf{p}_\perp|)^2 + m^2c^4 - [\mathcal{E} + V(r)]^2}. \quad (\text{B.4.3})$$

The energy potential $V(r)$ is either given by $V_{\text{out}}(r)$ (B.2.3) for $r > R_c$, or $V_{\text{in}}(r)$ (B.2.4) for $r < R_c$. The limits of integration (B.4.2): $R_b = R_L < R_c$ (B.2.16) or (B.3.7) indicating the location of the classical orbit (classical turning point) of semi-classical (bound) state; while another classical turning point R_n is determined by setting $p_r(r) = 0$ in Eq. (B.4.3). There are two cases: $R_n < R_c$ and $R_n > R_c$, depending on β and κ values.

To obtain a maximal WKB-probability amplitude (B.4.2) of pair production, we only consider the case that the charge core is bare and

- the lowest energy-levels of semi-classical (bound) states: $p_\phi/(Ze^2) = \kappa/\beta \rightarrow 0$, the location of classical orbit(B.2.16) $R_L = R_b \rightarrow 0$ and energy (B.2.17) $\mathcal{E} \rightarrow \mathcal{E}_{\text{min}} = -3\beta mc^2/2$ (B.2.20);
- another classical turning point $R_n \leq R_c$, since the probability is exponentially suppressed by a large tunneling length $\Delta = R_n - R_b$.

In this case ($R_n \leq R_c$), Eq. (B.4.3) becomes

$$p_r = \sqrt{(c|\mathbf{p}_\perp|)^2 + m^2c^4} \sqrt{1 - \frac{\beta^2 m^2 c^4}{4[(c|\mathbf{p}_\perp|)^2 + m^2c^4]} \left(\frac{r}{R_c}\right)^4}, \quad (\text{B.4.4})$$

and $p_r = 0$ leads to

$$\frac{R_n}{R_c} = \left(\frac{2}{\beta mc^2} \right)^{1/2} [(c|\mathbf{p}_\perp|)^2 + m^2 c^4]^{1/4}. \quad (\text{B.4.5})$$

Using Eqs. (B.4.2,B.4.4,B.4.5), we have

$$\begin{aligned} W_{\text{WKB}}(|\mathbf{p}_\perp|) &= \exp \left\{ -\frac{2^{3/2}[(c|\mathbf{p}_\perp|)^2 + m^2 c^4]^{3/4} R_c}{c\hbar(mc^2\beta)^{1/2}} \int_0^1 \sqrt{1-x^2} dx \right\} \\ &= \exp \left\{ -0.87 \frac{2^{3/2}[(c|\mathbf{p}_\perp|)^2 + m^2 c^4]^{3/4} R_c}{c\hbar(mc^2\beta)^{1/2}} \right\}. \end{aligned} \quad (\text{B.4.6})$$

Dividing this probability amplitude by the tunneling length $\Delta \simeq R_n$ and time interval $\Delta t \simeq 2\hbar\pi/(2mc^2)$ in which the quantum tunneling occurs, and integrating over two spin states and the transverse phase-space $2 \int d\mathbf{r}_\perp d\mathbf{p}_\perp / (2\pi\hbar)^2$, we approximately obtain the rate of pair-production per the unit of time and volume,

$$\Gamma_{\text{NS}} \equiv \frac{d^4 N}{dt d^3 x} \simeq \frac{1.15}{6\pi^2} \left(\frac{Z\alpha}{\tau R_c^3} \right) \exp \left\{ -\frac{2.46}{(Z\alpha)^{1/2}} \left(\frac{R_c}{\lambda} \right)^{3/2} \right\}, \quad (\text{B.4.7})$$

$$= \frac{1.15}{6\pi^2} \left(\frac{\beta}{\tau \lambda R_c^2} \right) \exp \left\{ -\frac{2.46 R_c}{\beta^{1/2} \lambda} \right\}, \quad (\text{B.4.8})$$

$$= \frac{1.15}{6\pi^2} \left(\frac{1}{\tau \lambda^2 R_c} \right) \left(\frac{E_s}{E_c} \right) \exp \left\{ -2.46 \left(\frac{R_c}{\lambda} \right)^{1/2} \left(\frac{E_c}{E_s} \right)^{1/2} \right\}, \quad (\text{B.4.9})$$

where $E_s = Ze/R_c^2$ being the electric field on the surface of the core and the Compton time $\tau = \hbar/mc^2$.

To have the size of this pair-production rate, we compare it with the Sauter-Euler-Heisenberg-Schwinger rate of pair-production in a constant field E (43; 58; 59),

$$\Gamma_{\text{S}} \equiv \frac{d^4 N}{dt d^3 x} \simeq \frac{1}{4\pi^3 \tau \lambda^3} \left(\frac{E}{E_c} \right)^2 \exp \left\{ -\pi \frac{E_c}{E} \right\}. \quad (\text{B.4.10})$$

When the parameter $\beta \simeq (R_c/\lambda)^2$, Eq. (B.4.8) becomes

$$\Gamma_{\text{NS}} \equiv \frac{d^4 N}{dt d^3 x} \simeq \frac{1.15}{6\pi^2} \left(\frac{1}{\tau \lambda^3} \right) \exp \{-2.46\} = 1.66 \cdot 10^{-3} / (\tau \lambda^3), \quad (\text{B.4.11})$$

which is close to the Sauter-Euler-Heisenberg-Schwinger rate (B.4.10) $\Gamma_{\text{S}} \simeq 3.5 \cdot 10^{-4} / (\tau \lambda^3)$ at $E \simeq E_c$. Taking a neutron star with core mass $M = M_\odot$ and radius $R_c = 10\text{km}$, we have $R_c/\lambda = 2.59 \cdot 10^{16}$ and $\beta = 3.86 \cdot 10^{-17} Z\alpha$,

leading to $Z \simeq 2.4 \cdot 10^{51}$ and the electric field on the core surface $E_s/E_c = Z\alpha(\lambda/R_c)^2 \simeq 2.6 \cdot 10^{16}$. In this case, the charge-mass ratio $Q/(G^{1/2}M) = 2 \cdot 10^{-6}|e|/(G^{1/2}m_p) = 2.2 \cdot 10^{12}$, where where G is the Newton constant and proton's charge-mass ratio $|e|/(G^{1/2}m_p) = 1.1 \cdot 10^{18}$.

Let us consider another case that the electric field on the core surface E_s (B.2.5) is about the critical field ($E_s \simeq E_c$). In this case, $Z = \alpha^{-1}(R_c/\lambda)^2 \simeq 9.2 \cdot 10^{34}$, $\beta = Z\alpha\lambda/R_c = R_c/\lambda \simeq 2.59 \cdot 10^{16}$, and the rate (B.4.8) becomes

$$\Gamma_{\text{NS}} \equiv \frac{d^4N}{dt d^3x} \simeq \frac{1.15}{6\pi^2} \left(\frac{1}{\tau\lambda^3} \right) \left(\frac{\lambda}{R_c} \right) \exp \left\{ -2.46 \left(\frac{R_c}{\lambda} \right) \right\}, \quad (\text{B.4.12})$$

which is exponentially smaller than Eq. (B.4.11) for $R_c \gg \lambda$. In this case, the charge-mass ratio $Q/(G^{1/2}M) = 8.46 \cdot 10^{-5}$.

It is interesting to compare this rate of electron-positron pair-production with the rate given by the Hawking effect. We take $R_c = 2GM/c^2$ and the charge-mass ratio $Q/(G^{1/2}M) \simeq 10^{-19}$ for a naive balance between gravitational and electric forces. In this case $\beta = \frac{1}{2}(Q/G^{1/2}M)(|e|/G^{1/2}m) \simeq 10^2$, the rate (B.4.8) becomes,

$$\Gamma_{\text{NS}} = \frac{1.15}{6\pi^2} \left(\frac{25}{\tau\lambda^3} \right) \left(\frac{1}{mM} \right) \exp \{-0.492(mM)\}, \quad (\text{B.4.13})$$

where $mM = R_c/(2\lambda)$. This is much larger than the rate of electron-positron emission by the Hawking effect (88),

$$\Gamma_{\text{H}} \sim \exp \{-8\pi(mM)\}, \quad (\text{B.4.14})$$

since the exponential factor $\exp \{-0.492(mM)\}$ is much larger than $\exp \{-8\pi(mM)\}$, where $2mM = R_c/\lambda \gg 1$.

B.5. Summary and remarks

In this letter, analogously to the study in atomic physics with large atomic number Z , we study the classical and semi-classical (bound) states of electrons in the electric potential of a massive and charged core, which has a uniform charge distribution and macroscopic radius. We have found negative energy states of electrons inside the core, whose energies can be smaller than $-mc^2$, and the appearance of energy-level crossing to the negative energy spectrum. As results, quantum tunneling takes place, leading to electron-positron pairs production, electrons then occupy these semi-classical (bound) states and positrons are repelled to infinity. Assuming that massive charged cores are bare and non of these semi-classical (bound) states are occupied, we analytically obtain the maximal rate of electron-positron pair production in terms of core's radius, charge and mass, and we compare it with the Sauter-

Euler-Heisenberg-Schwinger rate of pair-production in a constant field. We have seen that even for very small charge-mass ratio of the core that is given by the naive balance between gravitational and electric forces, this rate is much larger than the rate of electron-positron pair-production by the Hawking effect.

Any electron occupations of these semi-classical (bound) states must screen core's charge and the massive core is no longer bare. The electric potential inside the core is changed. For the core consists of a large number of electrons, the Thomas-Fermi approach has to be adopted. We recently study (13; 71) the electron distribution inside and outside the massive core, i.e., the distribution of electrons occupying stable states of the massive core, and find the electric field on the surface of the massive core is overcritical.

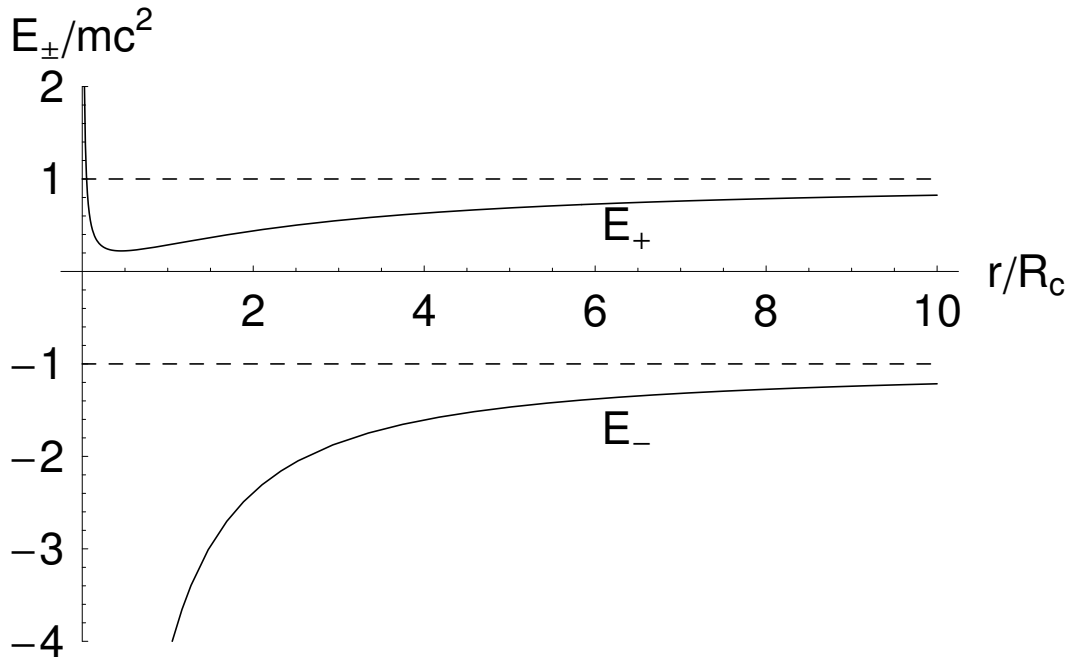


Figure B.1.: In the case of point-like charge distribution, we plot the positive and negative effective potential energies E_{\pm} (B.2.2), $p_{\phi}/(mcR_c) = 2$ and $Ze^2 = 1.95mc^2R_c$, to illustrate the radial location R_L (B.2.6) of stable orbits where E_+ has a minimum (B.2.7). All stable orbits are described by $cp_{\phi} > Ze^2$. The last stable orbits are given by $cp_{\phi} \rightarrow Ze^2 + 0^+$, whose radial location $R_L \rightarrow 0$ and energy $\mathcal{E} \rightarrow 0^+$. There is no any stable orbit with energy $\mathcal{E} < 0$ and the energy-level crossing with the negative energy spectrum E_- is impossible.

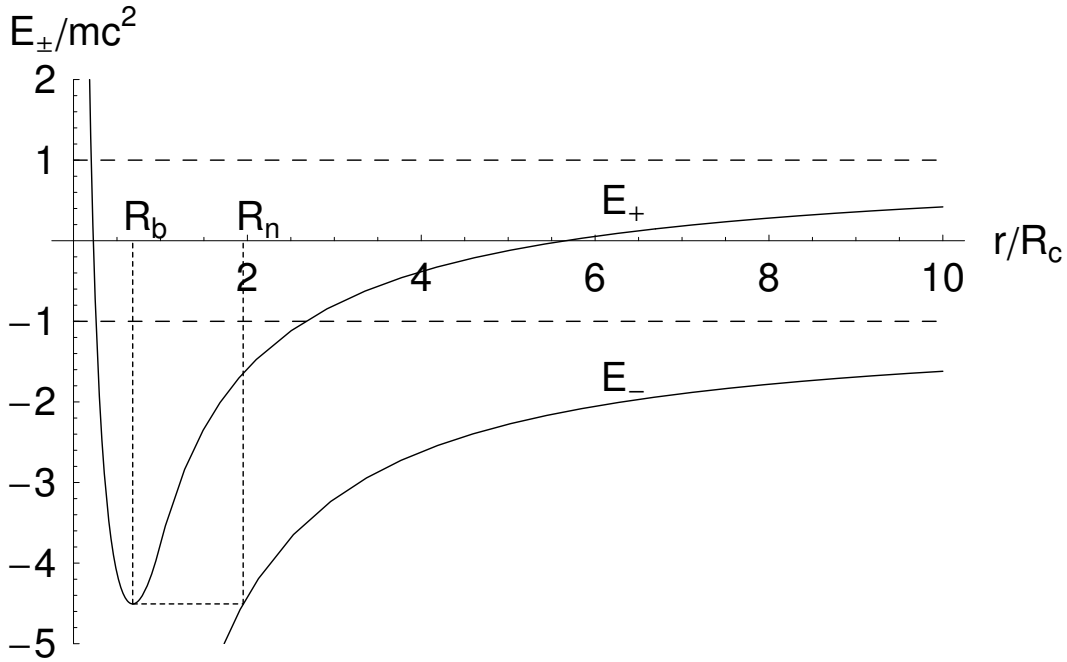


Figure B.2.: For the core $\kappa = 2$ and $\beta = 6$, we plot the positive and negative effective potentials E_{\pm} (B.2.2), in order to illustrate the radial location (B.2.16) $R_L < R_c$ of stable orbit, where E_+ 's minimum (B.2.17) $\mathcal{E} < mc^2$ is. All stable orbits inside the core are described by $\beta > \kappa > 1$. The last stable orbit is given by $\kappa/\beta \rightarrow 0$, whose radial location $R_L \rightarrow 0$ and energy $\mathcal{E} \rightarrow \mathcal{E}_{\min}$ (B.2.20). We indicate that the energy-level crossing between bound state (stable orbit) energy at $R_L = R_b$ and negative energy spectrum E_- (B.2.17) at the turning point R_n .

C. On the self-consistent general relativistic equilibrium equations of neutron stars

One of the fundamental issues in physics and astrophysics is the creation of an electron-positron plasma in overcritical electric fields larger than $E_c = m_e^2 c^3 / (e\hbar)$ (see (1) and references therein). Basic progress toward the understanding of the thermalization process of such a plasma have been achieved (118). The existence of such an electron-positron plasma has a central role in a variety of problems ranging from the acceleration process in gamma ray bursts (GRBs) (1) to the sharp trigger process in supernova phenomena (119; 120). This has motivated us to reconsider the standard treatment of neutron stars in order to find a theoretical explanation for the emergence of a wide variety of astrophysical situations involving such overcritical electric fields. In a classic article Baym, Bethe and Pethick (26) presented the problem of matching to the crust in a neutron star a liquid core composed of N_n neutrons, N_p protons and N_e electrons. After discussing various aspects of the problem they conclude: ‘the details of this picture requires further elaboration; this is a situation for which the Thomas-Fermi method is useful.’ In this letter we focus on relaxing the traditional condition of local charge neutrality $n_e = n_p$, which appears to have been assumed only for mathematical convenience without any physical justification. Instead, we adopt the more general condition of global charge neutrality $N_e = N_p$. The corresponding equilibrium equations then follow from self-consistent solution of the relativistic Thomas-Fermi equation, the Einstein-Maxwell equations and the β -equilibrium condition, properly expressed in general relativity.

The pressure and the density of the core are mainly due to the baryons while the pressure of the crust is mainly due to the electrons with the density due to the nuclei and possibly some free neutrons due to neutron drip (see e.g. (26)). The boundary conditions determined by the matching of the electron distribution in the core with that of the electrons of the crust are fundamental for the self-consistent construction of the equilibrium configurations.

We consider the case of a non-rotating neutron star with metric

$$ds^2 = e^\nu dt^2 - e^\lambda dr^2 - r^2 d\theta^2 - r^2 \sin^2 \theta d\phi^2, \quad (\text{C.0.1})$$

where ν and λ are functions only of r . We assume units where $G = \hbar = c = 1$

and let α denote the fine structure constant. As usual we define the mass of the star $M(r)$ by $e^{-\lambda} = 1 - 2M/r + r^2 E^2$, and denote the Coulomb potential by $V(r)$, which determines the electric field $E = e^{-(\nu+\lambda)/2} V'$, where a prime indicates the radial derivative. The combined energy-momentum tensor of the matter and fields $T_{\mu\nu}$ is given by

$$T_{\beta}^{\alpha} = \text{diag}(\mathcal{E} + \mathcal{E}^{em}, -P - P^{em}, -P + P^{em}, -P + P^{em}), \quad (\text{C.0.2})$$

where $\mathcal{E}^{em} = P^{em} = E^2/(8\pi)$, and \mathcal{E} and P are the energy density and pressure of matter. With all the above definitions, the time-independent Einstein-Maxwell field equations read

$$M' = 4\pi r^2 \mathcal{E} + 4\pi e^{\lambda/2} r^3 e E (n_p - n_e), \quad (\text{C.0.3})$$

$$e^{-\lambda} \left(\frac{\nu'}{r} + \frac{1}{r^2} \right) - \frac{1}{r^2} = -8\pi T_1^1, \quad (\text{C.0.4})$$

$$e^{-\lambda} \left[\nu'' + (\nu' - \lambda') \left(\frac{\nu'}{2} + \frac{1}{r} \right) \right] = -16\pi T_2^2, \quad (\text{C.0.5})$$

$$(eV)'' + (eV)' \left[\frac{2}{r} - \frac{(\nu' + \lambda')}{2} \right] = -4\pi \alpha e^{\nu/2} e^{\lambda} (n_p - n_e). \quad (\text{C.0.6})$$

In order to close the system of equilibrium equations, the condition of local charge neutrality $n_e = n_p$ has been traditionally imposed for mathematical simplicity. In this case the problem is reduced to solving only the Einstein equations for a Schwarzschild metric. When this condition is relaxed, imposing only global charge neutrality $N_e = N_p$, we need to satisfy the Einstein-Maxwell equations (C.0.3)–(C.0.6). In order to impose global charge neutrality as well as quantum statistics on the leptonic component, the general relativistic Thomas-Fermi equation must also be satisfied.

The general relativistic electron Fermi energy is given by

$$E_e^F = e^{\nu/2} \mu_e - eV = \text{constant}, \quad (\text{C.0.7})$$

where $\mu_e = \sqrt{(P_e^F)^2 + m_e^2}$ and $P_e^F = (3\pi^2 n_e)^{1/3}$ are respectively the chemical potential and Fermi momentum of degenerate electrons. From Eqs. (C.0.6) and (C.0.7) we obtain the general relativistic Thomas-Fermi equation

$$(eV)'' + (eV)' \left[\frac{2}{r} - \frac{(\nu' + \lambda')}{2} \right] = -4\pi \alpha e^{\nu/2} e^{\lambda} \left\{ n_p - \frac{e^{-3\nu/2}}{3\pi^2} [(E_e^F + eV)^2 - m_e^2 e^{\nu}]^{3/2} \right\}. \quad (\text{C.0.8})$$

The β -equilibrium condition is expressed by

$$\mu_n = \mu_e + \mu_p. \quad (\text{C.0.9})$$

In order to take into account the effect of the compression of the crust on the leptonic component of the core we solve the equilibrium conditions for the core within a Wigner-Seitz cell (33). The radius R_{WS} of this cell determines the Fermi energy of the electrons of the core which has to be matched with the Fermi energy of the leptonic component of the crust. Global charge neutrality is specified by

$$\int_0^{R_{WS}} e^{\lambda/2} n_p d^3r = \int_0^{R_{WS}} e^{\lambda/2} n_e d^3r. \quad (\text{C.0.10})$$

From Eqs. (C.0.9) and (C.0.10) we can determine self-consistently the proton, neutron, electron fractions inside the core as well as the radius R_{WS} of the Wigner-Seitz cell of the core (33).

The coupled system of equations consisting of the Einstein-Maxwell equations (C.0.3)–(C.0.5), the general relativistic Thomas-Fermi equation (C.0.8), the β -equilibrium condition (C.0.9) along with the constraint (C.0.10) needs, in order to be closed, an equation of state (EOS) for the baryonic component in the core and for the leptonic component of the crust.

In order to illustrate the application of this approach we adopt, as an example, the Baym, Bethe, and Pethick (BBP) (26) strong interaction model for the baryonic matter in the core as well as for the white-dwarf-like material of the crust. The general conclusions we reach will in fact be independent of the details of this model.

At the neutron star radius $r = R$, all the electro-dynamical quantities must be zero as a consequence of the global charge neutrality condition. Consequently, we have a matching condition with the Schwarzschild spacetime which imposes the boundary condition

$$e^{v(R)/2} = \sqrt{1 - \frac{2M(R)}{R}}. \quad (\text{C.0.11})$$

The boundary conditions at the center correspond to $M(0) = 0$ and the regularity condition to $n_e(0) = n_p(0)$. From the β -equilibrium condition (C.0.9), we can evaluate the central chemical potentials $\mu_e(0)$, $\mu_p(0)$, and $\mu_n(0)$, or equivalently, the central number densities $n_e(0)$, $n_p(0)$, and $n_n(0)$ (121). From Eq. (C.0.7) we also have the relation

$$e^{v(0)/2} = \frac{E_e^F + eV(0)}{\mu_e(0)}. \quad (\text{C.0.12})$$

Having determined the boundary conditions at infinity and at the center, we turn now to the matching conditions at the surface of the core. Following BBP (26), the neutron profile at the core-crust interface is given by

$$n_n(z) = n_n^{crust} + (n_n^{core} - n_n^{crust})f(z/b). \quad (\text{C.0.13})$$

We have defined $n_n^{core} = n_n(R_c)$ and $n_n^{crust} = n_n(R_{WS})$. Here R_c is the radius of the core defined as the point where the rest-mass density reaches the nuclear saturation density, i.e., $\rho(R_c) = \rho_0 \simeq 2.7 \times 10^{14} \text{ g cm}^{-3}$ (26). The function $f(z/b)$ satisfies $f(-\infty) = 1$, $f(\infty) = 0$, where $b \simeq (n_n^{core} - n_n^{crust})^{-1/3} \simeq 1/m_\pi$ (26). As proposed by BBP, an appropriate choice for the function $f(z/b)$ is the Woods-Saxon profile $f(z/b) = (1 + e^{z/b})^{-1}$. The z -coordinate lines are perpendicular to the sharp surface separating two semi-infinite regions (core and crust) in the planar approximation (26); the neutron density approaches n_n^{core} as $z \rightarrow -\infty$ and n_n^{crust} as $z \rightarrow \infty$.

The matching between the core and the crust occurs at the radius R_{WS} , where we have $V'(R_{WS}) = 0$ by virtue of the global neutrality condition given by Eq. (C.0.10), and we also choose the value of the Coulomb potential $V(R_{WS}) = 0$. From the electron chemical potential $\mu_e(R_{WS})$ at the edge of the crust, we calculate the corresponding neutron chemical potential $\mu_n(R_{WS})$ according to the BBP treatment. If $\mu_n(R_{WS}) - m_n > 0$, neutron drip occurs. In this case, the pressure is due to the neutrons as well as to the leptonic component, so we have the inner crust (see Table C.1 and (26; 121) for details). For larger values of the radii, i.e., for $r > R_{WS}$ the condition $\mu_n(r) - m_n < 0$ is reached at $\rho_{drip} \simeq 4.3 \times 10^{11} \text{ g cm}^{-3}$ and there the outer crust starts, with the pressure only determined by the leptonic component. If $\mu_n(R_{WS}) - m_n < 0$, only the outer crust exists.

For a fixed central rest-mass density $\rho(0) \simeq 9.8 \times 10^{14} \text{ g cm}^{-3}$ and selected values of E_e^F we have integrated the system of equations composed by the general relativistic Thomas-Fermi equation (C.0.8), the β -equilibrium condition (C.0.9), the Einstein-Maxwell equations (C.0.3)-(C.0.5), with the constraint of overall neutrality (C.0.10).

We found that although the electro-dynamical properties of the core are very sensitive to the Fermi energy of the electrons (see Table C.1 for details), the bulk properties of the core like its mass and radius are not sensitive to the value of E_e^F . This is perfectly in line with the results of Ruffini et al. in (33).

Particularly interesting are the electro-dynamical structure and the distribution of neutrons, protons, and electrons as the surface of the core is approached (see Fig. C.1). It is interesting to compare and contrast these results with the preliminary ones obtained in the simplified model of massive nuclear density cores (33). The values of the electric field are quite close and are not affected by the constant proton density distribution assumed there. In the present case, the proton distribution is far from constant and increases outward as the core surface is approached.

In conclusion, for any given value of the central density an entire new family of equilibrium configurations exists. Each configuration is characterized by a strong electric field at the core-crust interface. Such an electric field extends over a thin shell of thickness $\sim 1/m_e$ and becomes largely overcritical in the limit of decreasing values of the crust mass and size (see Table C.1 and Fig. C.1).

$\frac{E_e^F}{m_\pi}$	$\frac{M(R_c)}{M_\odot}$	$R_c(\text{km})$	$\frac{eV(0)}{m_\pi}$	$\frac{eV(R_c)}{m_\pi}$	$\frac{E_{max}}{E_c}$	$\frac{\rho_{crust}}{\rho_{drip}}$	$\frac{M_{crust}}{M_\odot}$	$\Delta_r^{ic}(\text{m})$	$\Delta_r^{oc}(\text{km})$
0.10	0.24	5.98	1.085	0.60	388.72	0.125	2.45×10^{-6}	0.00	0.797
0.15	0.24	5.98	0.985	0.55	381.04	0.384	1.15×10^{-5}	0.00	1.251
0.20	0.24	5.98	0.935	0.50	370.89	1.000	4.45×10^{-5}	0.00	1.899
0.30	0.24	5.98	0.835	0.40	346.67	46.19	4.83×10^{-5}	1.89	1.899
0.35	0.24	5.98	0.785	0.35	332.43	80.83	5.42×10^{-5}	2.85	1.899

Table C.1.: Results of the numerical integration of the BBP model for selected values of E_e^F for $\rho(0) \simeq 9.8 \times 10^{14} \text{ g cm}^{-3}$. We show the mass and radius of the core $M(R_c)$ and R_c , the Coulomb potential at the center and at the core surface $eV(0)$ and $eV(R_c)$, the peak of the electric field in the core-crust interface E_{max} , the rest-mass density at the edge of the crust $\rho_{crust} \equiv \rho(R_{WS})$, the mass of the crust M_{crust} , and the inner and outer crust thickness Δ_r^{ic} and Δ_r^{oc} .

These configurations endowed with overcritical electric fields are indeed stable against the quantum instability of pair creation because of the Pauli blocking of the degenerate electrons (1). It is expected that during the gravitational collapse phases leading to the formation of a neutron star, a large emission of electron-positron pairs will occur prior to reaching a stable ground state configuration. Similarly during the merging of two neutron stars or a neutron star and a white-dwarf leading to the formation of a black hole, an effective dyadotorus (122) will be formed leading to very strong creation of an electron-positron plasma. In both cases the basic mechanism which makes gravitational collapse depart from a pure gravitational phenomena is due to the electro-dynamical process introduced in this letter.

Finally, it is appropriate to recall that the existence of overcritical fields on macroscopic objects of $M \sim M_\odot$ and $R \sim 10 \text{ km}$ was first noted in the treatment of quark stars (28; 27; 29; 30). In that case the relativistic Thomas-Fermi equations were also considered. However, in all of these investigations, a hybrid combination of general and special relativistic treatments was adopted, resulting in an inconsistency in the boundary conditions (see (121)). The treatment given here in this letter is the first self-consistent treatment of the general relativistic Thomas-Fermi equations, the beta equilibrium condition and the Einstein-Maxwell equations. Critical fields are indeed obtained on the surface of the neutron star core involving only neutrons, protons, and electrons, their fundamental interactions, and with no quarks present.

While we were preparing our work an extremely interesting observational problematic has emerged from the Chandra observations of Cas A CCO (123; 124). It is with a similar steadily emitting and non-pulsating neutron star that our theoretical predictions can be tested. In particular, the existence for each

C. On the self-consistent general relativistic equilibrium equations of neutron stars

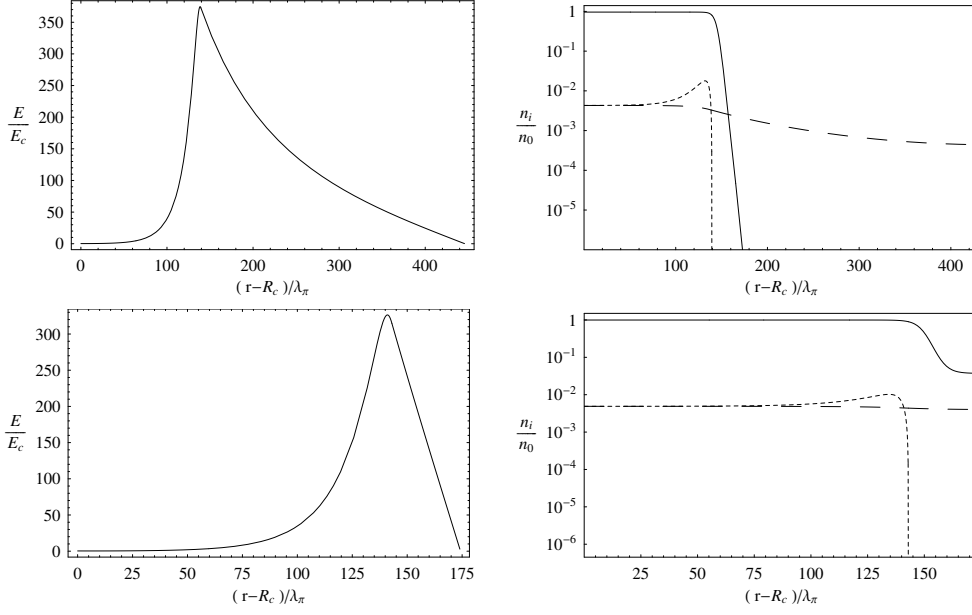


Figure C.1.: Left column: the surface electric field in units of the critical field. Right column: the surface particle number density of neutrons (solid), protons (short-dashed), and electrons (long-dashed) normalized to the nuclear density for selected values of E_e^F . First row: $E_e^F = 0.20m_\pi$, second row $E_e^F = 0.35m_\pi$.

central density of a new family of neutron stars with a smaller crust than the one obtained when the local neutrality condition is adopted.

Indeed, the existence of neutron stars with huge crusts, i.e., with both inner and outer crusts, is mainly a consequence of assuming no electrodynamical structure (i.e., assuming local neutrality) and of allowing electrons to have larger values of their Fermi energy E_e^F (see details in (121)). It can also be demonstrated that no consistent solution of the Einstein-Maxwell equations satisfying the local $n_e = n_p$ condition exists, even as a limiting case (121).

D. The Outer Crust of Neutron Stars

The General Relativistic Model. The Outer Crust of Neutron Stars is the region of Neutron Stars characterized by a mass density less than the “neutron drip” density $\rho_{drip} = 4.3 \cdot 10^{11} \text{ g cm}^{-3}$ (92) and composed by White Dwarf - like material (fully ionized nuclei and free electrons). Its internal structure can be described by the Tolman-Oppenheimer-Volkoff (TOV) equation

$$\frac{dP}{dr} = -\frac{G \left(\rho + \frac{P}{c^2} \right) \left(m + \frac{4\pi r^3 P}{c^2} \right)}{r^2 \left(1 - \frac{2Gm}{rc^2} \right)}, \quad (\text{D.0.1})$$

together with the equation

$$\frac{dm}{dr} = 4\pi r^2 \rho, \quad (\text{D.0.2})$$

where m , ρ and P are the mass, the density and the pressure of the system. We have determined M_{crust} and ΔR_{crust} by integrating eq. (D.0.1) and (D.0.2) from $r_{in} = R_{is}$, where R_{is} is the radius of the inner part of the star (the base of the Outer Crust).

The pressure and the mass density of the system are

$$P \approx P_e, \quad (\text{D.0.3})$$

$$\rho \approx \mu_e m_n n_e. \quad (\text{D.0.4})$$

P_e is the pressure of electrons, given by (93)

$$P_e = k_e \phi_e, \quad (\text{D.0.5})$$

where

$$k_e = \frac{m_e c^2}{8\pi^2 \lambda_e^3}, \quad (\text{D.0.6})$$

$$\phi_e = \quad (\text{D.0.7})$$

$$\zeta_e \left(\frac{2}{3} \zeta_e^2 - 1 \right) \sqrt{\zeta_e^2 - 1} + \log \left(\zeta_e + \sqrt{\zeta_e^2 - 1} \right), \quad (\text{D.0.8})$$

with λ_e the Compton wavelenght of electrons, $\xi_e = \sqrt{1 + x_e^2}$ and x_e the Fermi momentum of electrons normalized to $(m_e c)$. μ_e is the mean molecular weight per electron that, for a completely ionized element of atomic weight A and number Z , is equal to A/Z (for simplicity, we assume $\mu_e = 2$), m_n is the mass of neutrons and n_e is the number density of electrons

$$n_e = \frac{x_e^3}{3\pi^2 \lambda_e^3}. \quad (\text{D.0.9})$$

In eq. (D.0.4) we have assumed the local charge neutrality of the system.

The mass and the thickness of the crust. We have integrated eq. (D.0.1) and (D.0.2) for different sets of initial conditions; in fig. D.1 are shown the results obtained assuming

$$\begin{aligned} 10 \text{ km} &\leq R_{is} \leq 20 \text{ km}, \\ 1M_\odot &\leq M_{is} \leq 3M_\odot \end{aligned}$$

and an initial pressure equal to $1.6 \cdot 10^{30} \text{ dyne cm}^{-2}$, that corresponds to a mass density equal to ρ_{drip} .

It can be seen that M_{crust} has values ranging from $10^{-6}M_\odot$ to $10^{-3}M_\odot$; both M_{crust} and ΔR_{crust} increase by increasing R_{is} and decreasing M_{is} (see fig. D.1, D.2).

It's important to note that the values estimated for M_{crust} strongly depend on the values of M_{is} and R_{is} used; in particular, the values of M_{is} considered are greater than the maximum mass calculated for neutrons stars with a core of degenerate relativistic electrons, protons and neutrons in local charge neutrality ($M_{max} = 0.7M_\odot$ (47)). The outstanding theoretical problem to address is to identify the physical forces influencing such a strong departure; the two obvious candidate are the electromagnetic structure in the core and/or the strong interactions.

The Fireshell Model of GRBs. In the Fireshell Model (41) GRBs are generated by the gravitational collapse of the star progenitor to a charged black hole. The electron-positron plasma created in the process of black hole (BH) formation expands as a spherically symmetric "fireshell". It evolves and encounters the *baryonic remnant* of the star progenitor of the newly formed BH, then is loaded with baryons and expands until the transparency condition is reached and the Proper - GRB is emitted. The afterglow emission starts due to the collision between the remaining optically thin fireshell and the Circum-Burst Medium. A schematization of the model is shown in fig. D.3.

The baryon loading is measured by the dimensionless quantity

$$B = \frac{M_B c^2}{E_{dya}}, \quad (\text{D.0.10})$$

GRB	M_B/M_\odot
970228	5.0×10^{-3}
050315	4.3×10^{-3}
061007	1.3×10^{-3}
991216	7.3×10^{-4}
011121	9.4×10^{-5}
030329	5.7×10^{-5}
060614	4.6×10^{-6}
060218	1.3×10^{-6}

Table D.1.: GRBs and correspondent values of M_B used to reproduce the observed data within the Fireshell Model (94), in units of solar masses.

where M_B is the mass of the baryonic remnant and E_{dya} is the energy of the dyadosphere, the region outside the horizon of a BH where the electric field is of the order of the critical value for electron positron pair creation (43), (58) and (59)

$$E_c = \frac{m_e^2 c^3}{e \hbar} \approx 10^{16} \text{ V cm}^{-1}. \quad (\text{D.0.11})$$

B and E_{dya} are the two free parameters of the model.

The mass of the crust and M_B . Using the values of B and E_{dya} constrained by the observational data of several GRBs (94) and eq. (D.0.10), we have obtained the correspondent values of M_B (see table D.1). It can be seen that these values are compatible with the ones of M_{crust} .

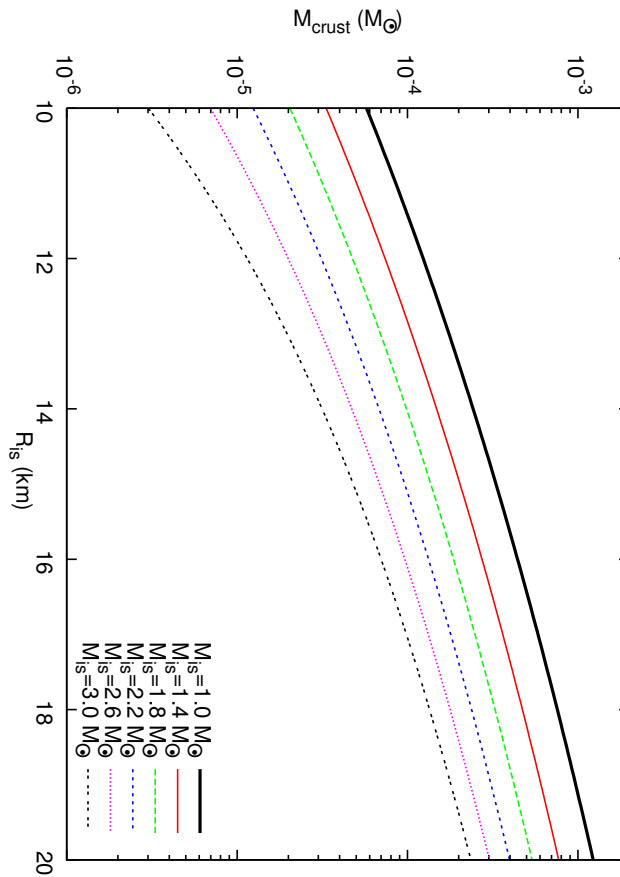


Figure D.1.: Values of M_{crust} in units of solar masses, as function of R_{is} , for different values of M_{is} (see legend).

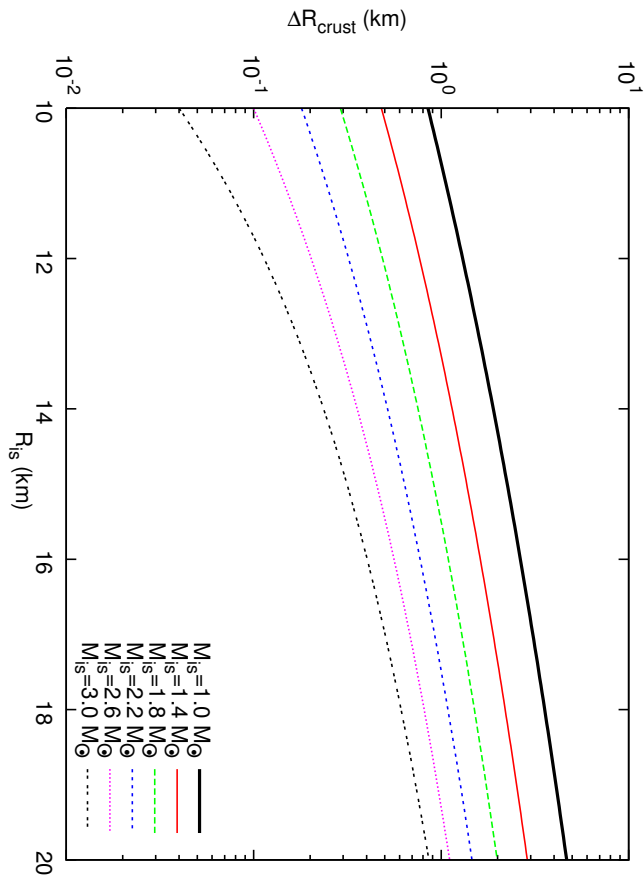


Figure D.2.: Values of thickness of the Outer Crust ΔR_{crust} in km, as function of R_{is} , for different values of M_{is} (see legend).

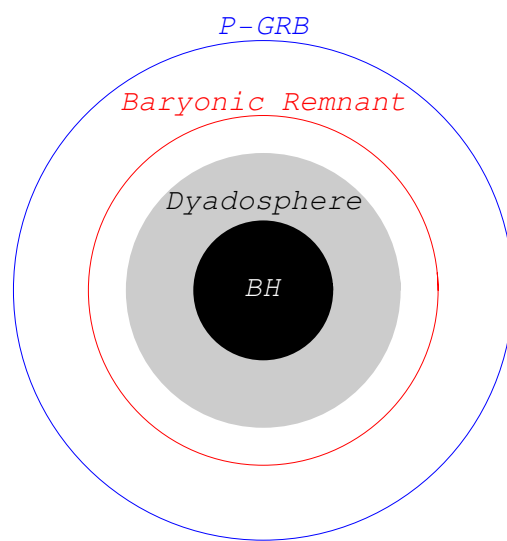


Figure D.3.: Schematization of the Fireshell Model of GRBs.

E. The Role of Thomas - Fermi approach in Neutron Star Matter

Introduction.

We first recall how certainly one of the greatest success in human understanding of the Universe has been the research activity started in 1054 by Chinese, Korean and Japanese astronomers by the observations of a "Guest Star" (see e.g. Shklovsky (95)), followed by the discovery of the Pulsar *NPO532* in the Crab Nebula in 1967, (see e.g. Manchester and Taylor (96)), still presenting challenges in the yet not identified physical process originating the expulsion of the remnant in the Supernova explosion (see e.g. Mezzacappa and Fuller (40) and Fig. E.1(a)). We are currently exploring the neutron star equilibrium configuration for a missing process which may lead to the solution of the above mentioned astrophysical puzzle.

We also recall an additional astrophysical observation which is currently capturing the attention of Astrophysicists worldwide: the Gamma ray Bursts or for short GRBs. Their discovery was accidental and triggered by a very unconventional idea proposed by Yacov Borisovich Zel'dovich (see e.g. (97)). It is likely that this idea served as an additional motivation for the United States of America to put a set of four Vela Satellites into orbit, 150,000 miles above the Earth. They were top-secret omnidirectional detectors using atomic clocks to precisely record the arrival times of both X-rays and γ -rays (see Fig. E.1(b)). When they were made operational they immediately produced results (see Fig. E.1(b)). It was thought at first that the signals originated from nuclear bomb explosions on the earth but they were much too frequent, one per day! A systematic analysis showed that they had not originated on the earth, nor even in the solar system. These Vela satellites had discovered GRBs! The first public announcement of this came at the AAAS meeting in San Francisco in a special session on neutron stars, black holes and binary X-ray sources, organized by Herb Gursky and myself (98).

A few months later, Thibault Damour and myself published a theoretical framework for GRBs based on the vacuum polarization process in the field of a Kerr–Newman black hole (45). We showed how the pair creation predicted by the Heisenberg–Euler–Schwinger theory (43; 59) would lead to a transfor-

mation of the black hole, asymptotically close to reversibility. The electron-positron pairs created by this process were generated by what we now call the blackholic energy (97). In that paper we concluded that this “naturally leads to a very simple model for the explanation of the recently discovered GRBs”. Our theory had two very clear signatures. It could only operate for black holes with mass M_{BH} in the range $3.2-10^6 M_{\odot}$ and the energy released had a characteristic value of

$$E = 1.8 \times 10^{54} M_{BH}/M_{\odot} \text{ ergs.} \quad (\text{E.0.1})$$

Since nothing was then known about the location and the energetics of these sources we stopped working in the field, waiting for a clarification of the astrophysical scenario.

The situation changed drastically with the discovery of the “afterglow” of GRBs (100) by the joint Italian-Dutch satellite BeppoSAX (see Fig. E.1(b)). This X-ray emission lasted for months after the “prompt” emission of a few seconds duration and allowed the GRB sources to be identified much more accurately. This then led to the optical identification of the GRBs by the largest telescopes in the world, including the Hubble Space Telescope, the KECK telescope in Hawaii and the VLT in Chile (see Fig. E.1(b)). Also, the very large array in Socorro made the radio identification of GRBs possible. The optical identification of GRBs made the determination of their distances possible. The first distance measurement for a GRB was made in 1997 for GRB970228 and the truly enormous of isotropical energy of this was determined to be 10^{54} ergs per burst. This proved the existence of a single astrophysical system emitting as much energy during its short lifetime as that emitted in the same time by all other stars of all galaxies in the Universe!^a It is interesting that this “quantum” of astrophysical energy coincided with the one Thibault Damour and I had already predicted, see Eq. (E.0.1). Much more has been learned on GRBs in recent years confirming this basic result (see e.g. (41)). The critical new important step now is to understand the physical process leading to the critical fields needed for the pair creation process during the gravitational collapse process from a Neutron Stars to a Black Hole.

As third example, we recall the galactic ‘X-ray bursters’ as well as some observed X-ray emission precursor of supernovae events (101). It is our opinion that the solution of: **a)** the problem of explaining the energetics of the emission of the remnant during the collapse to a Neutron Star, **b)** the problem of formation of the supercritical fields during the collapse to a Black Hole, **c)** the less energetics of galactic ‘X-ray bursters’ and of the precursor of the supernovae explosion event, will find their natural explanation from a yet unexplored field: the electro-dynamical structure of a neutron star. We will

¹Luminosity of average star = 10^{33} erg/s, Stars per galaxy = 10^{12} , Number of galaxies = 10^9 . Finally, $33 + 12 + 9 = 54!$

outline a few crucial ideas of how a Thomas-Fermi approach to a neutron star can indeed represent an important step in identify this crucial new feature.

Thomas-Fermi model.

We first recall the basic Thomas-Fermi non relativistic Equations (see e.g. Landau and Lifshitz (102)). They describe a degenerate Fermi gas of N_{el} electrons in the field of a point-like nucleus of charge Ze . The Coulomb potential $V(r)$ satisfies the Poisson equation

$$\nabla^2 V(r) = 4\pi en, \quad (\text{E.0.2})$$

where the electron number density $n(r)$ is related to the Fermi momentum p_F by $n = p_F^3 / (3\pi^2 \hbar^3)$. The equilibrium condition for an electron, of mass m , inside the atom is expressed by $\frac{p_F^2}{2m} - eV = E_F$. To put Eq. (E.0.2) in dimensionless form, we introduce a function ϕ , related to Coulomb potential by $\phi(r) = V(r) + \frac{E_F}{e} = Ze \frac{\chi(r)}{r}$. Assuming $r = bx$, with $b = \frac{(3\pi)^{3/2}}{2^{7/3}} \frac{1}{Z^{1/3}} \frac{\hbar^2}{me^2}$, we then have the universal equation (64; 65)

$$\frac{d^2 \chi(x)}{dx^2} = \frac{\chi(x)^{3/2}}{x^{1/2}}. \quad (\text{E.0.3})$$

The first boundary condition for this equation follows from the request that approaching the nucleus one gets the ordinary Coulomb potential therefore $\chi(0) = 1$. The second boundary condition comes from the fact that the number of electrons N_{el} is $1 - \frac{N_{el}}{Z} = \chi(x_0) - x_0 \chi'(x_0)$.

White dwarfs and Neutron Stars as Thomas-Fermi systems.

It was at the 1972 Les Houches organized by Bryce and Cecille de Witt summer School (see Fig. E.2(a) and (103)) that, generalizing a splendid paper by Landau (104), I introduced a Thomas-Fermi description of both White Dwarfs and Neutron Stars within a Newtonian gravitational theory and describing the microphysical quantities by a relativistic treatment. The equilibrium condition for a self-gravitating system of fermions, in relativistic regime is $c\sqrt{p_F^2 + m_n^2 c^2} - m_n c^2 - m_n V = -m_n V_0$, where p_F is the Fermi momentum of a particle of mass m_n , related to the particle density n by $n = \frac{1}{3\pi^2 \hbar^3} p_F^3$. $V(r)$ is the gravitational potential at a point at distance r from the center of the configuration and V_0 is the value of the potential at the boundary R_c of the configuration $V_0 = \frac{GNm_n}{R_c}$. N is the total number of particles. The Poisson equation is $\nabla^2 V = -4\pi Gm_n n$. Assuming $V - V_0 = GNm_n \frac{\chi(r)}{r}$ and $r = bx$, with $b = \frac{(3\pi)^{2/3}}{2^{7/3}} \frac{1}{N^{1/3}} \left(\frac{\hbar}{m_n c}\right) \left(\frac{m_{\text{Planck}}}{m_n}\right)^2$ we obtain the gravitational Thomas-Fermi equation

$$\frac{d^2 \chi}{dx^2} = -\frac{\chi^{3/2}}{\sqrt{x}} \left[1 + \left(\frac{N}{N^*}\right)^{4/3} \frac{\chi}{x} \right]^{3/2}, \quad (\text{E.0.4})$$

where $N^* = \left(\frac{3\pi}{4}\right)^{1/2} \left(\frac{m_{\text{Planck}}}{m_n}\right)^3$. Eq.(E.0.4) has to be integrated with the boundary conditions $\chi(0) = 0$, $-x_b \left(\frac{d\chi}{dx}\right)_{x=x_b} = 1$. Eq. (E.0.4) can be applied as well to the case of white dwarfs.

It is sufficient to assume

$$b = \frac{(3\pi)^{2/3}}{2^{7/3}} \frac{1}{N^{1/3}} \left(\frac{\hbar}{m_e c}\right) \left(\frac{m_{\text{Planck}}}{\mu m_n}\right)^2,$$

$$N^* = \left(\frac{3\pi}{4}\right)^{1/2} \left(\frac{m_{\text{Planck}}}{\mu m_n}\right)^3,$$

$$M = \int_0^{R_c} 4\pi r^2 n_e(r) \mu m_n dr.$$

For the equilibrium condition $c\sqrt{p_F^2 + m^2 c^2} - mc^2 - \mu m_n V = -\mu m_n V_0$, in order to obtain for the critical mass the value $M_{\text{crit}} \approx 5.7 M_{\text{sun}} \mu_e^{-2} \approx 1.5 M_{\text{sun}}$.

The relativistic Thomas-Fermi equation.

In the intervening years my attention was dedicated to an apparently academic problem: the solution of a relativistic Thomas-Fermi Equation and extrapolating the Thomas-Fermi solution to large atomic numbers of $Z \approx 10^4 - 10^6$. Three new features were outlined: **a)** the necessity of introducing a physical size for the nucleus, **b)** the penetration of the electrons in the nucleus, **c)** the definition of an effective nuclear charge (42; 23). The electrostatic potential is given by $\nabla^2 V(r) = 4\pi e n$, where the number density of electrons is related to the Fermi momentum p_F by $n = \frac{p_F^3}{3\pi^2 \hbar^3}$. In order to have equilibrium we have $c\sqrt{p_F^2 + m^2 c^2} - mc^2 - eV(r) = E_F$. Assuming $\phi(r) = V(r) + \frac{E_F}{e} = Ze\frac{\chi(r)}{r}$, $Z_c = \left(\frac{3\pi}{4}\right)^{1/2} \left(\frac{\hbar c}{e^2}\right)^{3/2}$, and $r = bx$, with $b = \frac{(3\pi)^{3/2}}{2^{7/3}} \frac{1}{Z^{1/3}} \frac{\hbar^2}{me^2}$, the Eq. (E.0.3) becomes

$$\frac{d^2\chi(x)}{dx^2} = \frac{\chi(x)^{3/2}}{x^{1/2}} \left[1 + \left(\frac{Z}{Z_c}\right)^{4/3} \frac{\chi(x)}{x} \right]^{3/2}. \quad (\text{E.0.5})$$

The essential role of the non point-like nucleus.

The point-like assumption for the nucleus leads, in the relativistic case, to a non-integrable expression for the electron density near the origin. We assumed a uniformly charged nucleus with a radius r_{nuc} and a mass number A given by the following semi-empirical formulae

$$r_{\text{nuc}} = r_0 A^{1/3}, \quad r_0 \approx 1.5 \times 10^{-13} \text{cm}, \quad (\text{E.0.6})$$

$$Z \simeq \left[\frac{2}{A} + \frac{3}{200} \frac{1}{A^{1/3}} \right]^{-1}, \quad (\text{E.0.7})$$

Eq.(E.0.5) then becomes

$$\frac{d^2\chi(x)}{dx^2} = \frac{\chi(x)^{3/2}}{x^{1/2}} \left[1 + \left(\frac{Z}{Z_c} \right)^{4/3} \frac{\chi(x)}{x} \right]^{3/2} - \frac{3x}{x_{nuc}^3} \theta(x_{nuc} - x), \quad (\text{E.0.8})$$

where $\theta = 1$ for $r < r_{nuc}$, $\theta = 0$ for $r > r_{nuc}$, $\chi(0) = 0$, $\chi(\infty) = 0$.

Eq.(E.0.8) has been integrated numerically for selected values of Z (see Fig. E.2(b) and (42; 23)). Similar results had been obtained by Greiner and his school and by Popov and his school with special emphasis on the existence of critical electric field at the surface of heavy nuclei. Their work was mainly interested in the study of the possibility of having process of vacuum polarization at the surface of heavy nuclei to be possibly achieved by heavy nuclei collisions (see for a review (106)). Paradoxically at the time we were not interested in this very important aspect and we did not compute the strength of the field in our relativistic Thomas-Fermi model which is indeed of the order of the Critical Field $E_c = m^2 c^3 / e \hbar$.

Nuclear matter in bulk: $A \approx 300$ or $A \approx (m_{\text{Planck}}/m_n)^3$.

The situation clearly changed with the discovery of GRBs and the understanding that the process of vacuum polarization unsuccessfully sought in earthbound experiments could indeed be observed in the process of formation of a Black Hole from the gravitational collapse of a neutron star (106). The concept of a Dyadosphere, (107; 108), was introduced around an already formed Black Hole and it became clear that this concept was of paramount importance in the understanding the energy source fo GRBs. It soon became clear that the initial conditions for such a process had to be found in the electro-dynamical properties of neutron stars. Similarly manifest came the crucial factor which had hampered the analysis of the true electro dynamical properties of a neutron star; the unjustified imposition of local charge neutrality as opposed to the global charge neutrality of the system. We have therefore proceeded to make a model of a nuclear matter core of $A \approx (m_{\text{Planck}}/m_n)^3$ nucleons (13). We generalized to this more general case the concept introduced in their important work by W. Greiner and V. Popov (see Fig. E.3) as follows.

I have assumed that the proton number density is constant inside the core $r \leq R_c$ and vanishes outside the core $r > R_c$:

$$n_p = \frac{1}{3\pi^2 \hbar^3} (P_p^F)^3 = \frac{3N_p}{4\pi R_c^3} \theta(R_c - r), \quad R_c = \Delta \frac{\hbar}{m_{\pi} c} N_p^{1/3},$$

where P_p^F is the Fermi momentum of protons, $\theta(R_c - r)$ is the step-function

and Δ is a parameter. The proton Fermi energy is

$$\mathcal{E}_p(P_p^F) = [(P_p^F c)^2 + m_p^2 c^4]^{1/2} - m_p c^2 + eV, \quad (\text{E.0.9})$$

where e is the proton charge and V is the Coulomb potential. Based on the Gauss law, $V(r)$ obeys the Poisson equation $\nabla^2 V(r) = -4\pi e [n_p(r) - n_e(r)]$ and boundary conditions $V(\infty) = 0$, $V(0) = \text{finite}$, where the electron number density $n_e(r)$ is given by

$$n_e(r) = \frac{1}{3\pi^2 \hbar^3} (P_e^F)^3, \quad (\text{E.0.10})$$

being P_e^F the electron Fermi momentum. The electron Fermi energy is

$$\mathcal{E}_e(P_e^F) = [(P_e^F c)^2 + m^2 c^4]^{1/2} - m c^2 - eV. \quad (\text{E.0.11})$$

The energetic equation for an electrodynamic equilibrium of electrons in the Coulomb potential $V(r)$ is $\mathcal{E}_e(P_e^F) = 0$, hence the Fermi momentum and the electron number density can be written as

$$n_e(r) = \frac{1}{3\pi^2 \hbar^3 c^3} \left[e^2 V^2(r) + 2m c^2 eV(r) \right]^{3/2}.$$

Introducing the new variable $x = r/(\hbar/m_\pi c)$ (the radial coordinate in unit of pion Compton length ($\hbar/m_\pi c$), $x_c = x(r = R_c)$), I have obtained the following relativistic Thomas-Fermi Equation ((109; 89)):

$$\frac{1}{3x} \frac{d^2 \chi(x)}{dx^2} = -\alpha \left\{ \frac{1}{\Delta^3} \theta(x_c - x) - \frac{4}{9\pi} \left[\frac{\chi^2(x)}{x^2} + 2 \frac{m}{m_\pi} \frac{\chi}{x} \right]^{3/2} \right\}, \quad (\text{E.0.12})$$

where χ is a dimensionless function defined by $\frac{\chi}{r} = \frac{eV}{\hbar c}$ and α is the fine structure constant $\alpha = e^2/(\hbar c)$. The boundary conditions of the function $\chi(x)$ are $\chi(0) = 0$, $\chi(\infty) = 0$ and $N_e = \int_0^\infty 4\pi r^2 dr n_e(r)$. Instead of using the phenomenological relation between Z and A , given by Eqs. (E.0.6) and (E.0.7), we determine directly the relation between A and Z by requiring the β -equilibrium

$$\mathcal{E}_n = \mathcal{E}_p + \mathcal{E}_e. \quad (\text{E.0.13})$$

The number-density of degenerate neutrons is given by $n_n(r) = \frac{1}{3\pi^2 \hbar^3} (P_n^F)^3$, where P_n^F is the Fermi momentum of neutrons. The Fermi energy of degenerate neutrons is

$$\mathcal{E}_n(P_n^F) = [(P_n^F c)^2 + m_n^2 c^4]^{1/2} - m_n c^2, \quad (\text{E.0.14})$$

where m_n is the neutron mass. Substituting Eqs. (E.0.9, E.0.11, E.0.14) into

Eq. (E.0.13), we obtain $[(P_n^F c)^2 + m_n^2 c^4]^{1/2} - m_n c^2 = [(P_p^F c)^2 + m_p^2 c^4]^{1/2} - m_p c^2 + eV$. These equations and boundary conditions form a close set of non-linear boundary value problem for a unique solution for Coulomb potential $V(r)$ and electron distribution (E.0.10), as functions of the parameter Δ , i.e., the proton number-density n_p . The solution is given in Fig. E.4(a). A relevant quantity for exploring the physical significance of the solution is given by the number of electrons within a given radius r , $N_e(r) = \int_0^r 4\pi(r')^2 n_e(r') dr'$. This allows to determine, for selected values of the $A = N_p + N_n$ parameter, the distribution of the electrons within and outside the core and follow the progressive penetration of the electrons in the core at increasing values of A (see Fig. E.4(b)). We can then evaluate, generalizing the results in (42; 23) , the net charge inside the core $N_{\text{net}} = N_p - N_e(R_c) < N_p$, and consequently determine of the electric field at the core surface, as well as within and outside the core (see Fig. A.15).

The energetically favorable configurations.

Introducing the new function ϕ defined by $\phi = \Delta \left[\frac{4}{9\pi} \right]^{1/3} \frac{\chi}{x}$, and putting $\hat{x} = \Delta^{-1} \sqrt{\alpha} (12/\pi)^{1/6} x$, $\zeta = \hat{x} - \hat{x}_c$ the ultra-relativistic Thomas-Fermi equation can be written as

$$\frac{d^2 \hat{\phi}(\zeta)}{d\zeta^2} = -\theta(-\zeta) + \hat{\phi}(\zeta)^3, \quad (\text{E.0.15})$$

where $\hat{\phi}(\zeta) = \phi(\zeta + \hat{x}_c)$. The boundary conditions on $\hat{\phi}$ are: $\hat{\phi}(\zeta) \rightarrow 1$ as $\zeta \rightarrow -\hat{x}_c \ll 0$ (at massive core center) and $\hat{\phi}(\zeta) \rightarrow 0$ as $\zeta \rightarrow \infty$. We must also have the continuity of the function $\hat{\phi}$ and the continuity of its first derivative $\hat{\phi}'$ at the surface of massive core $\zeta = 0$.

Eq. (E.0.15) admits an exact solution

$$\hat{\phi}(\zeta) = \begin{cases} 1 - 3 \left[1 + 2^{-1/2} \sinh(a - \sqrt{3}\zeta) \right]^{-1}, & \zeta < 0, \\ \frac{\sqrt{2}}{(\zeta+b)}, & \zeta > 0, \end{cases} \quad (\text{E.0.16})$$

where integration constants a and b are: $\sinh a = 11\sqrt{2}$, $a = 3.439$; $b = (4/3)\sqrt{2}$.

We than have for the Coulomb potential energy, in terms of the variable ζ , $eV(\zeta) = \left(\frac{1}{\Delta^3} \frac{9\pi}{4} \right)^{1/3} m_\pi c^2 \hat{\phi}(\zeta)$, and at the center of massive core $eV(0) = \hbar c (3\pi^2 n_p)^{1/3} = \left(\frac{1}{\Delta^3} \frac{9\pi}{4} \right)^{1/3} m_\pi c^2$, which plays a fundamental role in order to determine the stability of the configuration.

It is possible to compare energetic properties of different configurations satisfying the different neutrality conditions $n_e = n_p$ and $N_e = N_p$, with the same core radius R_c and total nucleon number A . The total energy in the case

$n_e = n_p$ is

$$\begin{aligned}\mathcal{E}_{\text{tot}}^{\text{loc}} &= \sum_{i=e,p,n} \mathcal{E}_{\text{loc}}^i \\ \mathcal{E}_{\text{loc}}^i &= 2 \int \frac{d^3r d^3p}{(2\pi\hbar)^3} \epsilon_{\text{loc}}^i(p) = \\ & \frac{cV_c}{8\pi^2\hbar^3} \left\{ \bar{P}_i^F [2(\bar{P}_i^F)^2 + (m_i c)^2] [(\bar{P}_i^F)^2 + (m_i c)^2]^{1/2} - (m_i c)^4 \text{Arsh} \left(\frac{\bar{P}_i^F}{m_i c} \right) \right\}\end{aligned}$$

The total energy in the case $N_e = N_p$ is

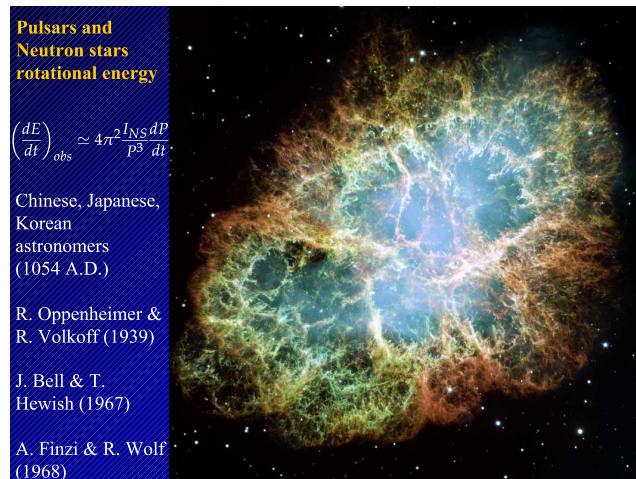
$$\begin{aligned}\mathcal{E}_{\text{tot}}^{\text{glob}} &= \mathcal{E}_{\text{elec}} + \mathcal{E}_{\text{binding}} + \sum_{i=e,p,n} \mathcal{E}_{\text{glob}}^i \\ \mathcal{E}_{\text{elec}} &= \int \frac{E^2}{8\pi} d^3r \approx \frac{3^{3/2}\pi^{1/2}}{4} \frac{N_p^{2/3}}{\sqrt{\alpha}\Delta c} m_\pi \int_{-\kappa R_c}^{+\infty} dx [\phi'(x)]^2 \\ \mathcal{E}_{\text{binding}} &= -2 \int \frac{d^3r d^3p}{(2\pi\hbar)^3} eV(r) \approx -\frac{V_c}{3\pi^2\hbar^3} (P_e^F)^3 eV(0) \\ \mathcal{E}_{\text{glob}}^i &= 2 \int \frac{d^3r d^3p}{(2\pi\hbar)^3} \epsilon_{\text{glob}}^i(p) = \\ & \frac{cV_c}{8\pi^2\hbar^3} \left\{ P_i^F [2(P_i^F)^2 + (m_i c)^2] [(P_i^F)^2 + (m_i c)^2]^{1/2} - (m_i c)^4 \text{Arsh} \left(\frac{P_i^F}{m_i c} \right) \right\}.\end{aligned}$$

We have indicated with \bar{P}_i^F ($i = n, e, p$) the Fermi momentum in the case of local charge neutrality ($V = 0$) and with P_i^F ($i = n, e, p$) the Fermi momentum in the case of global charge neutrality ($V \neq 0$). The energetic difference between local neutrality and global neutrality configurations is positive, $\Delta\mathcal{E} = \mathcal{E}_{\text{tot}}^{\text{loc}} - \mathcal{E}_{\text{tot}}^{\text{glob}} > 0$, so configurations which obey to the condition of global charge neutrality are energetically favorable with respect to one which obey to the condition of local charge neutrality (109; 110). For a core of 10 Km the difference in binding energy reaches 10^{49} ergs which gives an upper limit to the energy emittable by a neutron star, reaching its electrodynamic ground state.

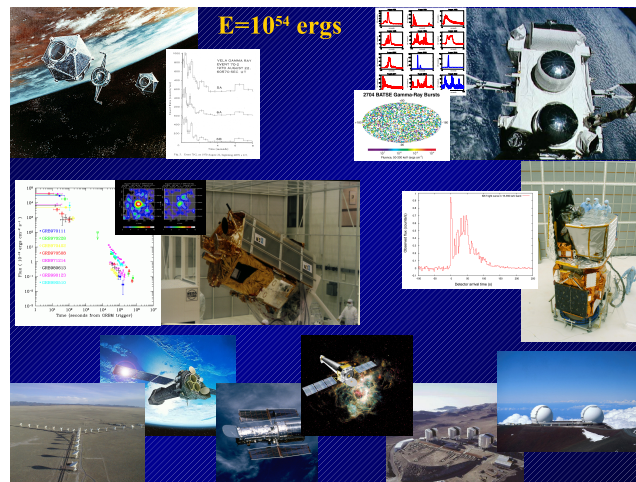
The current work is three fold: **a)** generalize our results considering the heavy nuclei as special limiting cases of macroscopic nuclear matter cores (89), **b)** describe a macroscopic nuclear matter core within the realm of General Relativity fulfilling the generalized Tolman, Oppenheimer, Volkoff equation (111), **c)** Generalize the concept of a Dyadosphere to a Kerr-Newman Geometry (112).

Conclusions.

It is clear that any neutron star has two very different components: the core with pressure dominated by a baryonic component and the outer crust with pressure dominated by a leptonic component and density dominated by the nuclear species. The considerations that we have presented above apply to the first component where the baryonic pressure dominates. It is clear that when the density increases and baryons become ultra-relativistic is this baryonic component which undergoes the process of gravitational collapse and its dynamics is completely dominated by the electro-dynamical process which we have presented in this talk.

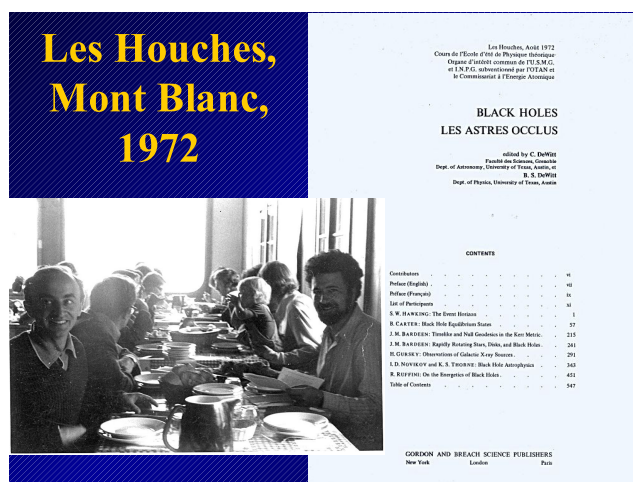


(a)

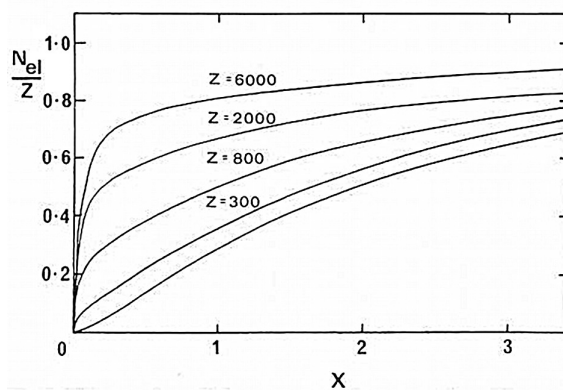


(b)

Figure E.1.: (a) The expanding shell of the remnant of the Crab Nebulae as observed by the Hubble Space Telescope. Reproduced from Hubble Telescope web site with their kind permission (News Release Number: STScI-2005-37). (b) On the upper left the Vela 5A and 5B satellites and a typical event as recorded by three of the Vela satellites; on the upper right the Compton satellite and the first evidence of the isotropy of distribution of GRB in the sky; on the center left the Beppo Sax satellite and the discovery of the after glow; on the center right a GRB from Integral satellite; in the lower part the Socorro very large array radiotelescope, the Hubble, the Chandra and the XMM telescopes, as well as the VLT of Chile and KECK observatory in Hawaii. All these instruments are operating for the observations of GRBs (99).



(a)



(b)

Figure E.2.: (a) Lunch at Les Louces summer school on 'Black Holes'. In front, face to face, Igor Novikov and the author; in the right the title of the book in English and in French. It is interesting that in that occasion Cecile de Witt founded the French translation of the word 'Back Hole' in 'Trou Noir' objectionable and she introduced instead the even more objectionable term 'Astres Occlus'. The French nevertheless happily adopted in the following years the literally translated word 'Trou Noir' for the astrophysical concept I introduced in 1971 with J.A. Wheeler ((105)). (b) The number of electrons contained within a distance x of the origin, as a function of the total number Z for a neutral atom. The lowest curve is that given by the solution of the non-relativistic Thomas-Fermi equation.

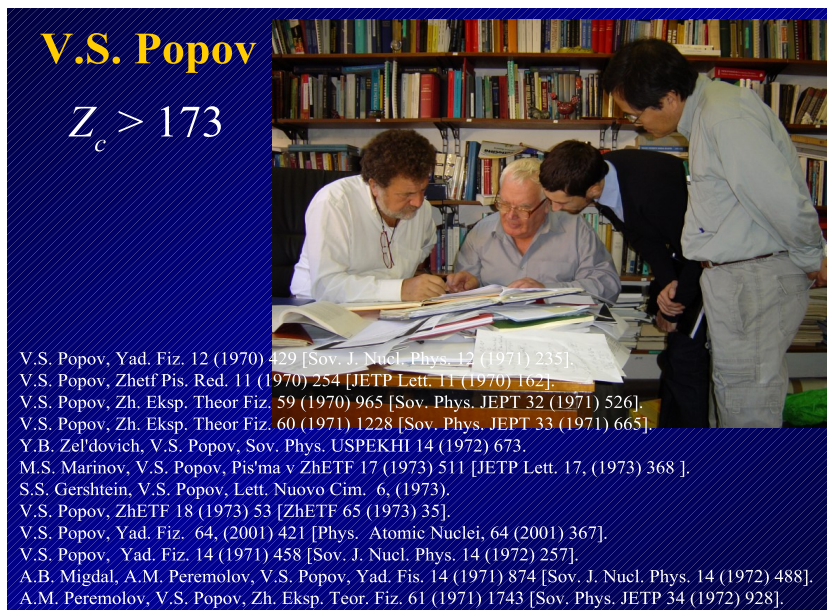
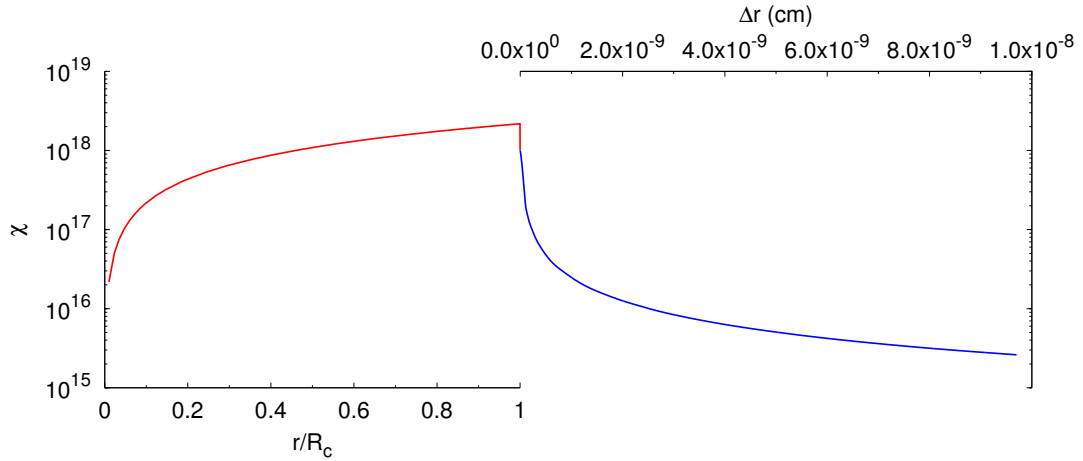
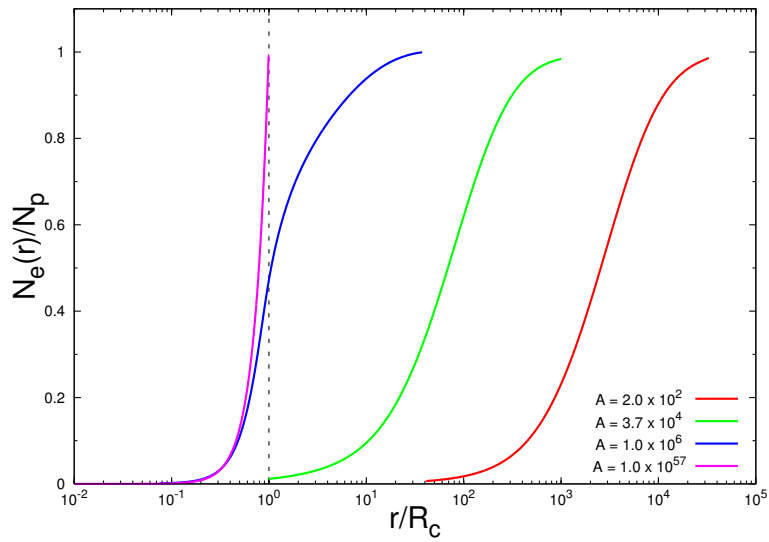


Figure E.3.: Vladimir Popov discussing with the author and Professors She Sheng Xue and Gregory Vereshchagin (Roma 2007). Also quoted the classical contributions of Popov and his school.



(a)



(b)

Figure E.4.: (a) The solution χ of the relativistic Thomas-Fermi Equation for $A = 10^{57}$ and core radius $R_c = 10\text{km}$, is plotted as a function of radial coordinate. The left solid line corresponds to the internal solution and it is plotted as a function of radial coordinate in unit of R_c in logarithmic scale. The right dotted line corresponds to the solution external to the core and it is plotted as function of the distance Δr from the surface in the logarithmic scale in centimeter. (b) The electron number in the unit of the total proton number N_p , for selected values of A , is given as function of radial distance in the unit of the core radius R_c , again in logarithmic scale. It is clear how by increasing the value of A the penetration of electrons inside the core increases.

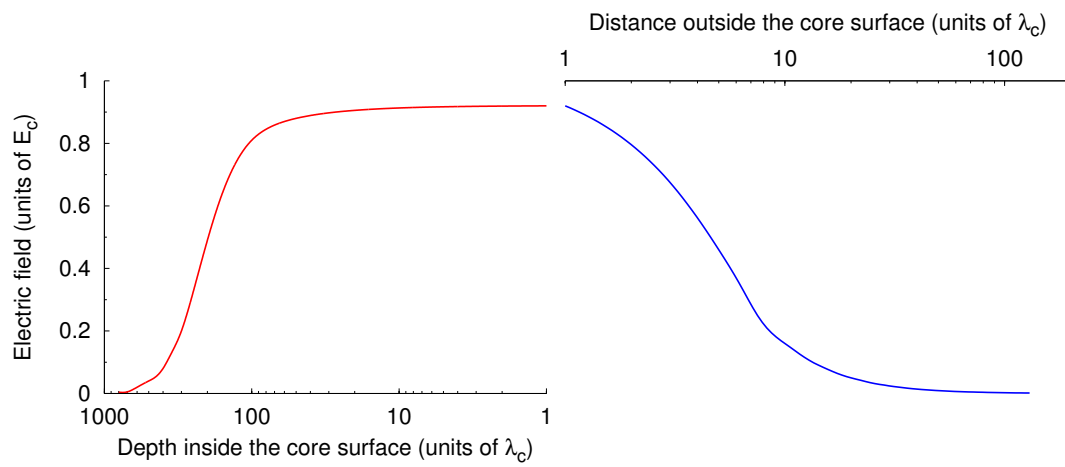


Figure E.5.: The electric field in the unit of the critical field E_c is plotted around the core radius R_c . The left (right) solid (dotted) diagram refers to the region just inside (outside) the core radius plotted logarithmically. By increasing the density of the star the field approaches the critical field.

Bibliography

- [1] R. Ruffini, S.-S. Xue and G. V. Vereshchagin, Phys. Rep. in press (2009).
- [2] C. Cherubini et al., Phys. Rev. D **79**, 124002 (2009).
- [3] A. G. Aksenov, R. Ruffini and G. V. Vereshchagin, Phys. Rev. Lett. **99**, 125003 (2007).
- [4] R. C. Tolman, Phys. Rev. **55**, 364 (1939).
- [5] J. R. Oppenheimer and G. Volkoff, Phys. Rev. **55**, 374 (1939).
- [6] B. K. Harrison et al., "Gravitational theory and gravitational collapse" (1965).
- [7] W. Pieper and W. Greiner, Z. Phys. **218**, 327 (1969).
- [8] B. Müller, *et al.*, Phys. Rev. Lett. **28**, 1235 (1972).
- [9] J. S. Greenberg and W. Greiner, Physics Today, **24** (August 1982) and references therein.
- [10] V. S. Popov, Sov. Phys. JETP **32**, 526 (1971).
- [11] Ya. B. Zeldovich and V. S. Popov, Sov. Phys. USP. **14**, 673 (1972).
- [12] A. B. Migdal, D. N. Voskresenskii and V. S. Popov, Sov. Phys. JETP Lett. **24**, 186 (1976).
- [13] R. Ruffini, M. Rotondo and S.-S. Xue, Int. J. Mod. Phys. D **16**, 1 (2007).
- [14] R. Ruffini, Proceedings of the 9th International Conference 'Path Integrals,' World Scientific, 207 (2008).
- [15] R. P. Feynman, N. Metropolis and E. Teller, Phys. Rev. **75**, 1561 (1949).
- [16] E. Fermi, "Nuclear Physics," Revised Edition, The University of Chicago Press, 1950.
- [17] *Ibid.*, p. 6.
- [18] *Ibid.*, p. 6.
- [19] *Ibid.*, p. 7.

- [20] Ibid., p. 164.
- [21] A. Bohr and B. R. Mottelson "Nuclear Structure," W. A. Benjamin (1969).
- [22] J. Ferreira, R. Ruffini and L. Stella, Phys. Lett. B **91**, 314 (1980).
- [23] R. Ruffini and L. Stella, Phys. Lett. B **102**, 442 (1981).
- [24] R. L. Liboff, "Introductory Quantum Mechanics," Addison-Wesley (2002).
- [25] S. Chandrasekhar, "The Mathematical Theory of Black Holes," Oxford University Press (1998).
- [26] G. Baym, H. A. Bethe and C. J. Pethick, Nucl. Phys. A **175**, 225 (1971).
- [27] N. Itoh, Prog. Theor. Phys. **44**, 291 (1970).
- [28] E. Witten, Phys. Rev. D, **30**, 272 (1984).
- [29] C. Alcock, E. Farhi and A. Olinto, Apj. **310**, 261 (1986).
- [30] Ch. Kettner et al., Phys. Rev. D **51**, 1440 (1995).
- [31] V. Usov, Phys. Rev. Lett. **80**, 230 (1998).
- [32] P. Haensel, A.Y. Potekhin, D.G. Yakovlev, Neutron Stars, Springer, (2007).
- [33] M. Rondono, J. Rueda, R. Ruffini and S.-S. Xue, in preparation (2009).
- [34] J. A. Rueda, R. Ruffini and S.-S. Xue, in preparation (2009).
- [35] J. Madsen, Phys. Rev. Lett. **100**, 151102 (2008).
- [36] P. C. C. Freire et al., arXiv:0711.2028v1.
- [37] P. C. C. Freire et al., ApJ, **679**, 1433 (2008).
- [38] C.E. Rhoades and R. Ruffini, Phys. Rev. Lett. **28**, 1235 (1972).
- [39] J.M. Lattimer and M. Prakash, Phys. Rep. **442**, 109 (2007).
- [40] A. Mezzacappa and G.M. Fuller, "Open Issues in Core Collapse Supernova Theory," World Scientific 2005.
- [41] R. Ruffini, in *Proceedings of the Eleventh Marcel Grossman Meeting*, R. Jantzen, H. Kleinert, R. Ruffini (eds.), (World Scientific, Singapore, 2008).

-
- [42] J. Ferreira, R. Ruffini and L. Stella, *Phys. Lett. B* **91**, 314 (1980).
- [43] W. Heisenberg and H. Euler, *Z. Phys.* **98**, 714 (1936).
- [44] E. Segré, "Nuclei and Particles", Second Edition, W. A. Benjamin 1977.
- [45] T. Damour and R. Ruffini, *Phys. Rev. Lett.* **35**, 463 (1975).
- [46] R. P. Kerr, *Phys. Rev. Lett.* **11**, 273 (1963).
- [47] R. Oppenheimer and G. M. Volkoff, *Phys. Rev.* **55**, 374 (1939).
- [48] G. Baym, H. A. Bethe and C. J. Pethick, *Nuc. Phys. A* **175**, 225 (1971).
- [49] B. Patricelli, M. Rotondo, J. A. Rueda H. and R. Ruffini., in *Proceedings of the Fifth Italian-Sino Workshop*, D. Lee, W. Lee, S.-S. Xue (eds.), AIP Conf. Proc., Vol. 1059, pp. 68-71 (2008).
- [50] B. Patricelli, J. A. Rueda H. and R. Ruffini, in *Proceedings of the Third Stueckelberg Workshop*, G. Montani and G. W. Vereshchagin (eds.), (World Scientific, 2008, in preparation).
- [51] J. A. Rueda H., B. Patricelli, M. Rotondo, R. Ruffini and S. S. Xue, in *Proceedings of the Third Stueckelberg Workshop*, G. Montani and G. W. Vereshchagin (eds.), (World Scientific, 2008, in preparation).
- [52] H. Andréasson, arXiv:0804.1882v1.
- [53] E. Lieb and B. Simon, *Phys. Rev. Lett.* **31**, (1973) 681.
- [54] I. Pomeranchuk and Ya. Smorodinsky, *J. Phys., USSR* **9**, (1945) 97.
- [55] S. S. Gershtein and Ya. B. Zeldovich, *Soviet Physics JETP*, Vol. **30**, (1970) 385.
- [56] B. Muller and J. Rafelski, *Phys. Rev. Lett.*, Vol. **34**, (1975) 349.
- [57] A. B. Migdal, D. N. Voskresenskii and V. S. Popov, *JETP Letters*, Vol. **24**, No. 3 (1976) 186.
- [58] F. Sauter, *Z. Phys.* **69** (1931) 742.
- [59] J. Schwinger, *Phys. Rev.* **82** (1951) 664; J. Schwinger, *Phys. Rev.* **93** (1954) 615; J. Schwinger, *Phys. Rev.* **94** (1954) 1362.
- [60] G. Gamow, "Constitution of Atomic Nuclei and Radioactivity", Clarendon Press, Oxford, 1931.
- [61] R. Ruffini and S. Bonazzola, *Phys. Rev. D* **187**, (1969) 1767.

- [62] H. A. Bethe, G. Börner and K. Sato, *Astron. & Astrophys.* 7, (1970) 279.
- [63] A. G. W. Cameron *Annual Reviews Inc.* (1970) 179.
- [64] L. H. Thomas, *Proc. Cambridge Phil. Society*, 23, (1927) 542-548.
- [65] E. Fermi, *Rend. Accad. Lincei* 6, (1927) 602-607.
- [66] G. Scorza-Dragoni, *Rend. Accad. Lincei* 8, (1928) 301; 9, (1929) 378 .
- [67] A. Sommerfeld, *Z. Physik* 78, (1932) 283 .
- [68] C. Miranda, *Mem. Accad. Italia* 5, (1934) 285-322.
- [69] E. Lieb, *Rev. Mod. Physics* 53, (1981) 603-642.
- [70] L. Spruch, *Rev. Mod. Physics* 63, (1991) 151-209.
- [71] R. Ruffini, M. Rotondo and S.-S. Xue, submitted to *Phys. Rev. Lett.* .
- [72] P. A. M. Dirac, *Proc. Roy. Soc.* 117 (1928) 610; P. A. M. Dirac, *Proc. Roy. Soc.* 118 (1928) 341.
- [73] P. A. M. Dirac, "Principles of Quantum Mechanics", Clarendon Press, Oxford, 1958.
- [74] W. Gordon, *Z. Phys.* 48 (1928) 11.
- [75] C. G. Darwin, *Proc. Roy. Soc.* A118 (1928) 654.
- [76] A. Sommerfeld, *Atomau und Spektrallinien*, 4. Aufl. ,6. Kap.
- [77] N. Case, *Phys. Rev.* 80 (1950) 797.
- [78] F. G. Werner and J. A. Wheeler, *Phys. Rev.* 109 (1958) 126.
- [79] V. Vorankov and N. N. Kolesinkov, *Sov. Phys. JETP* 12 (1961) 136.
- [80] V. S. Popov, *Yad. Fiz.* 12 (1970) 429 [*Sov. J. Nucl. Phys.* 12 (1971) 235].
- [81] V. S. Popov, *Zhetf Pis. Red.* 11 (1970) 254 [*JETP Lett.* 11 (1970) 162]; V. S. Popov, *Zh. Eksp. Theor Fiz.* 59 (1970) 965 [*Sov. Phys. JEPT* 32 (1971) 526].
- [82] V. S. Popov, *Zh. Eksp. Theor Fiz.* 60 (1971) 1228 [*Sov. Phys. JEPT* 33 (1971) 665].
- [83] M. S. Marinov and V. S. Popov, *Pis'ma v ZhETF* 17 (1973) 511 [*JETP Lett.* 17, (1973) 368]; G. Siff, B. Müller and J. Rafelski, *Zeits. Naturforsch* 292 (1974) 1267.

-
- [84] V. S. Popov, *Yad. Fiz.* 64, (2001) 421 [*Phys. Atomic Nuclei*, 64 (2001) 367].
- [85] Review article: J. Rafelski, L.P. Fulcher and A. Klein, *Phys. Repts.* 38 (1978) 227.
- [86] Review article: W. Greiner, B. Müller and J. Rafelski, "Quantum Electrodynamics of Strong Fields" Monograph in Physics, ISBN 3-540-13404-2 Springer-Verlag Berlin Heidelberg (1985) (references there in).
- [87] H. Kleinert, R. Ruffini and S.-S. Xue, to appear in *Phys. Rev. D* (2008).
- [88] S. W. Hawking, *Nature* 238 (1974) 30; S. W. Hawking, *Commun. Math. Phys.* 43, 199 (1975); G. W. Gibbons and S. W. Hawking, *Phys. Rev. D* 15 2752 (1977).
- [89] B. Patricelli, M. Rotondo and R. Ruffini, "On the Charge to Mass Ratio of Neutron Cores and Heavy Nuclei, AIP Conference Proceedings", Vol. 966 (2008), pp. 143-146.
- [90] R. Eisberg, R. Resnick, "Quantum Physics of Atoms, Molecules, Solids, Nuclei, and Particles", Second Edition, J. Wiley & Sons, 1985
- [91] E. Olson, M. Bailyn, *Phys. Rev. D*, Vol. 18, pp. 6, 1978
- [92] G. Baym, C. Pethick and P. Sutherland, *Astrophysical Journal*, Vol. 170, pp. 299, 1971
- [93] S. L. Shapiro, S. A. Teukolsky, "Black Holes, White Dwarfs, and Neutron Stars - The Physics of Compact Objects", WILEY - VCH, 2004
- [94] M. G. Dainotti et al., in preparation
- [95] I. S. Shlikvoskii, *Supernovae*, (Wiley, New York, 1968).
- [96] R. N. Manchester and J. H. Taylor, *Pulsars*, (Freeman and Co., San Francisco, CA, 1977).
- [97] R. Ruffini, From the ergosphere to the dyadosphere in *Festschrift in Honor of Roy Kerr*, D. Wildshire (ed.), (Cambridge University Press, 2008).
- [98] H. Gursky and R. Ruffini, *Neutron Stars, Black Holes and Binary X-Ray Sources*, (Springer, 1975).

- [99] R. Ruffini, M. G. Bernardini, C. L. Bianco, L. Caito, P. Chardonnet, M. G. Dainotti, F. Fraschetti, R. Guida, M. Rotondo, G. Vareshchagin, L. Vitagliano and S. S. Xue, in *Cosmology and Gravitation: XII th Brazilian School of Cosmology and Gravitation*, M. Novello, S. E. Perez Bergliaffa (eds.), AIP Conf. Proc., 910, 55 (2007).
- [100] E. Costa et al., *Nature* **387**, 783 (1997).
- [101] A. M. Soderberg et al., arXiv:0802.1712v1.
- [102] L. D. Landau and E. M. Lifshitz, *Non-Relativistic Quantum Mechanics*, (Pergamon Press, Oxford, 1975).
- [103] R. Ruffini, On the energetics of Black Holes in *Black Holes - Les astres occlus*, C. and B.S. De Witt (eds.), (Gordon and Breach, New York, 1972).
- [104] L. D. Landau, *Phys. Z. Sowjetunion* **1**, 285 (1932).
- [105] R. Ruffini and J. A. Wheeler, *Phys. Today* **24**, 30 (1971).
- [106] R. Ruffini, G. Vereshchagin and S. S. Xue, Progress Report, in preparation, (2008).
- [107] R. Ruffini, in *Black Holes and High Energy Astrophysics*, H. Sato and N. Sugiyama (eds.), 167 (Universal Academic Press, Tokyo, 1998).
- [108] G. Preparata, R. Ruffini and S. S. Xue, *Astron. Astroph.* 338, L87 (1998).
- [109] M. Rotondo, R. Ruffini and S. S. Xue, in *Relativistic Astrophysics: 4th Italian-Sino Workshop*, C.L. Bianco, S.S. Xue (eds.), AIP Conf. Proc., 966, 147 (2007).
- [110] R. Ruffini, M. Rotondo and S. S. Xue, in preparation, (2008).
- [111] J. Rueda, M. Rotondo and R. Ruffini, in preparation, (2008).
- [112] C. Cherubini, A. Geralico, J. A. H. Rueda and R. Ruffini, in *Relativistic Astrophysics: 4th Italian-Sino Workshop*, C.L. Bianco, S.S. Xue (eds.), AIP Conf. Proc., 966, 123 (2007).
- [113] V. Popov, M. Rotondo, R. Ruffini and S.-S. Xue, submitted to *Phys. Rev. C* (2009).
- [114] L. H. Thomas, *Proc. Camb. Phil. Soc.* **23**, 542 (1927).
- [115] E. Fermi, *Rend. Accad. Lincei* **6**, 602 (1928).
- [116] T. J. Bürvenich, I. N. Mishustin and W. Greiner, *Phys. Rev. C* **76**, 034310 (2007).

- [117] A. G. Aksenov, R. Ruffini and G. V. Vereshchagin, *Phys. Rev. D* **79**, 043008 (2009).
- [118] A. G. Aksenov, R. Ruffini, and G. V. Vereshchagin, *Phys. Rev. Lett.* **99**, 125003 (2007).
- [119] G. Pagliaroli, F. Vissani, M. L. Costantini, and A. Ianni, *Astropart. Phys.* **31**, 163 (2009).
- [120] G. Pagliaroli, F. Vissani, E. Coccia, and W. Fulgione, *Phys. Rev. Lett.*, **103**, 031102 (2009).
- [121] Jorge A. Rueda, R. Ruffini, and S.-S. Xue, To be submitted to *Phys. Rev. D*, (2009).
- [122] C. Cherubini, A. Geralico, J. A. Rueda H., and R. Ruffini, *Phys. Rev. D* **79**, 124002 (2009).
- [123] G. G. Pavlov and G. J. M. Luna, *Astrophys. Journal* **703**, 910 (2009).
- [124] Wynn C. G. Ho and Craig O. Heinke, *Nature* **462**, 71 (2009).

